12/82

CONTRACTOR REPORT - 165591

ENERGY EFFICIENT FACE SEAL

BY

J. SEHNAL
J. SEDY, A. ZOBENS

CRANE PACKING COMPANY
6400 OAKTON ST., MORTON GROVE, ILL. 60053

AND

I. ETSION
DEPT. OF MECHANICAL ENGINEERING
TECHNION, HAIFA, ISRAEL 32000

PREPARED FOR

NATIONAL AERONAUTICS AND SPACE ADMINISTRATION

LEWIS RESEARCH CENTER
CLEVELAND, OHIO 44135

UNDER

CONTRACT NAS 3-22128

APRIL 1982

(NASA-CR-165591) ENERGY EFFICIENT FACE SEAL (Crane Packing Co.) 113 p HC A06/MF A01 CSCL 11A

N83-15659

Unclas

1. Report No.	2. Government Accession No.	3. Recipient's Catalog No.
NASA CR-165591		

4. Title and Subtitle	5. Report Date
ENERGY EFFICIENT FACE SEAL	February 11, 1982
	6. Performing Organization Code

7. Author(s)	8. Performing Organization Report No.
J. Sehnal, J. Sedy, I. Etsion, A. Zobens	10. Work Unit No.

9. Performing Organization Name and Address	11. Contract or Grant No.
Crane Packing Company 6400 Oakton Street Morton Grove, IL 60053	NAS 3-22128

12. Sponsoring Agency Name and Address	13. Type of Report and Period Covered
National Aeronautics and Space Administration Lewis Research Center 21000 Brookpark Road Cleveland, Ohio 44135	Contract - one year
	14. Sponsoring Agency Code

15. Supplementary Notes
L. J. Kiraly, Lewis Contact
NASA Lewis Research Center
21000 Brookpark Road (MS 23-2)
Cleveland, Ohio 44135

16. Abstract

Torque, face temperature, leakage, and wear of a flat face seal were compared with three coned face seals at pressures up to 2758 kPa (400 psig) and speeds up to 8000 rpm. Axial movement of the mating seal parts was recorded using a digital data acquisition system. The coning of the tungsten carbide primary ring ranged from .51 μ -m (20 μ-in.) to 5.6 μ-m (220 μ-in.) The torque of the coned face seal balanced to 76.3% was an average 42% lower, the leakage eleven times higher, than that of the standard flat face seal. Reducing the balance of the coned face seal to 51.3% resulted in decreasing the torque by an additional 44% and increasing leakage 12 to 230 times, depending on the seal shaft speed. No measurable wear was observed on the face of the coned seals. All four seals operated in the stable region of the stability map.

17. Key Words (Suggested by Author(s))	18. Distribution Statement
Face Seals Liquid Lubricated Seals	Unclassified Unlimited

19. Security Classif. (of this report)	20. Security Classif. (of this page)	21. No. of Pages	22. Price*
Unclassified	Unclassified		

* For sale by the National Technical Information Service, Springfield, Virginia 22161

CONTENTS PAGE

SUMMARY

The effects of a face coning on seal performance, especially energy losses as indicated by torque, were studied by comparing one conventional flat face pusher type seal of 88.90 mm (3.5") mean face diameter with three seals of the same size where a convex cone was lapped on the face of the stationary flexibly mounted primary ring. One seal was a metal bellows type, the other two were pusher type seals equipped with the antirotation linkage drive. Measurements were made of the seal torque, face temperature, leakage, and of the axial movements of the seal mating parts.

The test conditions ranged from 0 to 2758 kPa (0 to 400 psig) for pressures and 1800 to 8000 rpm for the rotor speed which corresponds to a 8.08 m/sec. to 40.74 m/sec. (26.5 ft/sec. to 133.6 ft/sec.) sliding velocity at the face mean diameter. The cone height on the face of the tungsten carbide primary ring ranged from .51 micrometers (20 microinches) to 5.6 μ-m (220 μ-in.) per 3.175 mm to 6.36 mm (.125 in. to .25 in.) face width. The face material of the standard flat face seal was carbon.

The axial movement of the seal mating ring-rotor and its primary ring-stator was sensed using 5 miniature displacement sensors. The seal motion was then observed on an oscilloscope and digital displacement data stored on a magnetic tape using a fast analog to digital converter and a data acquisition system consisting of a microprocessor and a desktop computer.

Studies show that the cone lapped on the seal face results in energy reduction for the seal. The torque produced by the cone face seal, balanced to 76.3%, was on average 42% lower than that of the commercial flat face seal of the same balance and the same spring load. The friction torque of the flat face seal was sufficient to stall the rig driving motor when attempted to operate this seal at 8000 rpm.

The penalty for the lower torque was the increase in the seal leakage in proportion with the cone height at the same face width. The leakage averaged eleven times more for the coned pusher type seal and five times more for the coned bellows type seal. Reducing the spring closing force and the seal balance to 51.3% resulted in further reduction of the torque by 44%, while the leakage increased 12 to 230 times, depending on the shaft speed.

Due to the better cooling resulting from the increased flow through the seal interface, the face temperatures of the cone face seals were 33°C (60°F) to 56°C (140°F) lower.

The wear on the tungsten carbide faces of the coned seals was greatly reduced. Although the tests were short (15 to 20 hours total for each seal), the conventional seal experienced wear amounting to 2.5 μ-m (100 μ-in.) on the ID of its flat face carbon primary ring. No wear tracks could be observed on the mating parts of the coned seal, balanced to 51.3%, and only several microscopic wear tracks were visible on the face of the other two coned seals. Reduced wear on the seal parts is another indirect form of energy conservation.

The seal faces contacted during the runs with the flat face seal and were separated on the tests with the coned seals as indicated by the appearance of the seal faces. The exact amount of the clearance between the mating parts could not be measured accurately because of the temperature effect on the calibration of the displacement probes and on the rotor target ring.

In all tested seals, the flexibly mounted stationary primary ring synchronously tracked the angular misalignment (axial runout) of the rotor indicating a stable operation. A time dependent phase shift was detected in motion of the coned face seals, the flat face contacting seal experienced a pure axial translation motion without any lag between the stator and the rotor. During the tests with the pusher type seal, the maximum phase shift was measured 290° while on the bellows type seal it amounted to 37° because of lower inertia of the primary ring.

INTRODUCTION

Sealing technology can provide significant contributions to our national problem of energy conservation (1). Much recent and on-going research needs to be advanced and integrated in functional seal designs that offer substantial savings in energy (2). Such savings can be achieved in operating machines by improved performance as indicated by reduced friction (and, therefore, cooling), by lower leakage, and by extended service life with minimal maintenance. Also, energy conservative concepts can guide the selection of materials for construction and manufacturing methods.

The machine builders and operators that select mechanical components like seals choose to innovate with the components that they completely control in the design and manufacture; thus, they are reluctant to change, encourage or purchase new types of seals until service problems dictate that course. Energy losses in seals have not been an important design parameter for machine builders. For example, asbestos packings are still widely used although there can be little question that a properly selected shaft seal is more effective according to most any basis for performance comparison, but especially for energy conservation. Seal manufacturers must supply products that machine builders will purchase. It is not economical to pursue totally new concepts in seals, but rather to make incremental advancements in response to real or anticipated operational problems. Accordingly, most of the research and development attention has dealt with product improvement (as the economics dictate) and the rate of progress on a new energy conservative dynamic face seal has also followed that course.

One of the major requirements for an energy conservative seal is reduced friction and wear at the primary sealing interface, which can be accomplished by optimizing lubrication and pressure balance. Another requirement for sealing, also dependent on the above, is to maintain sufficiently precise geometry accomodation at that interface to minimize leakage flow; the leakage loss of any process fluid represents an energy loss for the system. NASA-Lewis, through its in-house, contract, grant programs, and special workshop seminars, has done much to identify, isolate, and quantify effective film formation parameters and geometric considerations of leakage paths in face

seals (3 to 15). The results from reported research studies were reviewed to select concepts for optimization and the design, fabrication, and evaluation with the objective of an energy conservative seal. There are problems in aerospace transportation (e.g. accessory seals for turbofan engines), in manufacturing process industries (e.g. pump seals for chemical process systems), and in other segments of this nation's present industrial complex where the technology of an energy conservative seal can be utilized to the national advantage.

The objective of this program was to design, fabricate, and experimentally evaluate an energy conservative face seal. The study utilized the technology on seal interface film lubrication advanced by Lewis and built on the expertise in sealing of Crane Packing Company. Thus, well established and successful sealing technology improved by utilization of NASA sponsored seal research could provide a significant advancement of the state of the art.

Recent analyses for NASA by I. Etsion and collaborators provide the background for experimental data on face seal liquid film concepts. An energy conservative seal was designed and built, modifying a successful, widely used, commercial seal. Design considerations concentrated on dynamic stability using coning to reduce the hydrodynamic transverse moment and, therefore, improve stability. The greatest probability for maintaining a liquid film,and thereby minimizing solid contacts at sealing interfaces,was sought for operating conditions relevant to real needs. Experimental evaluation was performed at rotation speeds to 8000 rpm, with pressures to 2758 kPa (400 psig) using a petroleum base turbine oil. Seal leakage, torque, and dynamic displacement measurements were made.

ANALYTICAL BACKGROUND

Nomenclature

- a - linearity constant, eq. (2)
- B - seal balance ratio, $(r_o^2-r_b^2)/(r_o^2-r_i^2)$
- C_o - equilibrium center-line clearance
- F^*_{spi} - initial spring load
- K^* - supporting springs constant
- m^* - ring mass
- p - pressure
- Δp - pressure differential, p_o-p_i
- Q - volumetric leakage
- R_i - dimensionless radius ratio, r_i/r_o
- r - radius
- r_b - seal balance radius
- r_g - ring radius of gyration
- r_{sp} - radius of spring location
- H - cone height, $\beta^*(r_o-r_i)$
- β^* - coning angle
- β - normalized coning, $\beta^* r_o/C_o$
- μ - viscosity
- ω - shaft angular velocity

Subscripts

- i - inner radius
- m - mid radius
- O - outer radius

The main objective in any seal is to minimize leakage. To this end the separation of the mating faces should be as small as possible. In conventional application this aim is achieved by using contacting seals where a complete or partial mechanical contact between the mating faces is maintained. When speed and pressure increase, mechanical contact results in excessive wear, high friction-loss, which may become intolerable, and short seal life. The solution to this problem is found in the use of non-contacting seals in which a complete fluid film is maintained between the faces in relative sliding. The presence of such lubricating fluid film reduces friction losses and increases seal life at the expense of some tolerable leakage. To avoid excessive leakage, the separation between the mating faces or the sealing gap should be very small, of the order of a few micrometers. Hence, any uncontrolled movement of the flexibly mounted seal ring can cause drastic changes in the sealing gap. This can eventually lead to seal failure due to rubbing contact or excessive leakage.

From the preceding discussion, it becomes evident that dynamic and static stability of the flexibly mounted ring is essential for safe operation of non-contacting seals. Damping and stiffness properties of the flexible support, as well as of the lubricating fluid film, mass-inertia of the seal ring, seal balance, and operating conditions are all important factors which affect seal stability. Flat face seals, for example, suffer from the lack of axial stiffness of the fluid film. Thus, it is impossible to maintain and control a desired sealing gap with flat face seals. One way to overcome this difficulty is to use coned face seals where proper coning is intentionally introduced to one of the mating faces. The dynamic behavior of non-contacting face seals was analyzed in (13) for the case of rigidly mounted rotating seat and a flexibly mounted stationary ring without damping in its flexible support.

Generally, three modes of seal operation were found. The results for a coned face seal of 0.9 radius ratio are shown in Figure 1 in the form of stability maps. Three dimensionless groups of parameters affect the seal's stability; the speed parameter $(r_g/r_{sp})^2 m^* \omega^2/K^*$, the pressure parameter $(r_m/r_{sp})^2 (p_o-p_i) r_o^2/K^* C_o$, and the coning parameter $\beta^* r_o/C_o$. As shown in Figure 1 when the seal operates at a given pressure and coning parameters

there is a critical speed parameter below which the seal is stable. In the stable region the flexibly mounted ring tracks the rotating seat synchronously. At equilibrium a desired design clearance is maintained between the mating faces and any disturbance of the seal ring from its equilibrium position disappears after a short period of time. If the speed parameter is increased above the critical value, the seal becomes unstable, the design clearance cannot be maintained, and rubbing contact occurs resulting in high friction losses and eventually seal failure. In the transition between the stable and unstable modes of operation, the flexibly mounted ring wobbles at a frequency that equals half the shaft speed, rubbing contact is avoided but high leakage may result from large relative misalignment between ring and seat. The three modes of operation mentioned above were observed experimentally elsewhere (14) but no quantitative results are yet available to confirm the prediction of Ref. (13). The critical speed parameter is related in (13) to the pressure and coning parameters by the expresssion

$$\left(\frac{r_g}{r_{sp}}\right)^2 \left(\frac{m^*\omega^2}{K^*}\right)_{cr} = 4 + a \frac{(p_o - p_i) r_o^2}{K^* C_o} \left(\frac{r_m}{r_{sp}}\right)^2 \tag{1}$$

where the linearity constant, a, depends on the coning parameter and has the form

$$a = -8\pi R_i^2 (1 - R_i)^2 \frac{1 - \beta R_i}{\left[2 + \beta(1 - R_i)\right]^2} \tag{2}$$

$$\beta = \beta^* \frac{r_o}{C_o} \tag{3}$$

An optimum coning exists which maximizes the value of the critical speed parameter at any given pressure parameter. This optimum coning is given by

$$\beta_{opt} = \frac{2}{R_i (1 - R_i)} \tag{4}$$

Designing the seal with the optimum coning as given by (4) provides the largest range for stable operation.

In practice the actual clearance C_o at standstill can be calculated from the quadratic equation

$$2K^*C_o^2 + \left[2F_{spi} + K^*H + 4\pi r_m(r_o - r_i)(B - \tfrac{1}{2})\Delta p\right] C_o$$
$$- 2\pi r_m(r_o - r_i)(1 - B)\ H\ \Delta p + F^*_{SPi}H = 0 \qquad (5)$$

where H is the cone height measured over the seal face width and related to the coning angle by

$$\beta^* = \frac{H}{r_o - r_i}$$

B is the balance ratio, and Δp is the pressure differential across the seal.

The values of C_o calculated by (5) for various Δp's can then be used in eqs. (3), (2), and (1) to calculate the corresponding critical speed values, ω_{cr}.

The leakage across the seal, assuming parallel faces, is given by (see ref. 15)

$$Q = \frac{\pi\Delta p}{6\mu} C_o^3 \frac{r_m}{r_o - r_i}\left(1 + \frac{3}{2}\ \frac{H}{C_o}\right) \qquad (6)$$

Hence, it can be seen that coning, expressed here in terms of cone height H, increases the leakage by $1.5\ H/C_o$ compared to a flat face seal with the same clearance C_o.

The critical parameters of the tested coned face seals were calculated using a computer program "CRPAPM" described and reproduced in Appendix 1. The program is based on expressions (1), (2), (3), and (5). From the results generated, the stability maps for the tested coned face seals were constructed with the location of test points indicating the character of seal operation. A total of three coned face seals operating in non-contacting manner were tested and their stability maps are shown in Figures 2, 3, and 4. Cone height as lapped was corrected for a deflection of the primary ring due to the sealed pressure on the OD.

EXPERIMENTAL SEALS

Two seals were needed for each experiment. The front seal with a probe target plate attached to its primary ring was the test seal. The rear seal was of an identical design, but without the target, served to close the back side of the seal cavity. Stationary flexibly mounted primary rings of both seals were running against the opposite sides of the common rotor shown in Figure 5 made of tungsten carbide. The rotor and the primary rings were re-lapped and repolished before each test if the damage on the faces was not severe.

A total of four different seals with the design characteristics in Table 1 were tested. The dimensions of the primary ring used in tests with the pusher type seal are shown in Figure 6.

a. Conventional flat face pusher type seal, balanced to 76.3%. This is Crane Packing Company's commercial Standard Type 8B Seal with an O-ring as a secondary seal. A pusher type seal is defined as a mechanical seal where the secondary sealing element is pushed along the shaft or sleeve to compensate for face wear. Non-pusher seals employ bellows or diaphragm as secondary sealing elements. The primary ring, shown in Figure 6, was held in place by a conventional round drive dent on the OD.

b. Coned face pusher type seal similar to the above Standard Type 8B Seal, but equipped with a low-friction, anti-rotation linkage drive. The seal shown in Figure 7 also used an O-ring as a secondary seal and was balanced to 76.3%.

c. Coned face bellows type seal, which is Crane Packing Company's Type 15 Seal. The design, as originally proposed, was modified several times in order to eliminate the effect of thermal distortion on the primary ring. Also, the seal balance was reduced by 8% to 79% at 345 kPa (50 psig). With this type of seal, the seal balance usually shifts when the pressure changes and at 1379 kPa

(200 psig) the balance was measured to be 68%. The latest design of the front and back seals, that were used in the testing, are shown in Figures 8 and 9.

d. Modified coned face pusher type seal shown in Figure 10 and similar to Type 8B Seal. This seal was of the same design as previously described except that the seal balance was reduced from 76.3% to 51.3% and the spring closing force decreased to 10.7 Newtons (2.4 lbs). A 3.17 mm (1/8") cross section O-ring in place of a secondary seal was replaced with the thinner 2.38 mm (3/32") O-ring and a spacer to reduce the damping effect of the O-ring on the primary ring. Those changes were made to obtain a seal capable of operating in the dynamically unstable region of operation (See Figure 4) at the speed range available on the test rig.

PREPARATION OF THE SEAL FACES

The flat faced primary rings for the initial run with the Standard Type 8B Seal were production lapped and hand polished to a .38 μ-m (15 μ-in.) flatness per 6.35 mm (1/4") face width. Both mating sides of the common rotor were also production lapped flat and polished to less than 2 helium light bands .58 μ-m (23 μ-in.). Unless the rotor was damaged beyond repair during the test, it was reused in the subsequent test runs.

For the tests with the coned seals only, the surface on the stationary primary ring had a cone, the other mating surface on the rotor was flat.

Convex coning on the seal ring was produced on Crane Packing Company's Lapmaster Model 12 lapping machine with the concave lapping plate. The set up that produced 2.8 to 3.8 μ-m (110 to 150 μ-in.) cone height on the tested seals is a result of many trials and it is reproduced in Figure 11. Boron Carbide No. 3600 lapping compound with the average particle size of .4 microns (15 micro inches) was used for lapping. Usually the seal ring was lapped 10 to 15 minutes and then the slope of the seal face was measured on the Talysurf Model 4 apparatus. This procedure was then repeated until the desired

slope on the seal primary ring was obtained.

The cone height was measured as an axial distance between the highest and lowest intersecting point of the straight profile line with the face OD and ID lines. The coning angle can then be expressed as a function of the cone height and the seal face width.

EXPERIMENTAL EQUIPMENT

An existing test rig (see photograph in Figure 12) with a new oil circulating loop and added instrumentation was used for the testing. The housing and mounting of the seals are shown in Figure 13.

A rotating seat, common to both front and rear seals, was rigidly mounted on the shaft using an adaptor. The spindle shaft was driven through the set of Poly-V pulleys by the 15 hp DC variable speed motor. The inner housing had freedom of motion to allow measurement of the friction torque of both seals.

The fluid circulating loop with the auxiliary equipment is schematically shown in Figure 14. A centrifugal pump was used to circulate Shell Turbo 46 Oil through the seal cavity and the heat exchanger. Oil leakage was replenished by the piston pump. The pressure in the system was maintained by using a piston type hydraulic accumulator with pressurized air on one side.

In the testing with the modified coned Type 8B Seal, balanced to 51.3%, the centrifugal oil pump was replaced with a gear pump of lower volumetric capacity, but of higher pressure rating which eliminated need for the piston pump. Tap water was used in the heat exchanger and in the circulating pump for cooling.

A list of all measured variables and measuring instruments is given in Table 2. A photograph of the test instrumentation is in Figure 15.

Test Rig Performance Data and Specifications

Rig Shaft Speed: Variable from 0 to 8000 RPM with pulley ratio 3.11

Tested Speeds: 1800, 3600, 5400, and 8000 RPM

Tested Pressure: 0 to 2758 kPa (400 psig)

Rig Maximum Pressure: 3447 kPa (500 psig) in the seal cavity

Rig Maximum Temperature: 121°C (250°F)

Fluid Circulation with the Centrifugal Pump: 11.4 liters/minute (3 GPM)
with the Gear Pump: 7.6 liters/minute (2 GPM)

Fluid Used in the Test: Shell Turbo 46 Oil, Viscosity in SSU, 223 at 38°C (100°F), 48 at 99°C (210°F), specific gravity 29.5° API (=.8789 g/cm^3 at 15.6°C (60°F)).

Motor: 15 HP, 220 Vac., 3 PH, DC variable from 0 to 2500 RPM

Centrifugal Circulating Pump: "Corcoran", made on special order per drawing D-208177

Gear Pump: Double A, Model B1.5

Piston Pump: Haskel AM35C, 2" Stroke

Spindle: Whitnon Model D693 with Air Mist Lubrication

Material: Pod Cylinder, Housing, and Seal Adaptors - Stainless Steel

Connecting Lines: Rigid - 1/2" OD x .035" wall, 316 SS Tubing
Flexible - 1/2" ID, Synflex #3030 Hose

Data Acquisition System

Acquisition of data was subject to stringent speed requirements. The analysis of the seal ring dynamics required at least one acquisition every 30 degree turn of the shaft. It was established that a minimum of five measures of individual ring displacements is needed to define the mutual position of the stationary and rotating seal rings. That, at the maximum shaft speed of 8000 rpm, translated into an acquisition rate of at least 8000 measurements per second, 125 μs per measurement.

To satisfy the above rate of data acquisition, a system with accurate, yet fast, analog-to-digital converter had to be chosen. Since nothing reasonably priced seemed to be available, the system was put together from individual components and its heart was Burr-Brown's 12 bit successive approximation A/D converter MP32BG. It was made part of a small microcomputer system, where the controlling unit was Texas Instrument's TM990/189 board with 16 bit TMS9980A microprocessor. To save the generated measurements, the RAM memory was increased to the full extent of its memory field (total available for data - 8192 bytes). In order that this data could be analyzed, a rudi-

mentary GPIB interface was simulated on TM990/189 with 8 data lines and control lines necessary for three wire handshakes. That made it possible to transfer the data from the TM990/189 system to the Hewlett Packard's HP-85 desktop microcomputer. Thereafter, the data could be conveniently stored or cartridge tapes for later analysis. Further, its printer and the HP7225A plotter peripheral made it possible to provide a permanent record of the data and products of data analysis.

The final speed of acquisition of this system turned out to be almost exactly 100 μs per measurement. This was split half and half between A/D conversion time (50 μs) and speed-optimized machine code written acquisition program (50 μs). This rate of acquisition was constant, yielding 15 acquisitions per shaft turn at 8000 rpm, 22 at 5400 rpm, and 66 acquisitions/rev. at 1800 rpm. Five measurement channels of this system were sensing DC voltage on output terminals of Kaman's eddy current system described later in a chapter on Displacement Measurement. Schematic of the whole system is illustrated in Figure 16.

Torque Sensing

The friction of the front and rear seal and in the pod cylinder bearings was measured. Force was transmitted through the restraining arm to a 0-445 Newton (0-100 lbs.) load cell. The point of contact between the arm and the load cell was 152.4 mm (6") distant from the center of the spindle shaft. The assembly is shown in Figure 17. The output from the load cell was recorded by a fast frequency response Gould Model 2400 Recorder.

During the 1800 rpm test run with the coned bellows type seal, the load cell became inoperative and the alternate strain gage beam arrangement was used. The response of the strain gage was slower than the response of the original load cell. After a repair, the load cell was reinstalled and used again.

Leakage Measurement

On the tests with the flat face seal, the leakage was small and was collected in graduated cylinders. They were placed below the end cover plate for the front seal and below the hose ended hole at the bottom of the rear end

plate for the rear seal. Leakage accumulation was recorded.

The same procedure, but with a larger graduated cylinder, was used on the tests with the coned face Type 8B and Type 15 Seals shown earlier.

To collect higher leakage and also to supply new oil into the system during the tests with the modified coned face seal (51.3% balance), the centrifugal oil circulating pump had to be replaced with the gear pump. A leakage draining hose with a valve was added to the front seal, which discharged the oil directly into the pump reservoir after the leakage was measured with the graduated container.

Displacement Measurement

Eddy current proximity probes manufactured by Kaman Sciences Corp. were mounted in threaded holes on a sleeve attached to the front seal adaptor. The brass sleeve was then inserted in the center of the front seal, bringing the probes close to the target ring pressed into the rotor and the target plate epoxied on the ID of the primary ring. The arrangement is illustrated in Figure 13. A digital volt meter was used to measure output of each probe while positioning the probe within the measuring range.

Initially eight probes were used to sense the seal motion, but three probes sensing the radial displacement were removed since the data was not needed for the analysis. Relative location of the probes is shown in Figure 18.

Two probes (#1 and #5) placed 180° apart sensed the axial movement of the rotating mating ring (rotor); the remaining three probes (#2, #3, and #4), placed 90° apart, sensed the axial movement of the flexibly mounted stationary primary ring (stator). The analog output from these probes was converted into the digital data, printed out in the form of displacement vs. time graph and then stored on the magnetic data tape cartridge using TM990/189 microprocessor and the HP-85 desktop computer. Part of the typical output from the computer with the added distance and time scales is shown in Figure 19. The large spikes on Traces #1 and #5 (Figure 19) were generated by a groove on the rotor made for the timing purposes; other irregular spikes of higher frequency and small amplitude are due to electrical noise.

The time duration of one recording was determined by counting the number

of large spikes and comparing it to the speed at which the seal is operating. The recorded time interval was thus .42 seconds long. One complete data acquisition run, i.e. the A/D conversion, data transmission to the HP-85, printing and storing the data on magnetic tape, took approximately 17 minutes.

The output of the probes was also supplied into the dual beam oscilloscope for a direct observation of the seal movement. Photographs on Figure 20 show the contacting seal under the stable conditions.

Calibration of the probes was done on a fixture using a micrometer head with the smallest graduation being .1 μ-m (= 4 microinches) to measure the target distance from the sensors. Signal voltage, which is proportional to the largest distance, was measured on a 4-1/2 digit voltmeter. Zero output was set at the target offset distance of 50 μ-m (= 1969 μ-in.). Output was adjusted to 2 volts at 100 μ-m displacement from the offset position. Linearity was less than 1 μ-m (40 μ-in.) within the 0 to 150 μ-m measuring range and less than 2 μ-m (80 μ-in.) within the 0 to 350 μ-m range. Most of the testing was done within the 0 to 150 μ-m range. The probes were calibrated at the 27°C (80°F) ambient temperature. Higher target and probe mounting sleeve temperature caused a shift in the sensor outputs, therefore, a calibration graph for each probe at the higher test temperature was developed and the output shift was compensated for. During the dynamic run, the test temperature of the stator target was several degrees less than the temperature measured at the seal face. The temperature of the probes mounting sleeve, measured approximately 10 mm (.39 in) away from the probe No. 3, was 10 to 30°C (18 to 54°F) lower than the temperature of the target. During the static measurements, both temperatures were the same as ambient temperature. The sensors and their oscilator-demodulator units broke down several times during the testing. Some failures were of electrical origin, some were caused by axial thermal expansion when the probe tip touched the rotating target. This was later avoided by inserting the probe sleeve with the probes inside the seal for a short period of time only to take a reading at the given test conditions.

To reduce a low frequency electrical noise resulting from interference of electromagnetic fields of the adjacent probes, the oscilator demodulator units were synchronized by a circuit modification in each unit. Also, isolation of

the sensors mounting sleeve and the grounding of the test pod housing reduced the electrical noise.

TESTING AND DISCUSSION

Seal Installation

Prior to assembly, the seal components were cleaned with a solvent and then ultrasonically in detergent. The seal was assembled and the thermocouples were epoxied to the primary rings.

Design of the rig required that the rear seal was installed first. Next, the rotor mounted on the shaft adaptor was secured in place by tightening the nut on the spindle shaft. The rotor axial runout (TIR) was measured with a dial indicator at the mean face diameter. If the runout was greater than .025 mm (.001"), the supporting back side of the rotor was shimmed until the runout was less than the above value. The front seal in assembly with the sleeve and the rig cover plate was then inserted into the seal cavity housing and the screws holding the cover plate were tightened. The probe mounting sleeve was positioned inside the front seal and individual probes were adjusted until they were within the measuring range. At the early stages of the testing, the sensors remained in the rig for most of the time. This required positioning the probes initially close to the maximum measuring range. This was done because the thermal expansion of the shaft brought the rotating target closer to the probes with the chance of touching and damaging the sensors. During the last test, the sleeve with the probes was kept at a safe distance and moved to within the measuring range only to take a reading. The initial static reading had to be taken then for each position and temperature.

Test Procedure

After closing the system, the piston pump was turned on filling the seal cavity and the connecting lines. Air was vented from the top of the seal cavity until the system was filled with oil and the piston pump was shut off.

A typical test started with taking of the displacement data under static conditions at pressures increasing up to 1379 kPa (200 psig) for the bellows type seal and up to 2758 kPa (400 psig) for the O-ring (pusher) type seal. The system was checked for leaks and the leakage from the seals measured.

The rotor axial runout was measured while turning the shaft by hand. The maximum and minimum readings were then taken using the dial indicator. The same measurements were also taken with the displacement probes #1 and #5 to verify a calibration of the probes.

The main pump circulating oil through the seal cavity was started for the dynamic test. The flow amounted to 11.35 liters/minute (3 gpm) when the centrifugal pump was used and 7.57 liters/minute (2 gpm) when the gear pump was installed in the system. Then the drive motor was energized and adjusted to give the required test speed on the seal shaft. The speed could be observed on the #4 channel of the Gould recorder and checked with a strobe light. Pressure in the seal cavity was increased by regulating air into the piston type accumulator until the required tested conditions were reached.

Duration of each test at a given pressure and speed was about 30 minutes. Data acquisition of the seal displacement, temperature, and torque recordings were taken at the end of this period when the oil temperature had stabilized. Leakage was also measured during this period. The procedure was repeated at higher pressures up to the maximum for the given seal. Then the speed was increased and the readings were taken again at the different pressures. A summary of the tests for each seal is shown in Table 3. The torque, leakage, and the face temperature of the tested seals were plotted against the pressure as shown in Figures 41 to 46 and Figures 52 to 61. The torque curves represent a sum of torque values for front and rear seals. The face temperature, as well as the displacement, was measured on the front seal only.

The oil circulating loop, as originally proposed, placed the seal cavity on the discharge line of the main oil pump and the heat exchanger on the suction line. Due to the head pressure of the pump, the minimum pressure in the seal cavity was 207 kPa (30 psig). To obtain 0 pressure in the seal cavity, the heat exchanger was placed on the discharge line of the main pump as it is shown in Figure 14. This arrangement was then used on tests with the bellows type seal and on the last test with the coned pusher type seal balanced to 51.3%.

Flat Face Seal, Standard Pusher Type 8B

The purpose of this test was to check the operation of the equipment and to establish baseline data for comparison. The seal was tested at pressures

of 207, 345, 689, 1034, 1379, and 2758 kPa (30, 50, 100, 150, 200, and 400 psig) and speeds of 1800, 3600, and 5400 rpm, which was the maximum speed of the rig at that time with the 355 mm (14") and 152 mm (6") diameter pulleys. Two identical seals were used on the front and rear sides, but the test readings were taken from the front seal only. Preventing the primary ring from rotation, was accomplished by eight circular dents on the ID of the retainer and the same number of mating notches on the primary ring OD, a standard design practice for this seal. A 3.175 mm (1/8") nominal diameter O-ring was in place of a secondary seal between the primary ring and the sleeve. The initial load on the primary ring was exerted by equally spaced compression type springs. The design data for this seal, as well as for other tested seals, is shown in Table 1.

The test started with a full complement of twelve springs, giving a total force of 320 newtons (72 lbs) on each seal head, but eight springs had to be removed to reduce the load on the 15 hp motor. The resulting spring force on the seal face was then 116.6 newtons (26.22 lbs.) for the front seal and 114.9 newtons (25.84 lbs.) for the rear seal at the seal working heights. When attempting to run at 8000 rpm with the 114 mm (4.5") driven pulley, the friction in the seal was enough to stall the motor and the test at the maximum speed was abandoned.

The Standard Type 8B is a contacting conventional seal where the hydraulic pressure and the spring load forces the mating surfaces into contact, creating a barrier against the pressurized fluid. The hydrostatic closing force amounted to 438.2 Newtons (98.5 lbs.) at 689.5 kPa (100 psig) and 1403 Newtons (315.4 lbs.) at 2758 kPa (400 psig) presuming a linear pressure distribution across the seal face (pressure gradient = .5). The torque and the face temperature produced by a rubbing action were subsequently highest among the tested seals and this seal could not be operated at the maximum rig speed of 8000 rpm without the stalling of the driving motor.

The face temperature was in excess of 149°C (300°F) when the seal was running at 5400 rpm. The wear on the carbon primary ring after only 20 hours of running can easily be seen in Figure 24. The ID location of the worn off material indicates that the seal face underwent a convex rotation due to the thermal expansion and that the 1.2 μ-m (50 μ-in.) waviness of the primary ring

(Figure 24) might also create some positive torque reducing hydrodynamic lift.

The leakage from this seal was more than ten times lower than from the comparable seal with the purposely lapped cone on its primary ring face. No leakage was observed at 1800 rpm up to 2068 kPa (300 psig); at 3600 and 5400 rpm, it ranged from 5 to 35 ml/hour. The displacement amplitude and frequency of the primary ring was same as that of the rotor, indicating on a pure axial translation motion without any phase shift between the stator and rotor.

Coned Face Pusher Type 8B Seal, 76.3% Balance

The objective of the coning was to allow the sealed liquid to form a lubricating film between the mating faces. This eliminated the material contact and reduced the friction losses, thus lowering the power requirements for the seal. The assembly and the design data of this seal are shown in Figure 7 and Table 1, respectively.

The front stationary primary ring was lapped to 2.7 μ-m (106 μ-in.) convex cone height per 6.33 mm (1/4") wide seal face, the rear seal was lapped to 3.04 μ-m (120 μ-in.) per same seal width. The same rotor used as a mating face from the previous testing with the flat face seal was relapped, polished, and used again. The spring force on the primary rings and the seal balance also remained the same. The only other change, besides the coning, was the method of holding the primary ring in the retainer. An unrestricted radial and axial movement of the primary ring is necessary for the ring to track the rotor and maintain a small clearance essential to proper operation of any non-contacting seal. This is not needed for a contacting seal where the friction in the dent type drive is insignificant in comparison to the closing force acting upon the primary ring. The holding of the primary ring in its retainer was, therefore, changed and a linkage type antirotation lock described below, was then used.

One end of each of the three links was mounted on a retainer pin, perpendicular to the seal centerline. The other end was rotatably attached to the disc. The springs between the retainer and the disc with the three pins supported the primary ring preventing it from rotation, but at the same time allowing it to move axially without the friction between the primary ring and

the retainer. The only direct external friction force acting upon the primary ring was then from the secondary seal, a 3.175 mm (1/8") nominal diameter O-ring.

The mating face materials on both seals were made out of tungsten carbide. Due to the lower power consumption of this seal, the rig could be operated at its maximum speed of 8000 rpm. The tests were run twice; once with the four axial probes and then repeated again with the five probes located as shown in Figure 18.

Better lubrication of the seal faces introduced by the coning of the primary ring was sufficient enough to reduce the torque produced by the seal and lower the seal face temperature. The recorded peak torque for this seal, shown in Figure 42, was an average 47% lower at 1800 rpm, 40% lower at 3600 rpm, and nearly equal, only 3% lower, at 5400 rpm than the torque of the flat face seal shown in Figure 41.

Measurements also indicated that the torque at 5400 rpm was 54% higher than the torque at 8000 rpm. This is assumed to be due to the phase change of the liquid because of the high shearing of the fluid in the interfacial film. Resulting reduction of the shearing area and change of viscosity of the oil caused lower torque reading at 8000 rpm. Still, more heat was generated at this speed and the measured temperature was higher than at 5400 rpm. Further investigation was not attempted since it was not within the scope of this project. At the end of the testing, an attempt was made to operate the seal at 0 kPa (0 psig) by shutting down the oil circulating pump temporarily at the shaft speed of 5400 rpm. After that, the seal face temperature quickly rose and within 30 seconds the rotor had cracked. Upon disassembly, the wear tracks and the heat checking marks were visible on the face ID of the seal primary ring confirming that the contact did occur. Photographs of the seal faces are shown in Figure 21.

The penalty for a lower power consumption of this seal was an increase in the leakage. At 1800 rpm and 2758 kPa (400 psig) pressure, the leakage was 14 times higher, but with the increased speed the difference was less. At 5400 rpm, the leakage was only 9 times higher than for the flat face seal. Also, the face temperatures did not change with the pressure and remained 28 to 50°C (50 to 90°F) lower (See Figures 58 and 59).

It is reasonable to expect that due to the face wear, the leakage of the flat face seal would increase with time while the leakage of the coned seal would remain the same, giving it a more favorable ratio in the endurance test.

The rotor axial runout (TIR) measured at the probes diameter was .01 mm (.0004 in.) which corresponds to the face axial angular misalignment of 164 μ rad. The primary ring again tracked synchronously the rotor axial runout, but in contrast to the flat face seal where no phase shift between the stator and the rotor occured, coned primary ring was lagging in tracking the angular misalignment of the rotor. The amount of lag or phase shift was variable with time.

Typical displacement recording for this seal is shown in Figure 62. The effect of the operating temperature on the calibration of the displacement probes had prevented the measuring of the face separation accurately at most of the tested pressures and speeds.

Coned Seal, Bellows Type

The front and rear seals of this type (Crane Packing Company's Type 15 Seal) are shown in Figures 8 and 9. Both seals were equipped with the coned face tungsten carbide inserts as a stationary primary ring. Because of the pressure limitation of the metal bellows, the maximum test pressure was lowered to 1379 kPa (200 psig). The seals also required several design changes described below to eliminate the damage to the seal faces occuring at the beginning of the testing.

a. The Standard Type 15 Seal initially had high spring force. Both front and rear seals had over 445 Newtons (100 lbs.) load at the bellows working height. The load was reduced in steps down to 89 Newtons (20 lbs.) by machining off the back side of the seal adaptor.

b. The designed seal balance for 6.35 mm (1/4") wide faces and for 92.71 mm (3.650") balance diameter was 75%. Measurements showed the seal balance diameter to be 91.11 mm (3.587") at 345 kPa (50 psig) giving a balance ratio of 87% and a high load on the seal face. The face OD was, therefore, reduced to 97.28 mm (3.830")

with the resulting balance 79% at 345 kPa (50 psig) and 68% at 1379 kPa (200 psig).

c. Mounting of the seal primary ring (insert) in the bellows adapter had to be changed also. During the first tests, the tungsten carbide face insert was rigidly mounted in 316 SS adapter using a structural adhesive. Elevated temperatures during the test and the subsequent thermal expansion of the bellows adapter then caused the seal face to rotate with the adapter to such an extent that the 2.65 μ-m (105 μ-in.) convex coning of the insert face had changed into the concave coning. The wear track was observed on the OD of the face instead of on the ID as could be expected. The front seal was more affected than the rear seal because of more massive adapter necessary to hold the target plate for the displacement probes. Profile measurements of the oven heated insert and adapter assembly showed that the face was 19 μ-m (745 μ-in.) concave at 117°C (248°F), flat at 49°C (120°F) and 2.65 μ-m (105 μ-in.) convex at the ambient temperature of 29°C (86°F). The inserts were then removed from the adapter and both were reworked. Two pins, O-ring, and reducing the mass of the adapter as shown in Figures 8 and 9 were used to eliminate the temperature effect and allow the free expansion of the inserts.

d. During the initial test runs with the Type 15 Seal, the thermal expansion of the brass ring press fitted and epoxied in the rotor also caused cracking of the rotor. The ring, which was used as a rotor target for the displacement measurement, was split in one place compensating for the expansion at higher temperature.

Initially the coning for both front and rear seal was nearly the same, 2.54 μ-m (100 μ-in.) and 3 μ-m (120 μ-in.). But after the run at 0 kPA (0 psig), the face of the front seal was damaged by a contact between the rotor and the stator. The cone height on the 12.7 mm (.5 in.) wide front seal face

was, therefore, increased to 5.6 μ-m (220 μ-in.) to increase the face separation and no damage or measurable wear was observed on the seal faces thereafter as shown in Figure 22.

Due to the lower initial spring force, the recorded torque at the test run at 0 kPa (0 psig) of the bellows seal was lower than the both previously tested flat face and coned face pusher type seals. At 1379 kPa (200 psig), the bellows type seal produced torque on average 43% lower than the flat face seal; this was about the same as with the coned face pusher type seal.

In addition to the torque peaks produced during each shaft revolution, there are other maximums and minimums of low frequency and inversely proportional to the shaft speed. For example, in Figure 49 the time interval at 5400 rpm is 1/2 second between the highs with the amplitude of 3.4 N/meter (2.5 ft. lbs.) which is 31% of the peak torque.

The leakage from the front and rear seals in this case was not averaged as in other tests because of the higher cone height on the front seal face. The rear seal leaked about half of the amount of fluid as the front seal and this was only slightly more than the leakage from the flat face seal.

The face temperature plotted against the system pressure shown in Figure 60 was measured on the front seal only. In comparison with the other pusher type coned seal, and depending on the shaft speed, the face temperature of the bellows seal was up to 6° to 22°C (10° to 40°F) higher at the 1379 kPa (200 psig) pressure. This and also the lower leakage could be attributed to the profile of the cone on the seal face. The lapping of the bellows primary ring produced a rounded profile with a variable slope angle across the face width. The cone angle was smaller at the face ID and larger at the face OD. The lapping of the pusher type primary ring resulted in less rounded profile line with the slope angle nearly constant.

The typical displacement traces for this seal are shown in Figure 63. The irregular shape of Traces #1 and #5 around the timing spikes was caused by the distortion of the split rotor target, which was replaced in the next testing again with the solid ring, but of a smaller contact area.

Rotor axial runout (TIR) in this test amounted to .025 mm (.001 in.) at the probes diameter. The tracking, i.e. phase shift or relative misalignment

of the rotor and stator was again variable with time and can be presented by a harmonic wave form of constant amplitude and frequency synchronous with the shaft revolutions. The phase lag amplitude was lower than in the tests with coned pusher type seals because of the smaller mass of the bellows type primary ring. A graph showing the phase shift of this seal is on Figure 66, the maximum amplitude measured was 37 degrees.

Coned Face, Pusher Type 8B Seal, 51.3% Balance

The purpose of the last test was to operate the seal in the unstable region of the stability maps as shown in Figure 4. The coned face pusher Type 8B Seal was selected over the Bellows Type 15 Seal because the greater mass of the primary ring and about seven times smaller spring rate would make the seal more susceptible to reaching the unstable region.

The main disadvantage was the necessity of using an O-ring in place of the secondary seal and its damping effect on the movements of the primary ring. This was hoped to be reduced by replacing the 3.175 mm (1/8") cross section O-ring by a smaller 2.38 mm (3/32") cross section slightly stretched over the sealing diameter of the sleeve. A spacer supported on a disc held the O-ring tight against a step on the ID of the primary ring. The assembly of this seal is shown in Figure 10. Other changes in the design of the seal involved:

a. Reducing the balance to 51.3% by grinding off the seal face OD to allow the seal to open.
b. Reducing the spring force to 8.9 Newtons (2 lbs.) by using 6 springs in the seal retainer.
c. Decreasing the height of the cone on the primary ring face to .5 µ-m (20 micro-inches) per 3.175 mm (1/8") face width.
d. Drilling of additional holes in the flange to allow adjustment of the spring force with the seal installed in the rig.
e. Modifying the probe brass target ring in the rotor to eliminate its thermal distortion. Several targets were tried, but none of them was completely free of distortion. Preferred solution would be sensing the rotor

displacement directly on its front side, but this would require some time consuming changes on the test rig and was not attempted.

The test seal was again on the front side, on the rear side was installed a contacting flat face carbon primary ring balanced to 56.5% to reduce the friction and to limit the leakage. But the carbon primary ring was later replaced with the cone faced ring identical to the ring on the front side in order to balance the axial forces on the rotor and to reduce the temperature of the rotor.

Static test at pressures up to 2758 kPa (400 psig) was run at the beginning and the face separation was directly measured by comparing the change in the displacement of Probes #2 and #4 (primary ring, stator) with that of Probes #1 and #5 (rotor). At the same time, the leakage was also measured.

For the dynamic run, several test points were selected from the stability map (Figure 4), in the stable and one in the unstable region to determine if the seal follows the theory described in the chapter "Analytical Background".

The displacement traces of this seal are shown in Figures 63 and 64, where the traces No. 2, 3, and 4 represent the axial movement of the flexibly mounted stationary primary ring as it tracks the angular misalignment of the rotor. The axial runout of the rotor was .009 mm (.00035 in.) at the probes diameter. The phase shift between the theoretical location of the stator and its actual position as detected by the probes is shown in a time graph in Figure 67. The distortion of the harmonic waveform is obvious indicating a beginning of the transition operation, which would eventually result in a contact between the stator and rotor if the shaft speed would increase further or if it would not be for a restriction in the axial movement of the stator. It is possible to say that the primary ring of this seal was not completely free to move and that it was limited in movement by the friction and flexing of the O-ring stretched over the sleeve and by the friction resulting from the contact between the primary ring and the sleeve. The sticking of the primary ring was observed several times during the static and dynamic tests and although the surface of the sleeve was hand lapped and burnished with PTFE the sticking could not be completely eliminated.

The timing spikes are not shown on Traces #1 and #5 because of solid target ring without the groove was used in the rotor. The leakage of this seal was heavy, but in contrast to seals tested previously, the leakage was indirectly proportional to the shaft speed, i.e. was highest at the speed of 1800 rpm and lowest at the maximum speed of 8000 rpm. When compared with the coned face pusher type seal balanced to 76.3%, the leakage was higher in order of 10^3 at 1800 rpm, 1034 kPa (150 psig) pressure, in order of 10^2 at 3600 rpm, 54 times higher at 5400 rpm and only 13.5 times at 8000 rpm and 2068 kPa (300 psig).

Obviously, the face temperature measured on this seal and plotted on Figure 58 was the lowest of all the tested seals because of the highest flow of cooling liquid through the seal interface. The face temperature at 5400 rpm was affected by a higher temperature of the surrounding test rig parts. After the test, conditions of the seal mating parts in Figure 23 showed the wear tracks of the contacting rear seal and not even a trace of wear on the faces of the non-contacting seal.

Analysis of Performance

The experimental test results indicate that the performance of the coned face seals was in agreement with the operation predicted by the calculation. Stable operation was attained under all tested conditions. The test run at 8000 rpm and 2068 kPa (300 psig) pressure with a pusher type seal balanced to 51.3% was expected to be unstable as per Figure 4, with the contact between the rotor and stator, but due to the restriction in motion of the primary ring no contact was detected. The primary ring synchronously tracked the rotor angular misalignment and a time dependent phase shift existed between the flexibly mounted stationary primary ring and the rotating mating ring.

The narrow face design of the primary ring made this seal sensitive to a change in balance diameter. For example, a reduction of the balance diameter by only .025 mm (.001 in.) would bring the 8000 rpm, 2068 kPa (300 psig) test point way into the stable region of the stability map on Figure 4.

The seal leakage for parallel faces calculated from the equation (6) with the effect of convergent coning included was in order of 10^2 smaller than the measured dynamic leakage. But, the amount of leakage under the dynamic

conditions is governed besides other factors also by the instantaneous mutual position of the stator and the rotor. If the phase shift between them is small, as in the test with the bellows type seal, then the difference in the fluid film thickness around the seal face circumference is also small and the leakage is close to the calculated value for parallel faces (eq. 6). When the phase shift and its amplitude are large as it was documented in the tests with the coned pusher type seal, the difference in the film circumferential thickness is greater and the leakage increases.

The static measurements of the face separation of the pusher type seal showed that as the pressure gradually increased, the primary ring moved away from the rotor in irregular jumps rather than in smooth continuous increases, which would be more desirable. When, still under the static conditions, the pressure became constant, the primary ring moved back and the face clearance and the leakage decreased. Depending on the pressure and, therefore, on the thickness of the film, this could be observed for a period of more than 30 minutes. The axial movement of the primary ring was not uniform over the circumference of the ring. Some sections had moved more than the others resulting in the tilting of the primary ring face in relation to the mating surface. Leakage through such non-parallel gap is more than the calculated leakage through the parallel gap with the effect of coning taken into consideration. This points out the need for solving and predicting damping effects of elastomeric secondary seal on primary ring, to assure a free movement of the primary ring and to provide a circumferentially uniform support for the primary ring. In this testing, softer springs with lower spring constant would be required. To reduce the high leakage of the coned face pusher type seal, the tracking of the rotor by the stator would have to be improved, i.e. phase shift held to a minimum by reducing the mass inertia of the primary ring.

From the stability maps, it is apparent that for all the tested seals, the speed within its practical limits has much less effect on inducing unstable operation than the pressure. Non-contacting seals are, therefore, capable of operating at speeds higher than comparable contacting seals as was shown in this report. Because of its design characteristics, Crane Packing's commer-

cial flat face Type 8B Seal would operate in the stable manner, i.e. synchronously tracked the rotor, if it was forced for some reason to run as a non-contacting seal.

CONCLUDING REMARKS

The conventional flat face seal commercially available, with 88.90 mm (3.5") mean face diameter was compared with three coned face seals of the same size to determine energy savings by providing positive interface lubrication by a means of convex type cone on the face of the stationary primary ring. The seal torque, leakage, face temperature, and the axial movement of the seal mating parts were measured and compared. The results of this testing could be summarized as follows:

1. Torque produced at the seal interface was reduced by 42% when the primary ring profile was changed from flat to a convergent cone.
2. The leakage increased with the cone height at a given face width. When the seal balance and the spring force were reduced, the leakage rates became excessive for practical purposes.
3. Face temperatures were 33°C (60°F) to 56°C (140°F) lower for the cone face seals due to face separation and better cooling resulting from the increased flow between the seal mating parts.
4. Wear on the tungsten carbide face of the coned seals during short duration (15 to 20 hours) test runs was greatly reduced. No wear tracks could be observed on the coned seal balanced to 51.3% and only several microscopic wear tracks were visible on the face of the other two coned seals. The Standard Type 8B Seal experienced wear amounting to 2.5 μ-m (100 μ-in.) on the ID of the flat face carbon primary ring.
5. In all tested seals, the flexibly mounted stationary primary ring synchronously tracked the angular misalignment (axial runout) of the rotor indicating a

stable operation. A time dependent phase shift was detected in motion of the coned face seals while the flat face contacting seal experienced a pure axial translation motion without any lag between the stator and the rotor. During the tests with the pusher type seal balanced to 51.3%, the maximum amplitude of the phase shift amounted to 290°. Because of lower inertia of the primary ring, the maximum amplitude in tracking motion of the bellows type seal was only 37°. The damping effect of the secondary seal and the possible contact between the primary ring and the sleeve prevented the cone seal balanced to 51.3% from reaching the unstable region.

ACKNOWLEDGEMENTS

The testing described here was carried out at the Crane Packing Company's Research and Mechanical Laboratory during the year of 1981 with partial support under Contract NAS3-22128 from NASA-Lewis Research Center, Cleveland, Ohio. Acknowledgement is also expressed to Mr. Terry Strand and Mr. Nyunt A. Hou.

APPENDIX 1

The equations introduced in the "Analytical Background" were incorporated into a computer program written in BASIC programming language for use on a Hewlett-Packard desktop computer HP-85. To use the program (as listed) on other computers, may require some modifications. Program flowchart is shown on the following page; complete listing of program and sample calculations appear in this Appendix. Comment statements indicated by (!) in the program list, give detailed description of the program. Seal input data should be entered in S.I units, i.e. seal dimensions in meters, pressure in kPa, force in Newtons, etc. It should be noted that if the seal clearance Co is negative, then the seal is of a contacting type and the equations derived here do not apply.

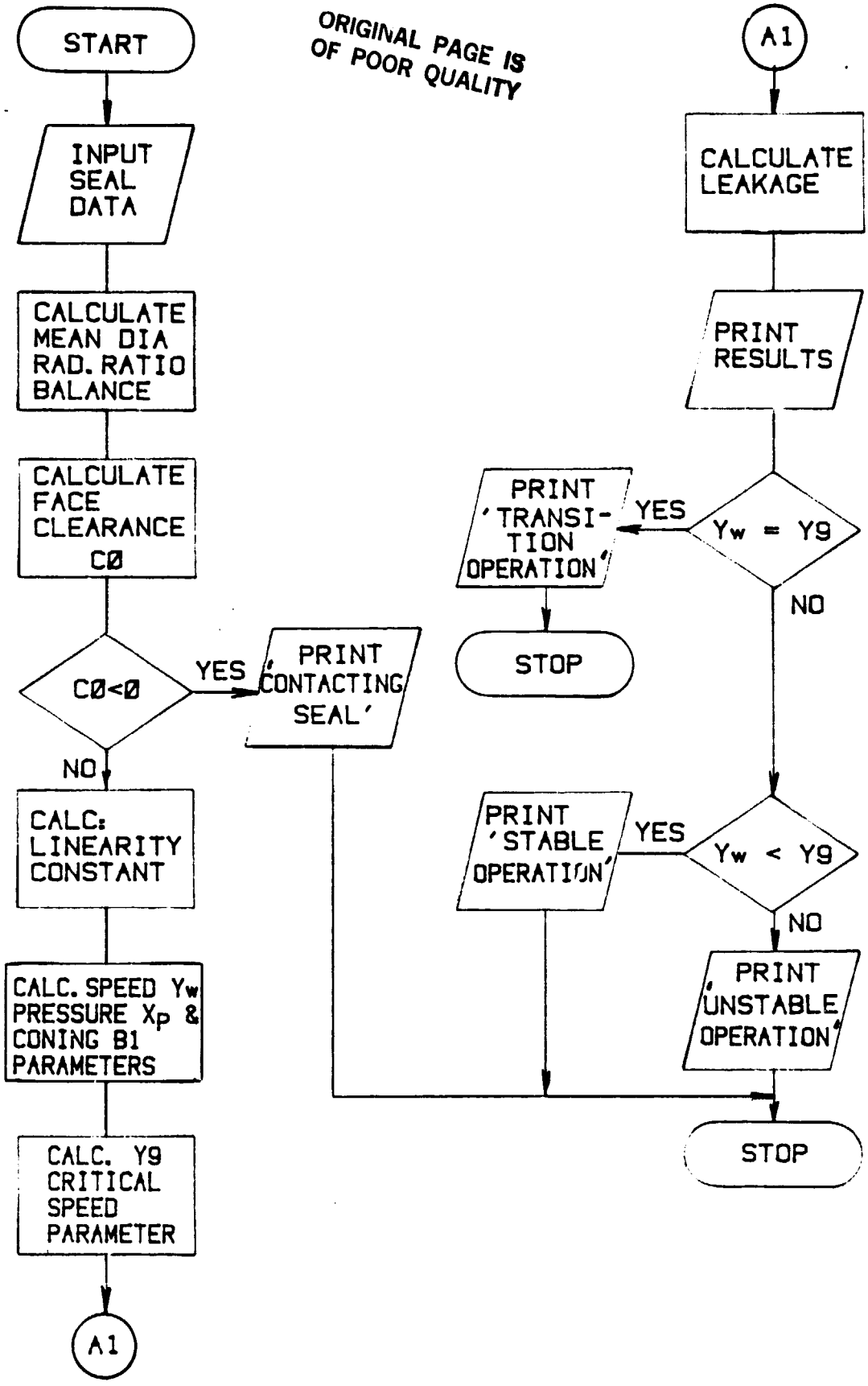

PROGRAM FLOWCHART

COMPUTER PROGRAM:


```
10 ! CPPARM
20 ! ******
30 ! EXPLANATION:
40 ! FOR A GIVEN CONED FACE SEA
   L PROGRAM CALCULATES:1)SPEED
    PARAMETER Yw 2)PRESSURE PAR
   AMETER Xp"
50 ! 3)CONING PARAMETER beta 4)
   CRITICAL SPEED PARAMETER Ycr
   it AT THE PRESSURE PARAMETER
    Xcrit=Xp
60 ! 5)LINEARITY CONSTANT a 6)L
   EAKAGE FOR PARALLEL FACES 7)
   SEAL BALANCE 8)RADIUS RATIO
   Ri/Ro
70 ! 9)FACE CLEARANCE C0 IN mic
   rometers(m-m) AND microinche
   s(m-in).BY COMPARING Yw AND
   Ycrit
80 ! SEAL OPERATION CAN BE DETE
   RMINED. IF Yw<Ycrit OPERATIO
   N IS STABLE, IF Yw>Ycrit OPE
   RATION
90 ! IS UNSTABLE. AT Yw=Ycrit T
   HE OPERATION IS IN TRANSITIO
   N MODE
100 DISP "ENTER SEAL DATA IN S.I
    .UNITS:   1-SPRING FORCE Fs(
    N) 2-SPRING   CONSTANT K1(Nm
    /S^2)"
110 DISP "3-FACE OUTSIDE RADIUS
    Ro(m) "
120 DISP "4-FACE INSIDE RADIUS R
    i(m)       5-CONE HEIGHT H(m)
     6-BALANCE"
130 DISP "RADIUS Rb(m) 7-RADIUS
    OF SPRING LOCATION Rsp(m) 8-
    RADIUS OF"
140 DISP "GYRATION Rg(m) 9-RING
    MASS m"
150 DISP "10-PRESSURE dP(kPA) 11
    -SPEED    N(RPM) 12-VISCOSIT
    Y M1"
160 DISP "ENTER Fs,K1,Ro,Ri,H,Rb
    ,Rsp,Rg,m,dP,N,M1"
170 INPUT F0,K1,R0,R1,H,R5,R2,R3
    ,M,P1,N,M1
180 !
190 ! CALCULATION
200 P=P1/10^-3 ! kPA INTO Pascal
    s
210 R4=(R0+R1)/2 ! MEAN RADIUS
220 A4=R1/R0 ! RADIUS RATIO
230 B=(R0^2-R5^2)/(R0^2-R1^2) !
    SEAL BALANCE
240 W=2*PI*N/60 ! ANGULAR SPEED
250 A0=2*K1 ! PARTIAL RESULT
260 A1=2*PI*R4*(R0-R1)*P ! PARTI
    AL RESULT
270 A2=2*F0+K1*H+2*A1*(B-.5) ! P
    ARTIAL RESULT
280 A3=F0*H-A1*(1-B)*H ! PARTIAL
     RESULT
290 IF A2^2-4*A0*A3<0 THEN PRINT
     "NEGATIVE SQUARE,CHECK THE
    ENTRY DATA" @ GOTO 680
300 C0=(-A2+SQR(A2^2-4*A0*A3))/2
    /A0 ! FACE CLEARANCE
310 IF C0<=0 THEN GOTO 650 ! CON
    TACTING SEAL
320 A5=H/C0
330 S=-(8*PI*A4^2*(1-A4)^2*(1-A4
    /(1-A4)*A5)/(2+A5)^2) ! LINE
    ARITY CONSTANT
340 Y=(R3/R2)^2*(M*W^2/K1) ! SPE
    ED PARAMETER
350 X=P*R0^2/K1/C0*(R4/R5)^2 ! P
    RESSURE PARAMETER
360 B1=H/(R0-R1)*R0/C0 ! CONING
    PARAMETER
370 S9=-(8*PI*A4^2*(1-A4)^2*((1-
    B1*A4)/(2+B1*(1-A4))^2))
380 Y9=S9*X+4 ! CRITICAL SPEED P
    ARAMETER
390 Q=PI*P*C0^3/(6*M1)*R4/(R0-R1
    )*(1+1.5*H/C0) ! LEAKAGE
400 ! END OF CALCULATION
410 !
420 ! ENTERED DATA ARE PRINTED O
    UT
430 PRINT "          ENTERED DATA
    :"
440 PRINT "Fs=";F0;"K1=";K1;"Ro=
    ";R0;"Ri=";R1;"H=";H;"Rb=";R
    5;"Rsp=";R2;"Rg=";R3;"m=";M
450 PRINT "PRESSURE=";P1;"kPA ="
    ;IP(P1*1.45037*10^-1+.5);"PS
    IG"
460 PRINT "SPEED=";N;"RPM visc="
    ;M1
470 PRINT
480 ! RESULTS ARE PRINTED OUT:
490 PRINT "          RESULTS:"
500 PRINT "Balanc=";FNR2(B*100);
    "%";" Ri/Ro=";FNR2(A4)
510 PRINT "C0=";FNR2(C0*10^6);"m
    -m = ";FNR2(C0*10^6*39.37);"
    m-in"
520 PRINT "Xp=";IP(X);"      Yw=
    ";FNR3(Y)
530 PRINT "a =";FNR6(S);"    bet
    a=";FNR3(B1)
540 PRINT "Xcrit=";IP(X);"   Ycr
    it=";FNR2(Y9)
550 PRINT "LEAKAGE=";FNR6(Q*10^6
    *60);"ml/HOUR"
560 IF Y=Y9 THEN PRINT "TRANSIT
    OPERATION"
570 IF Y<Y9 THEN PRINT "STABLE O
    PRATION" ELSE PRINT "UNSTABL
    E OPRATION"
```

CONTINUED...

```
580 PRINT USING "////"
590 !
600 ! ROUNDING FUNCTIONS LISTED:
610 DEF FNR1(N) = INT(N*10^1+.5)
    /10^1
620 DEF FNR2(N) = INT(N*10^2+.5)
    /10^2
630 DEF FNR3(N) = INT(N*10^3+.5)
    /10^3
640 DEF FNR6(N) = INT(N*10^6+.5)
    /10^6
650 IF C0>0 THEN GOTO 680
660 BEEP 114,11.4 @ DISP "CONTAC
    TING SEAL - REDUCE FACE LOAD
    "
670 ! J.Sehnal,DEC-20-1981
680 END
```

END OF PROGRAM.

SAMPLE OUTPUT #1

```
          ENTERED DATA
Fs= 8.9 K1= 15967 Ro= .04445 Ri=
  .041275 H= .00000041 Rb=
   04285 Rsp= .048 Rg= .0474 m=
  1147
PRESSURE= 2068 kPA = 300 PSIG
SPEED= 8000 RPM visc= .008184

             RESULTS:
Balanc= 51.32 % Ri/Ro= .93
C0= 5.4 m-m =  212.71 m-in
Xp= 47390        Yw= 4.916
a =-.000346      beta= 1.062
Xcrit= 47390     Ycrit=-12.42
LEAKAGE= 18.826944 ml/HOUR
UNSTABLE OPRATION
```

SAMPLE OUTPUT #2

```
          ENTERED DATA:
Fs= 8.9 K1= 15967 Ro= .04445 Ri=
  .041275 H= .00000046 Rb=
  .04285 Rsp= .048 Pg= .0474 m=
   1147
PRESSURE= 1034 kPA = 150 PSIG
SPEED= 8000 RPM visc= .008184

             RESULTS:
Balanc= 51.32 % Ri/Ro= .93
C0= 4.7 m-m =  184.87 m-in
Xp= 27264        Yw= 4.916
a = .00687     beta= 1.371
Xcrit= 27264     Ycrit= 191.31
LEAKAGE= 6.363429 ml/HOUR
STABLE OPRATION
```

APPENDIX 2

Units of measure used in the report.

Variable	SI Unit (Metric System)		U.S. Customary Unit (English System)
Pressure	Kilopascale (kPa)	=	.1449 Pounds per Square Inch (psi)
Length	Micrometer (μ-m)	=	39.37 Microinch (μ-in)
Force	Newton (N)	=	.22481 Pound-Force (lbs)
Torque	Newton-Meter (Nm)	=	1.355818 Pound-Force-Foot (ft-lbs)
Temperature	^{o}Kelvin (^{o}K)		^{o}Fahrenheit = 1.8 x ^{o}K - 459.7 (^{o}F)
Volume	Liters (l)	=	.26417 gallons (Gal)

REFERENCES

1. Pinkus, O., and Wilcock, D. F., Strategy for Energy Conservation through Technology, ASME Research Committee on Lubrication, Department of Energy (formerly ERDA) Sponsored Report, 1977.

2. Stair, W. K. and Ludwig, L. P., Energy Conservation through Sealing Technology, Lubrication Engineering, Vol. 34, No. 11, November 1978, pp 618-624.

3. Ludwig, L. P., Face Seal Lubrication, I Proposed and Published Models, NASA TN D-8101, April 1976.

4. Ludwig, L. P. and Allen, G. P., Face Seal Lubrication II Theory of Response to Angular Misalignment, NASA TN D-8102, March 1976.

5. Ludwig, L. P. and Greiner, H. F., Designing Mechanical Face Seals for Improved Performance - I Basic Configurations, Mechanical Engineering, Nov. 1978, pp 38 - 46.

6. Ludwig, L. P. and Greiner, H. F., Designing Mechanical Face Seals for Improved Performance - II Lubrication, Mechanical Engineering, December 1978, pp 18 - 23.

7. Etsion, I., Hydrodynamic Effects in a Misaligned Radial Face Seal, ASME, Journal of Lub. Tech., Vol. 101, No. 3, July 1979, pp 283 - 292.

8. Etsion, I., Squeeze Film Effects in Radial Face Seals, ASME Journal of Lub. Tech., Vol. 102, No. 2, April 1980, pp 145 - 152.

9. Etsion, I., Radial Forces in a Misaligned Radial Face Seal, ASME Journal of Lub. Tech., Vol. 101, No. 1, January 1979, pp 81 - 85.

10. Etsion, I., The Accuracy of the Narrow Seal Approximation in Analyzing Radial Face Seal, ASLE Trans., Vol. 23, No. 2, April 1980, pp 208 - 216.

11. Johnson, R. L. and Ludwig, L. P., Lubrication, Friction and Wear in Aircraft, NASA TM-X-67872 Technical Paper for Structures and Materials Panel, AGARD London, March-April 1971.

12. Etsion, I., Nonaxisymetric Incompressible Hydrostatic Pressure Effects in Radial Face Seals, ASME, Journal of Lub. Tech., Vol. 100, No. 3, July 1978, pp 379 - 385.

13. Etsion, I., Dynamic Analysis of Noncontacting Face Seals, ASME 81-Lub-10, ASLE-ASME Lubrication Conference, October 1981.

14. Metcalf, R., Dynamic Whirl in Well Aligned, Liquid Lubricated End Face Seals with Hydrostatic Tilt Instability, ASLE Preprint 80-LC-1B-1, ASLE-ASME Lubrication Conference, August 1980.

15. Etsion, I. and Sharoni, A., Performance of End Face Seals with Diametral Tilt and Coning - Hydrostatic Effects, ASLE Trans., Vol. 23, No. 3, July 1980, pp 279 - 288.

16. Hughes, W. F., Winowich, N. S., Birchok, M. J. and Kennedy, W. C., Phase Change in Liquid Face Seals, ASME Paper No. 77-LUB-12, 1977.

17. Banerjie, B. N., Burton, R. A., Experimental Studies of Thermoelastic Effects in Hydrodynamic Lubricated Face Seals, ASME Paper No. 73-LUB-11.

18. Banerjie, B. N. and Burton, R. A., Thin Film Flows with Thermoelastically Deformed Boundaries, Paper for NASA-Lewis Workshop on Seal Lubrication, September 29, 1977.

19. Lebeck, A. O., Teale, J. L., and Pierce, R. E., Hydrodynamic Lubrication and Wear in Wavy Contacting Face Seals, ASME Paper No. 77, LUB-18, October 1977.

20. Lebeck, A. O., Teale, J. L., and Pierce, R. E., Hydrodynamic Lubrication with Wear and Asperity Contact in Mechanical Face Seals, The University of New Mexico Annual Report ME-86 (78) ONR-414-1, January 1978.

21. Lebeck, A. O., Mechanical Loading - A Primary Source of Waviness in Mechanical Face Seals, ASLE Transaction 20, 3, 195-208, 1977.

22. Iny, E. H., The Design of Hydrodynamically Lubricated Seals with Predictable Operating Characteristics, Proc. 5th International Conference Fluid Sealing, Coventing, England, March 1971.

23. Schoenherr, K., Design Terminology for Mechanical Face Seals, Aerospace Fluid Power Systems and Equipment Conference, Los Angeles, Calif., May 18-20, 1965, SAE Paper No. 650301.

24. Koenig, Thomas H. (Editor), Review of Dynamic Seal Literature Through 1967, pp 37-48, Recent Developments in Seal Technology, ASLE Special Publication SP-2, 1969.

25. Nau, B. S., Hydrodynamic Lubrication in Face Seals, BHRA Third International Conference on Fluid Sealing Proceedings, Cambridge, England, April 1967, Paper E-5.

26. Nau, B. S., A Review of Recent Rotary Face Seal Literature, Review and Bibliography on Aspects of Fluid Sealing, 1972 BHRA, Cranfield, England.

27. Mayer, E., Mechanical Seals, Iliffe Books, Ltd., London, American Elsevier, New York 1973.

28. Eubank, W. J., Dynamic Seals - A Review of Recent Literature, ASME Paper 67-WA/LUB-24.

29. Brown, F. P., A Glossary of Seal Terms, ASLE Publication SP-1 , 1969.

TABLE 1 - DESIGN DATA OF THE EXPERIMENTAL SEALS

DESIGN PARAMETER	FLAT FACE STANDARD PUSHER TYPE 8B		CONED FACE PUSHER TYPE 8B		CONED FACE BELLOWS TYPE		MODIFIED CONED FACE PUSHER TYPE 8B BALANCED TO 51.3%		
	FRONT SEAL	REAR SEAL	FRONT SEAL	REAR SEAL	FRONT SEAL	REAR SEAL	FRONT SEAL	REAR SEAL #1	REAR SEAL #2[3]
Face Dimensions									
O.D. mm (in)	95.25 (3.750)		95.25 (3.750)		97.28 (3.830)		88.9 (3.5)	89.66 (3.530)	88.9 (3.5)
I.D. mm (in)	82.55 (3.250)		82.55 (3.250)		89.41 (3.520)		82.55(3.25	82.55 (3.250)	82.55 (3.25)
Face Width, mm (in)	6.35 (.25)		6.35 (.25)		3.935(.155)		3.175(.14)	3.555(.14)	3.175(.125)
Seal Balance:[1]	76.3%		76.3%		2) at 345kPa(50psig) 71%		51.3%	56.5%	51.3%
					at 690kPa(100psig) 75.5%				
					at 1034kPa(150psig) 74.9%				
					at 1379kPa(200psig) 67.7%				
Balance Diameter, mm (in)	85.725 (3.375)		85.725 (3.375)				85.70 (3.374)	85.70 (3.374)	85.70 (3.374)
Face Sliding Velocity at Mean Diameter, m/sec (ft/sec)	1800 rpm 8.38	(27.5)	8.38	(27.5)	9.17	(30.08)	8.08 (26.5)	8.11 (26.62)	8.08 (26.5)
	3600 rpm 16.76	(55)	16.76	(55)	18.33	(60.15)	16.21 (53.2)	16.22 (53.23)	16.21 (53.2)
	5400 rpm 25.15	(82.5)	25.15	(82.5)	27.5	(90.23)	24.23 (79.5)	24.34 (79.85)	24.23 (79.5)
	8000 rpm 35.36	(116)	35.36	(116)	40.74	(133.6)	35.87 (117.7)	36.1 (118.3)	35.87 (117.7)
Face Cone Height of the Primary Ring before Test, μm (μin)	Flat, less than .44 (17)		Cone 2.69 (106)	Cone 3.05(120)	Cone 2.54 (100)[5] 5.6 (220)	Cone 3.05(120)	Cone .51 (20)	Flat, less than .29 (11.6)	Cone .51 (20)
Material of the Primary Ring	Carbon		Tungsten Carbide		Tungsten Carbide		Tungsten Carbide	Carbon	Tungsten Carbide
Weight of the Primary Ring in Grams	195 (.43)	128 (.28)	1127 (2.48)	1060 (2.34)	254(.56)	203 (.45)	1125 (2.43)	127(.28)	1058 (2.33)
Spring Force on the Seal Face at Working Height, Newton (lbs)	116.6 (26.22)	114.9(25.84)	116.6(26.22)	114.9(25.84)	74.5(16.7)	88.3(19.8)	8.9 (2)	9.6(2.15)	9.6 (2.15)
Number of Springs	4	4	4	4	None	None	6	6	6
Spring Constant, N/m (lbs/in)	15702(89.6)	15287(87.2)	15702(89.6)	15287(87.2)	105958(605)	89380(510)	15967(91.2)	10519(60.1	10519 (60.1)

1) Balance is the ratio of the back side of the primary ring exposed to the test pressure to the seal face area.

2) Balance shown was calculated from the balance diameter determined in the CPC MTL test project 2034. Balance calculated using the values obtained in the test by CPC Slough, England is 6 to 10% higher.

3) This non-contacting seal #2) replaced contacting seal #1 to reduce the rotor face temperature and to equalize the forces acting on the rotor.

4) One entry in SI and English units indicates that the same data applies for the front and rear seals.

5) The seal face was damaged from the contact at this initial coning during the test at 0 kPa (0 psig) pressure. For the test runs at 345 kPa (50 psig) to 1379 kPa (200 psig), the cone height was then increased.

BLE 2 - INSTRUMENTATION AND MEASURED VARIABLES

ASURED VARIABLE	INSTRUMENT	DATA RECORDING METHOD	NOTE
Displacement of the Front Seal	"Kaman" Proximity Probes KD-2310 Models .25S and 2UB	Microprocessor Based D.A. System Data Stored on Magnetic Tapes. Tektronics Oscilloscope Model 5440, direct reading of signal output voltage of individual probes and photographing screen. Digital Voltmeter Keithly Model 135.	
a. Axial Displacement of Rotor	2 Probes #1 and #5, 180° apart, measuring range 0 to 250 μ-m (0 to .010 inches)		
b. Axial Displacement of Stationary Primary Ring	3 Probes #2, #3, and #4, 90° apart with the measuring range 0 to 250 μ-m (0 to .010")		
c. Radial Displacement of Stationary Primary Ring	Probes 2UB, range 0 to 1 mm (0 to .040")		Radial displacement was measured on standard flat faced seal only.
d. Radial Displacement of Rotor	Probe 2UB, range 0 to 1 mm (0 to .040")		
Torque produced by the 2 Seals and Housing Bearings	"Sensotec" Load Cell 0 to + 445 N (100 lbs) located 152.4 mm (6") from the shaft axis.	Goulds Model 2400 Recorder, Channel #1.	
	Strain Gage attached to beam	Goulds Model 2400 Recorder, Channel #1.	
DC Motor Input Power	Digital Voltmeter, Digital Ammeter	Recorded by Operator	

ABLE 2 - INSTRUMENTATION AND MEASURED VARIABLES

EASURED VARIABLE	INSTRUMENT	DATA RECORDING METHOD	NOTE
. Shaft Speed (RPM)	Displacement Probe 2UB	Gould Recorder, Channel #4	RPM's were not recorded on last test with modified coned Type 8B Seal due to design changes in target and probe mounting cylinder
	Stroboscope	Recorded by Operator	
. Circulating Oil Pressure measured in seal cavity and in line	Pressure Gauges, range as necessary for tested pressure	Recorded by Operator	
. Front Seal Face Temperaturemeasured as follows:	J-Type thermocouples		
a. Carbon Flat Faced Primary Ring at three locations per Dwg. X464-A3983:			
.76 mm (.030") from the face OD	Thermocouple #1	Gould Recorder #2 Channel	
at face mean dia.	Thermocouple #2	Leeds and Northrup 24 Point Recorder #2 Channel	
.76 mm (.030") from face ID	Thermocouple #3	Goulds Recorder #3 Channel	
b. Tungsten Carbide Coned Primary Ring Type 8B and Type 15 Seal. Thermocouple wasepoxied on ID of ring 1/16 away from face	J-Type thermocouple	Goulds Recorder, Channel #2	

TABLE 2 - INSTRUMENTATION AND MEASURED VARIABLES

MEASURED VARIABLE	INSTRUMENT	DATA RECORDING METHOD	NOTE
7. Circulating Oil Flow	"Hedland" Flowmeter .5 to 5.5 GPM	Recorded by Operator	
8. Circulating Oil Temp.	J-Type thermocouples	Leeds and Northrup Recorder	On tests with Type 15 Seal and modified coned face Type 8B Seal, the location of heat exchanger and pod cylinder was switched with respect to cir culating pump
a. on the inlet line to heat exchanger which is on outlet line from pod		#5 Point	
b. on the outlet line from heat exchanger		#4 point on Leeds & Northrup Recorder	
9. Cooling Water Flow thru Oil Heat Exchanger	"Brooks" Flowmeter, 0 to 5 GPM	Recorded by Operator	
0. Cooling Water Temp.	J-Type thermocouples	Leeds & Northrup Recorder	
a. on inlet line to heat exchanger		#7 Point	
b. on outlet line to heat exchanger		#6 Point	
1. Seal Leakage	Graduated Cylinder and Stop Watch	Recorded by Operator	
a. Front Seal			
b. Rear Seal			
2. Temperature of Probe holding cylinder measured on cylinder ID next to Probe #3	J-Type thermocouples	Leeds & Northrup Recorder	
3. Temperature of Probe brass target attached to stationary primary ring	J-Type thermocouples	Gould Recorder	
4. Pressure in the seal chamber	Pressure Gage	Recorded by Operator	

TABLE 3 - SUMMARY OF TESTS

TEST #	TYPE OF SEAL	DATE TESTED	SPEED (RPM)	PRESSURE IN KILOPASCAL (PSIG)							
				0 (0)	207 (30)	345 (50)	690 (100)	1034 (150)	1379 (200)	2068 (300)	2758 (400)
1	Standard Flat Face Type 8B, pusher type	November 1980	1800		X	X	X	X	X	X	X
			3600		X	X	X	X	X	X	X
			5400		X	X	X	X	X	X	X
			8000 1)								
2	Cone Face Type 8B 76% Balance, pusher type with linkage antirotation locks	December 1980 to January 1981	1800		X	X	X	X	X	X	X
			3600		X	X	X	X	X	X	X
			5400		X	X	X	X	X	X	X
			8000		X	X	X	X	X	X	X
3	Cone Face Bellows Type 15	April 1981	1800	X		X	X	X	X		
			3600	X		X	X	X	X		
			5900	X		X	X	X	X		
			8000	X		X	X	X	X		
4	Cone Face Type 8B, 51.3% Balance, pusher type with linkage antirotation locks	August-Sept. 1981	1800					X			
			3600					X		X	
			5400			X				X	
			8000			X				X	

X = Seal Tested and all data recorded at the indicated conditions.

1) = In some of the tests the maximum speed of the rig dropped to 7900 RPM due to the decreased power supply.

LIST OF FIGURES

FIGURE 34 - Profile Traces
35 - "
36 - "
37 - "
38 - "
39 - "
40 - "
41 - Torque Curves
42 - "
43 - "
44 - "
45 - Torque Comparison Curves
46 - " " "
47 - Torque Recording
48 - " "
49 - " "
50 - " "
51 - " "
52 - Leakage Curves
53 - " "
54 - " "
55 - " "
56 - " "
57 - Leakage Comparison Curves
58 - Face Temperature Curves
59 - " " "
60 - " " "
61 - " " "
62 - Axial Movement Traces
63 - " " "
64 - " " "
65 - " " "
66 - Phase Shift Curve
67 - " " "

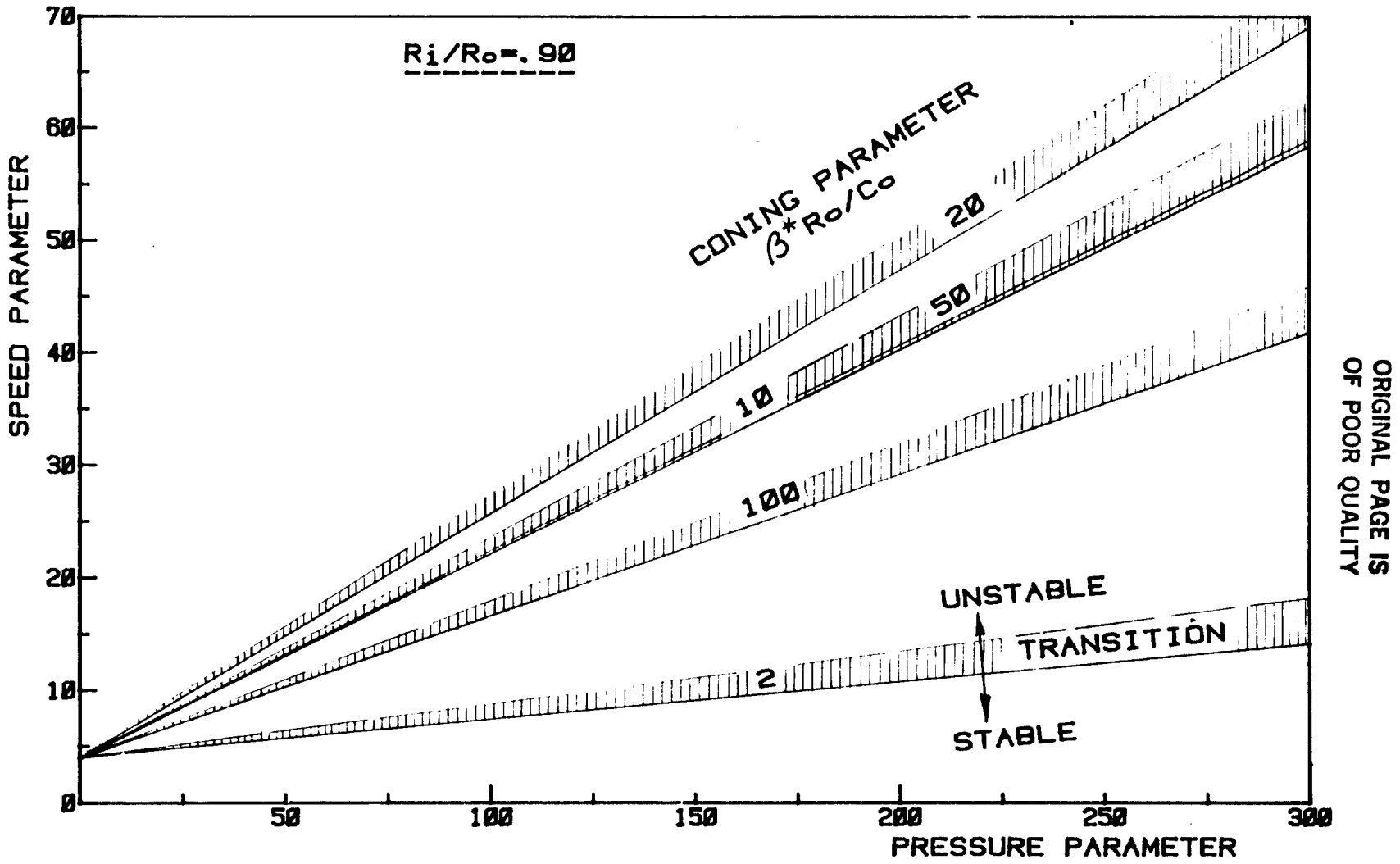

FIGURE 1 - STABILITY MAP FOR SEALS OF
RADIUS RATIO Ri/Ro = .90
(REFERENCE 13)

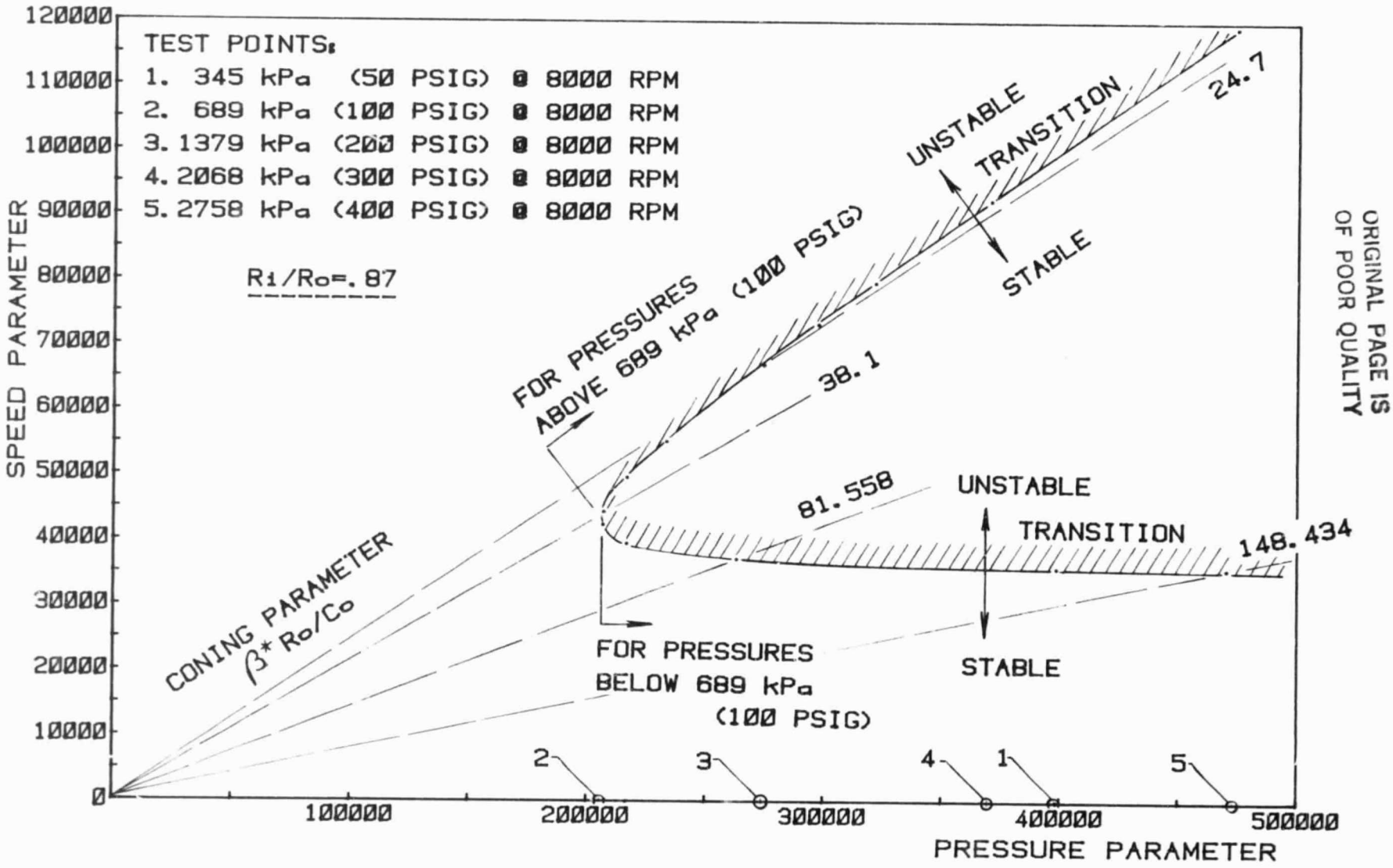

FIGURE 2 - STABILITY MAP IDENTIFYING SPECIFIC TEST POINTS FOR THE TESTED CONED FACE PUSHER TYPE SEAL, BALANCED TO 76.3%.

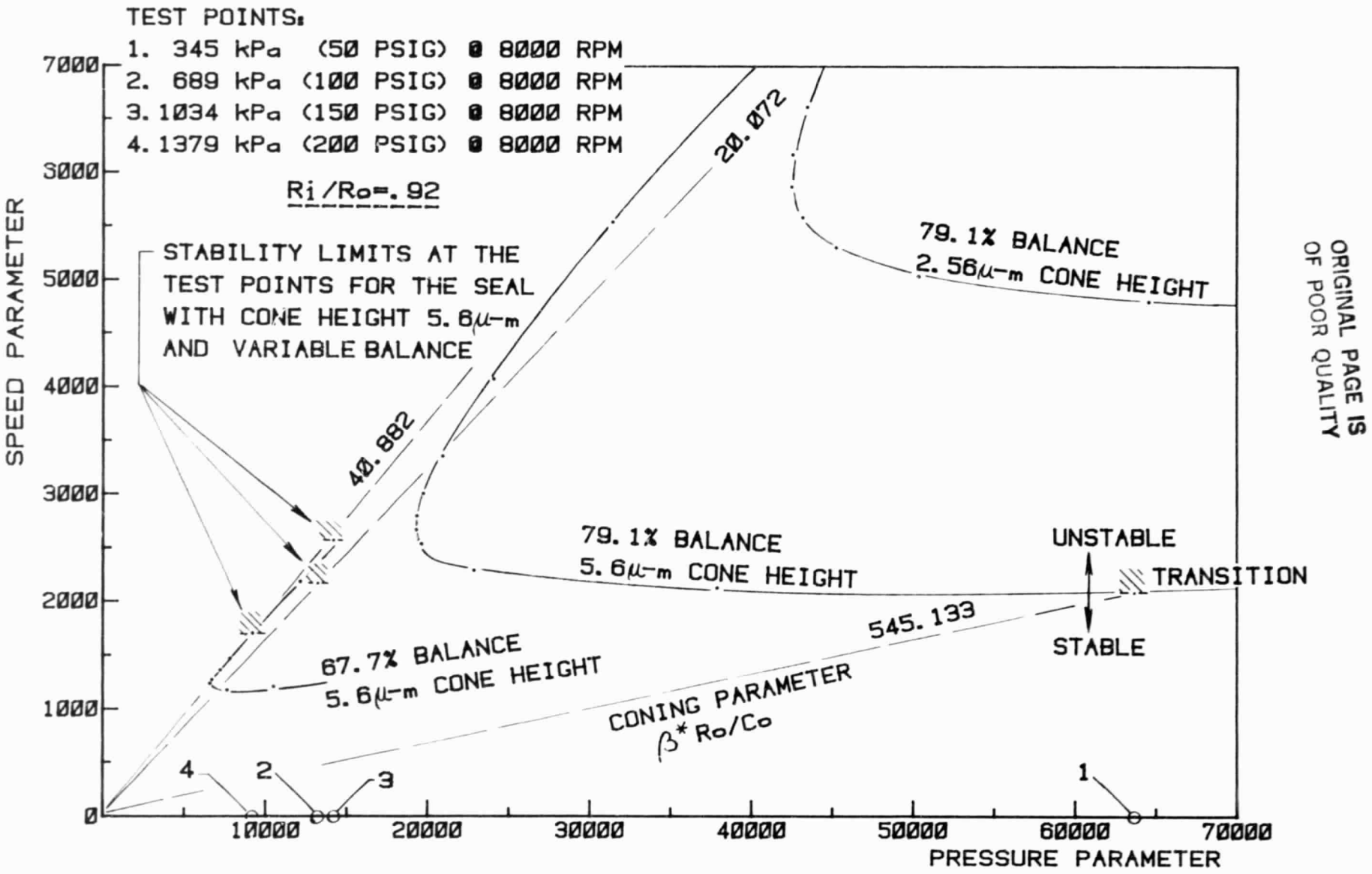

FIGURE 3 - STABILITY MAP IDENTIFYING SPECIFIC TEST POINTS FOR THE TESTED CONED FACE BELLOWS TYPE SEAL.

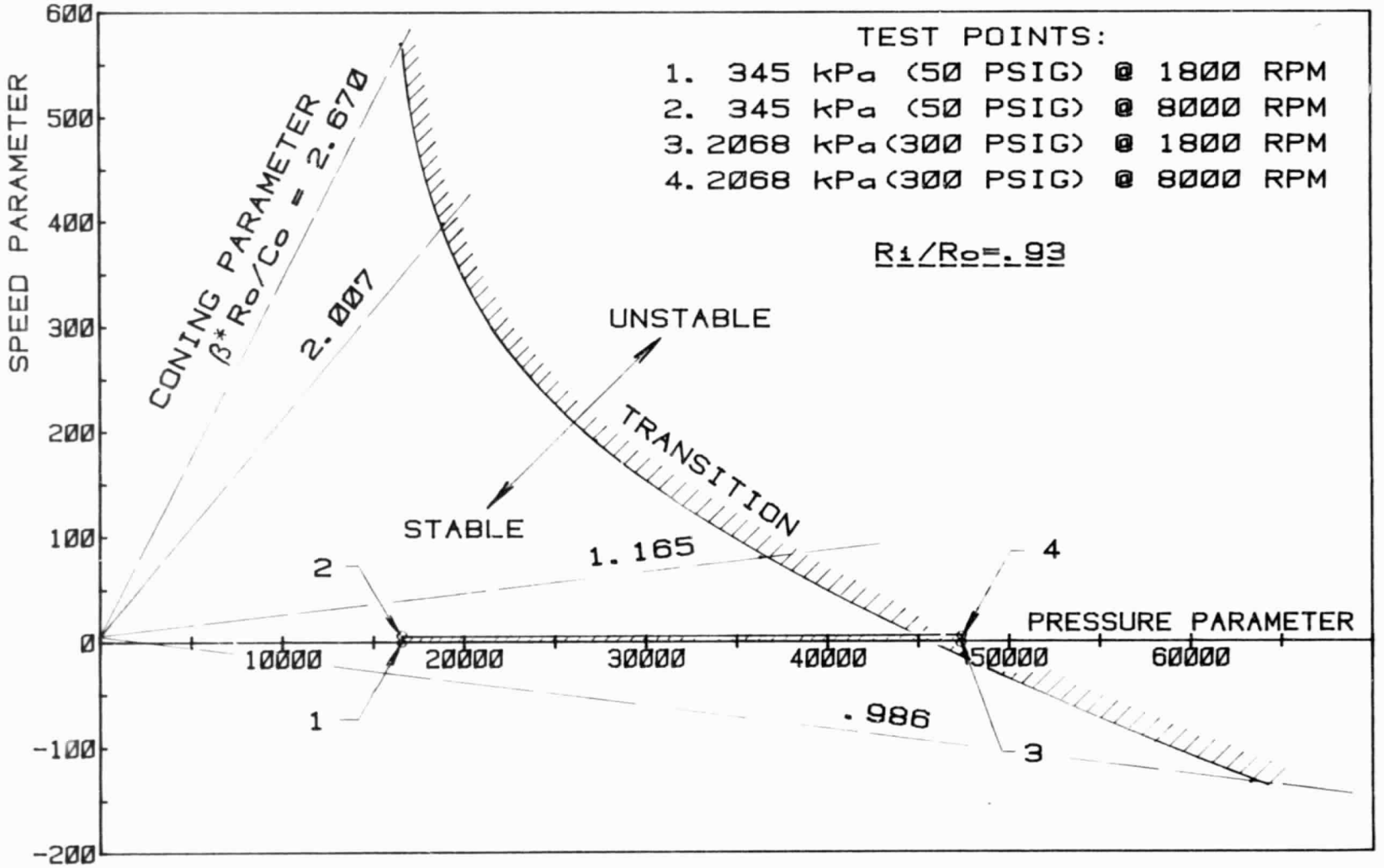

FIGURE 4 - STABILITY MAP IDENTIFING SPECIFIC TEST POINTS FOR THE TESTED CONED FACE PUSHER TYPE SEAL BALANCED TO 51.3%.

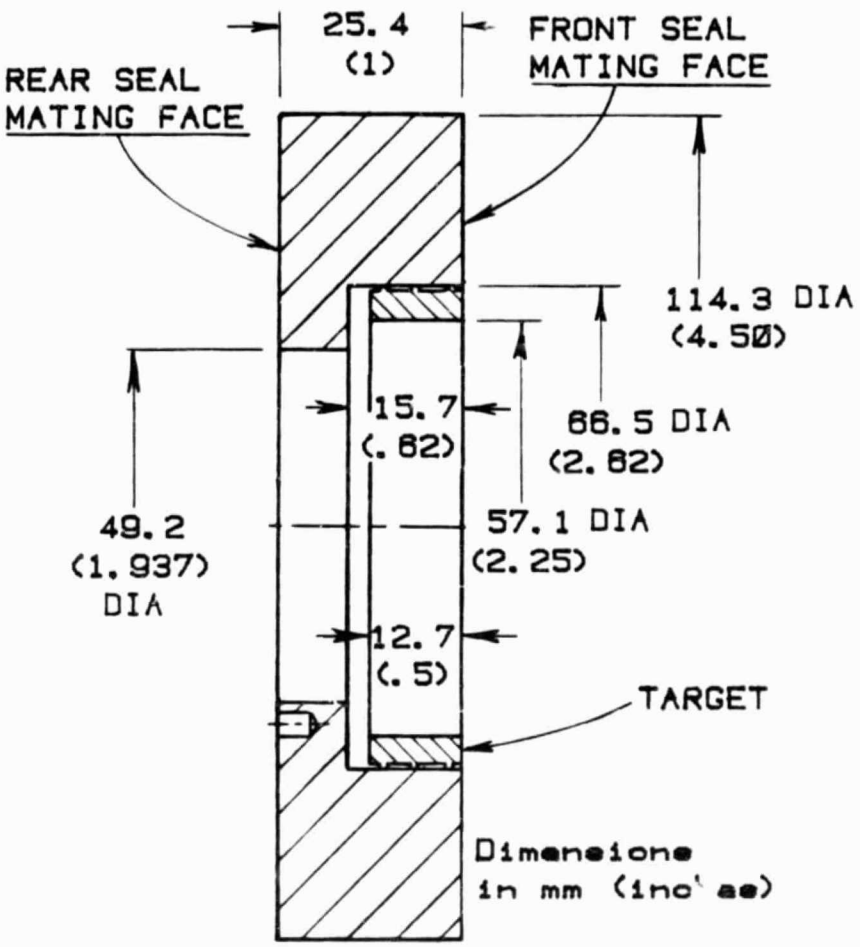

FIGURE 5 - ROTOR AND TARGET DIMENSIONS

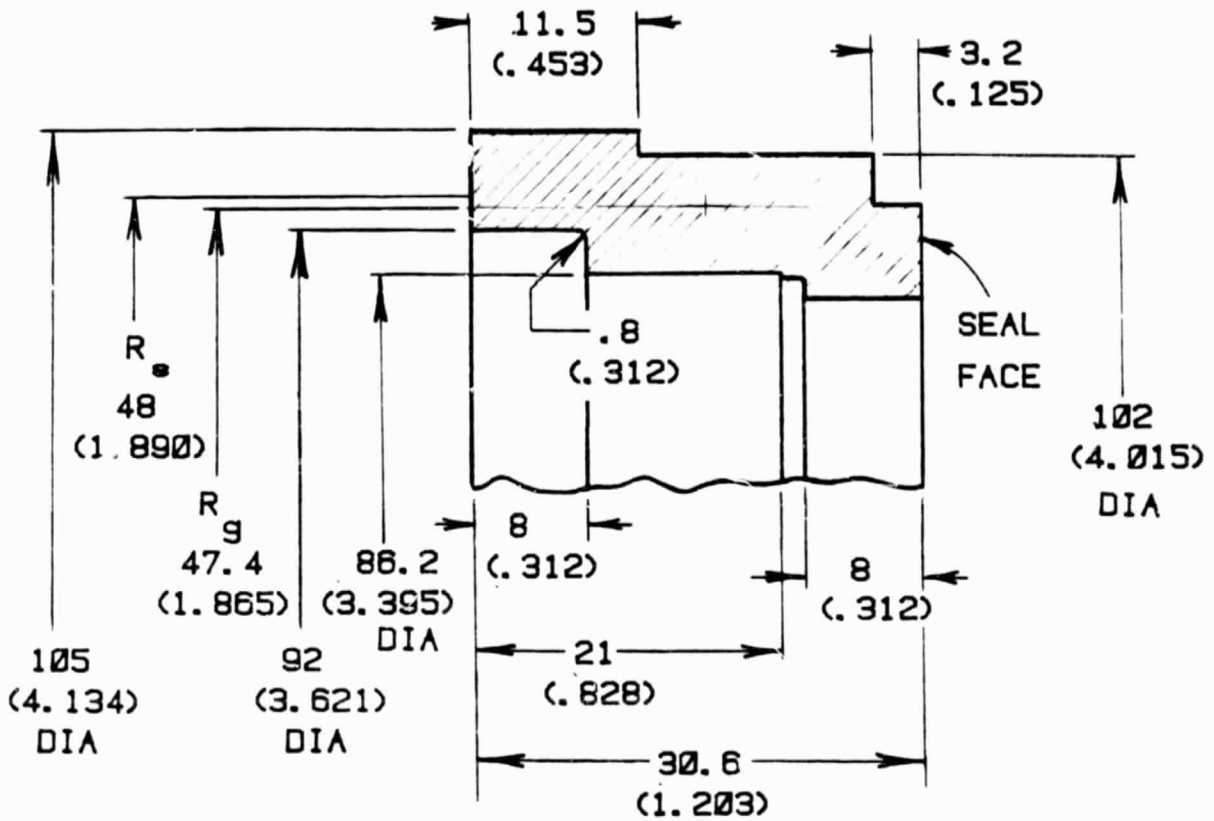

FIGURE 6 - PRIMARY RING USED ON TESTS WITH THE PUSHER TYPE SEAL.

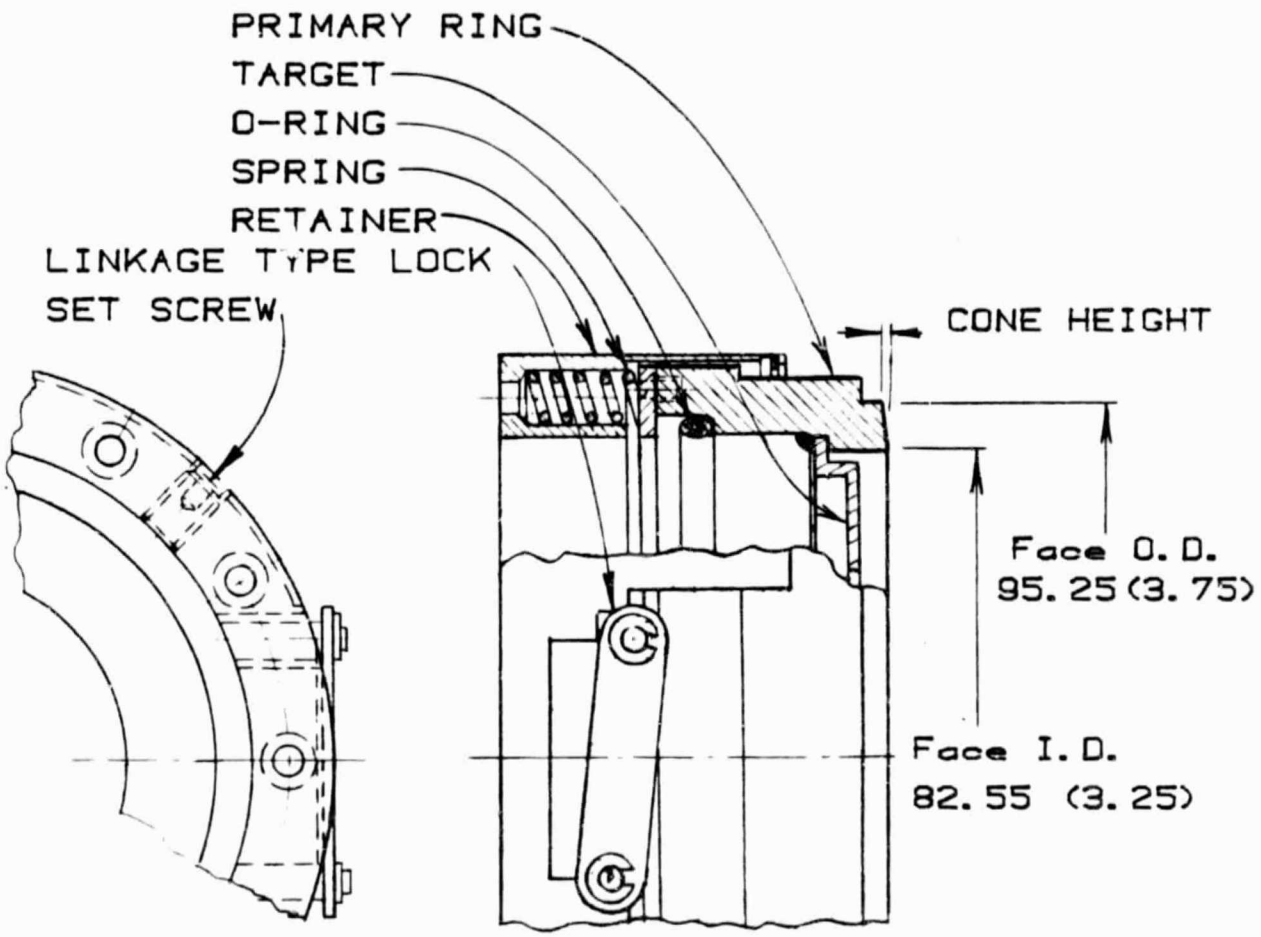

Dimensions in mm (inches)

Balance diameter = 85.72 (3.375)

FIGURE 7 - CONED FACE PUSHER TYPE SEAL BALANCED TO 76.3%.

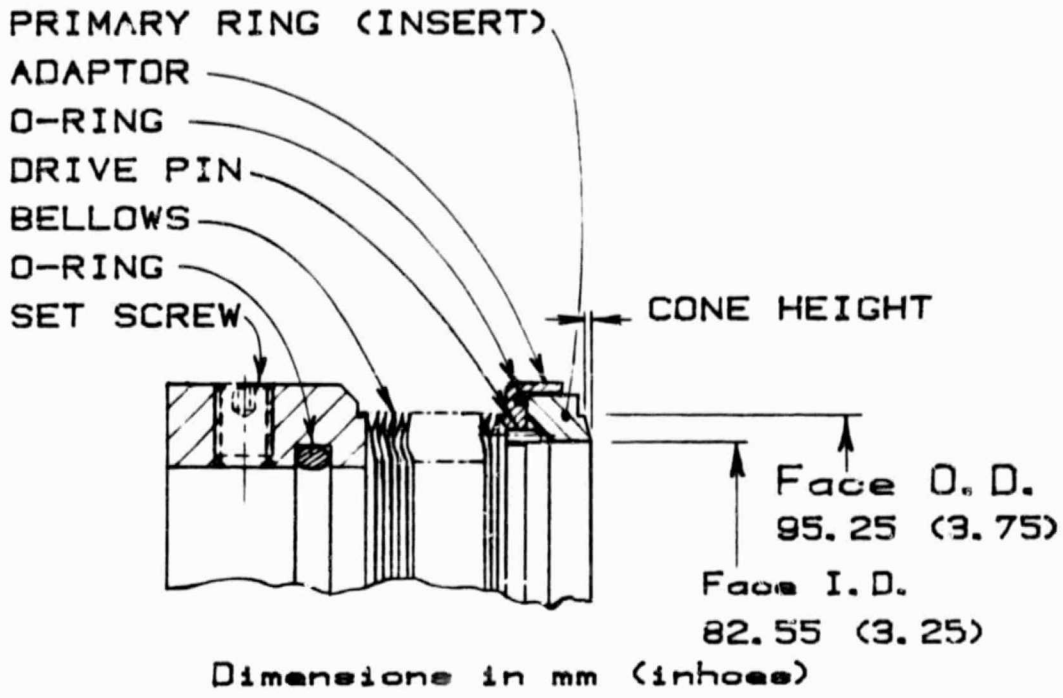

FIGURE 8 - REAR BELLOWS TYPE SEAL.

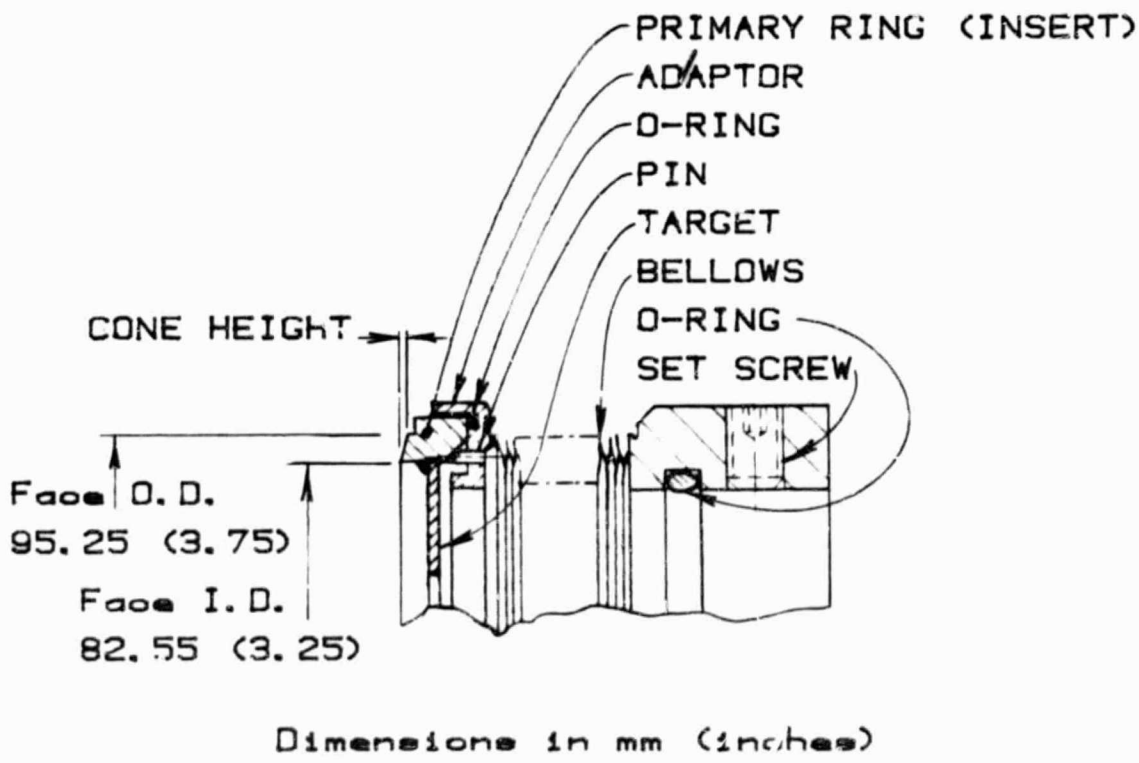

FIGURE 9 - FRONT BELLOWS TYPE SEAL.

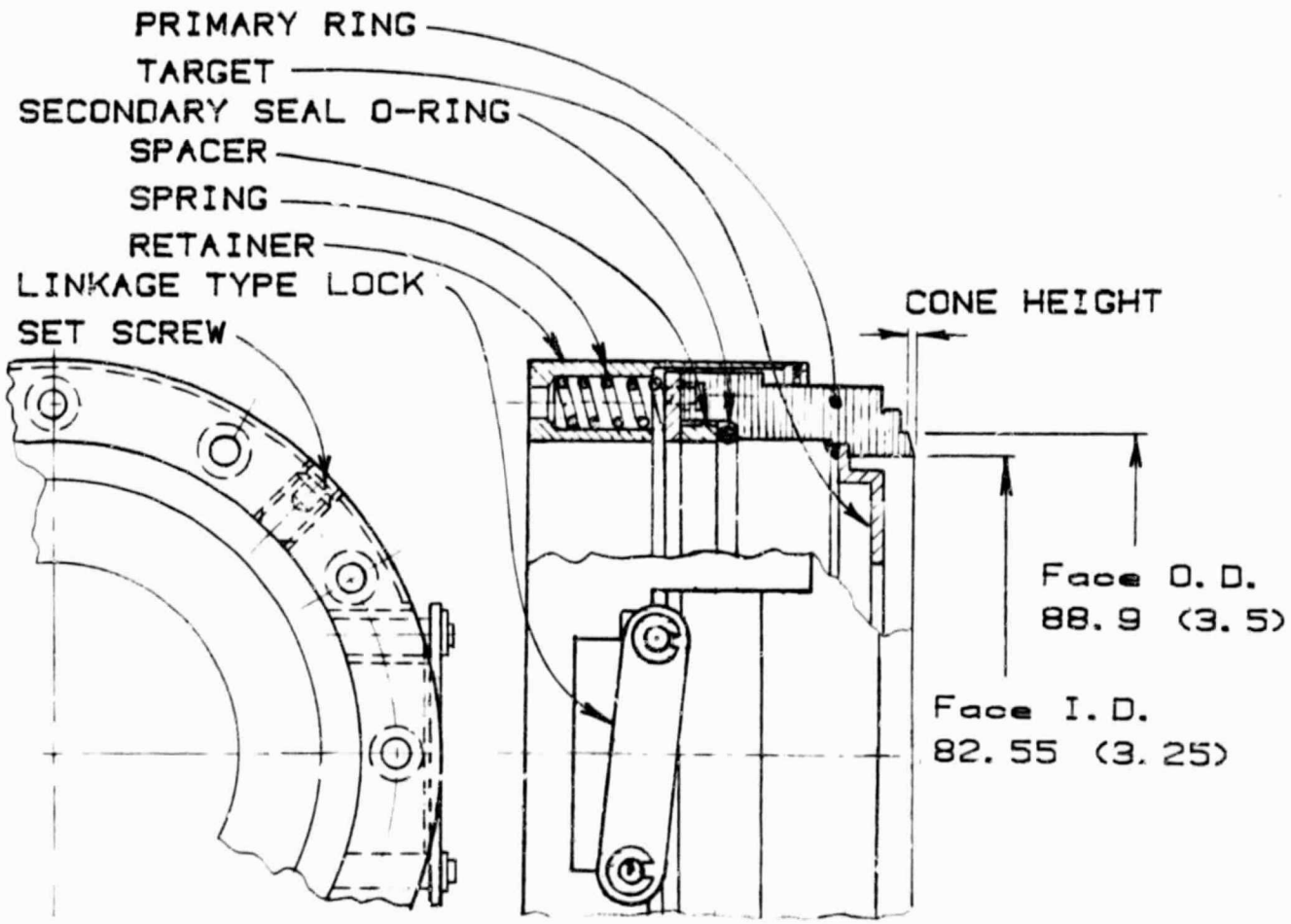

Dimensions in mm (inches)

Balance diameter = 85.7 (3.374)

FIGURE 10 - CONED FACE PUSHER TYPE SEAL BALANCED TO 51.3%.

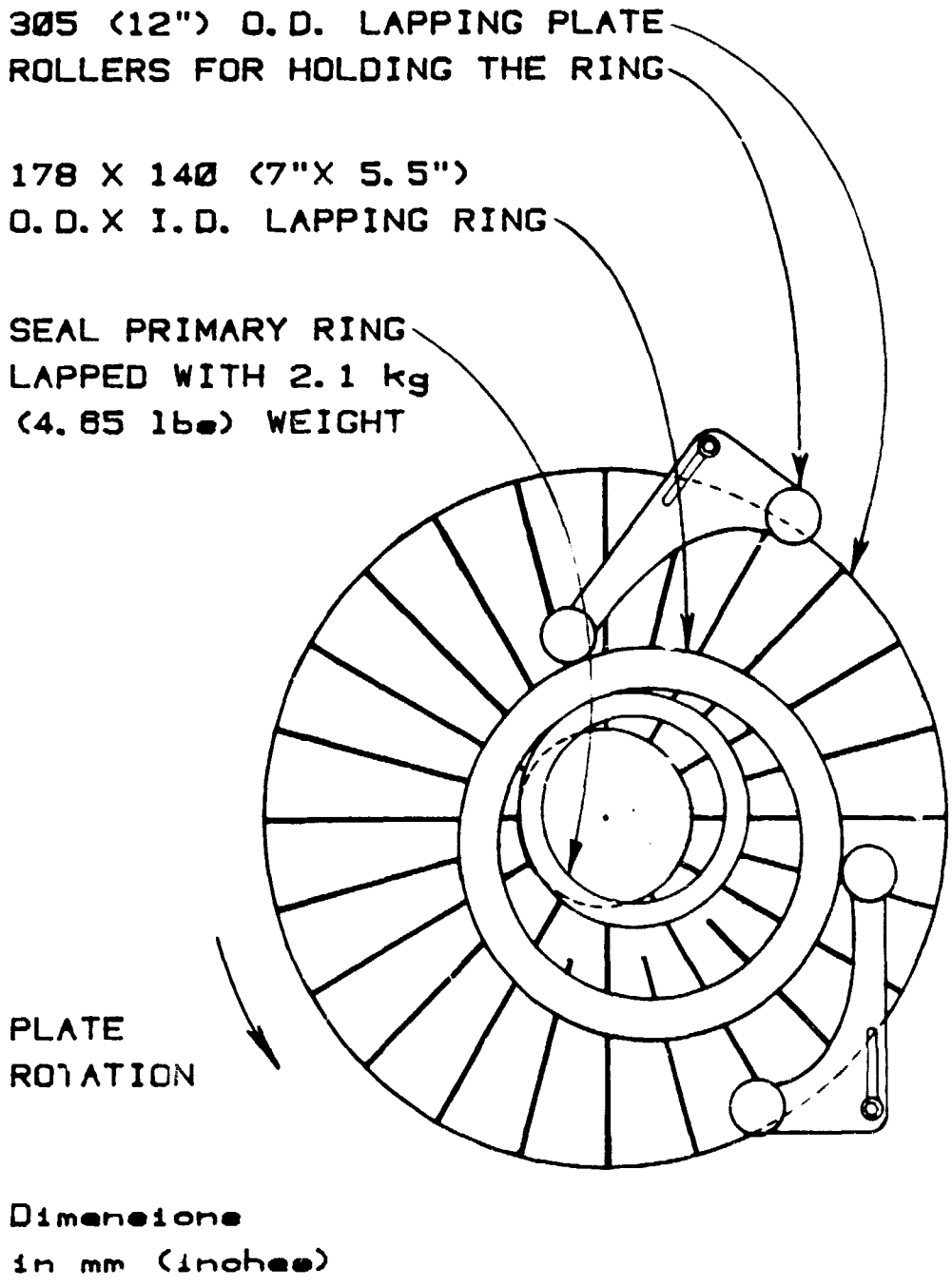

FIGURE 11 - CONE LAPPING SET-UP.

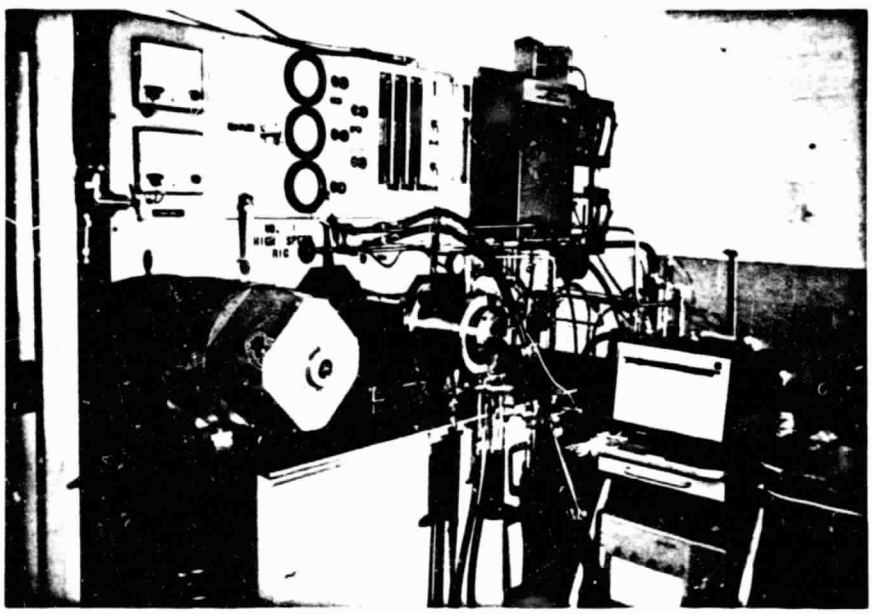

FIGURE 12 - PHOTOGRAPH OF THE TEST RIG WITH THE MAIN COMPONENTS. FROM THE LEFT: 15 HP MOTOR, BELT DRIVE HIDDEN BEHIND THE PANEL, TEST HEAD IN THE MIDDLE WITH LEAKAGE COLLECTING CYLINDERS BELOW AND OIL CIRCULATING SUPPORTING EQUIPMENT IN BACK-GROUND. RECORDERS ARE IN LOWER RIGHT CORNER.

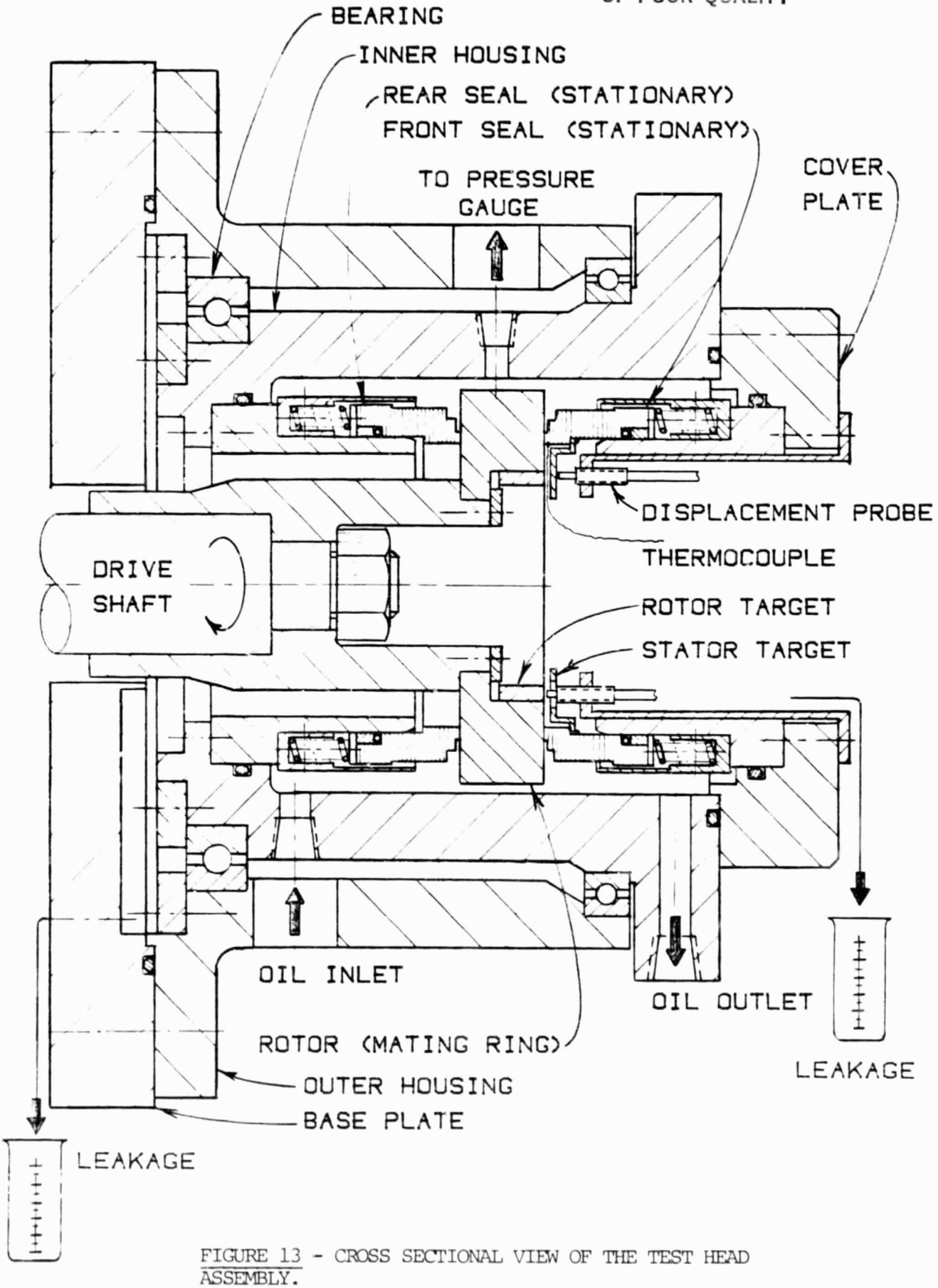

FIGURE 13 - CROSS SECTIONAL VIEW OF THE TEST HEAD ASSEMBLY.

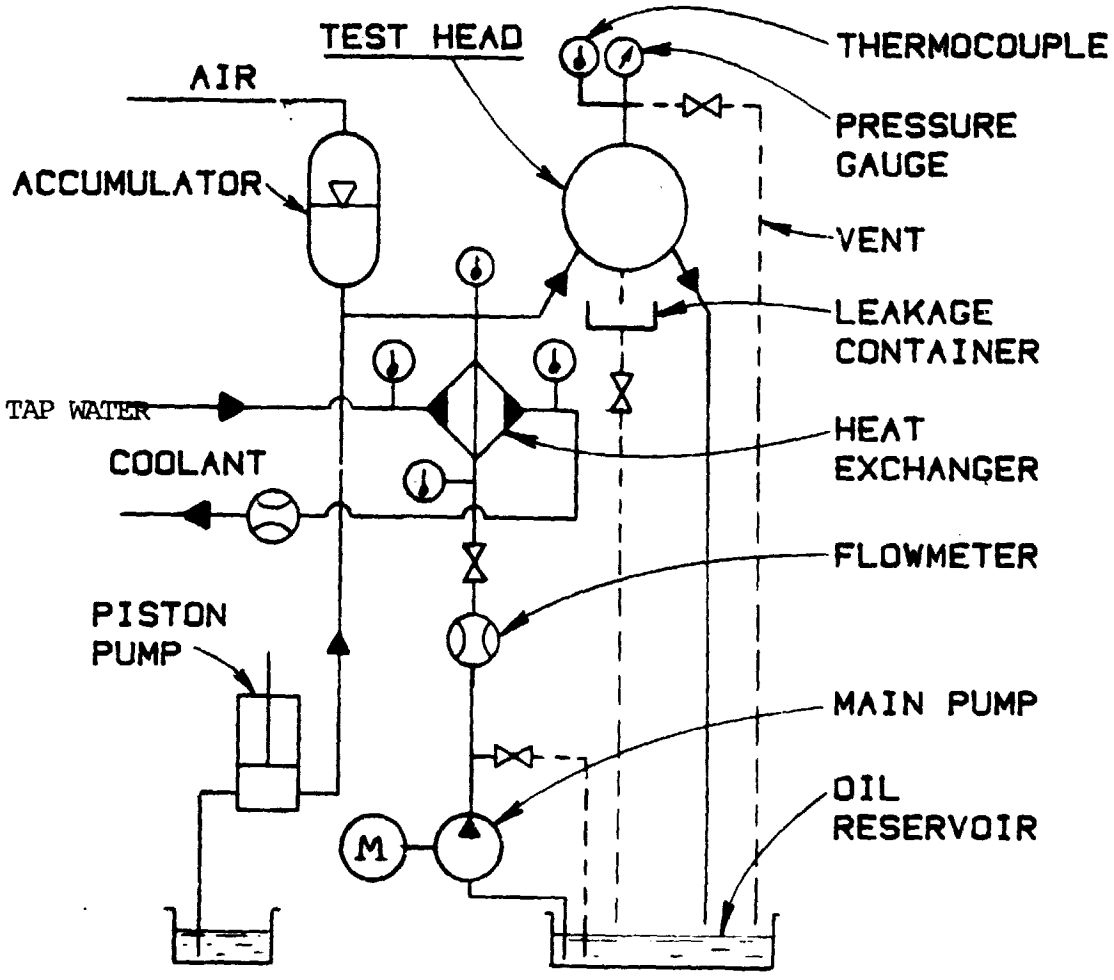

FIGURE 14 - SCHEMATIC OF SEAL TEST OIL CIRCULATING SYSTEM.

FIGURE 15 - PHOTOGRAPH OF INSTRUMENTATION AND DATA ACQUISITION SYSTEM USED IN THE TESTING. FROM THE LEFT: TEMPERATURE RECORDER, BELOW IS THE TORQUE RECORDER, IN THE MIDDLE ARE DEMODULATORS-OSCILLATORS FOR THE DISPLACEMENT PROBES AND POWER SUPPLIES, ABOVE THEM IS A MICROPROCESSOR AND HP-85 DESK TOP COMPUTER. OSCILLOSCOPE IS ON THE RIGHT SIDE.

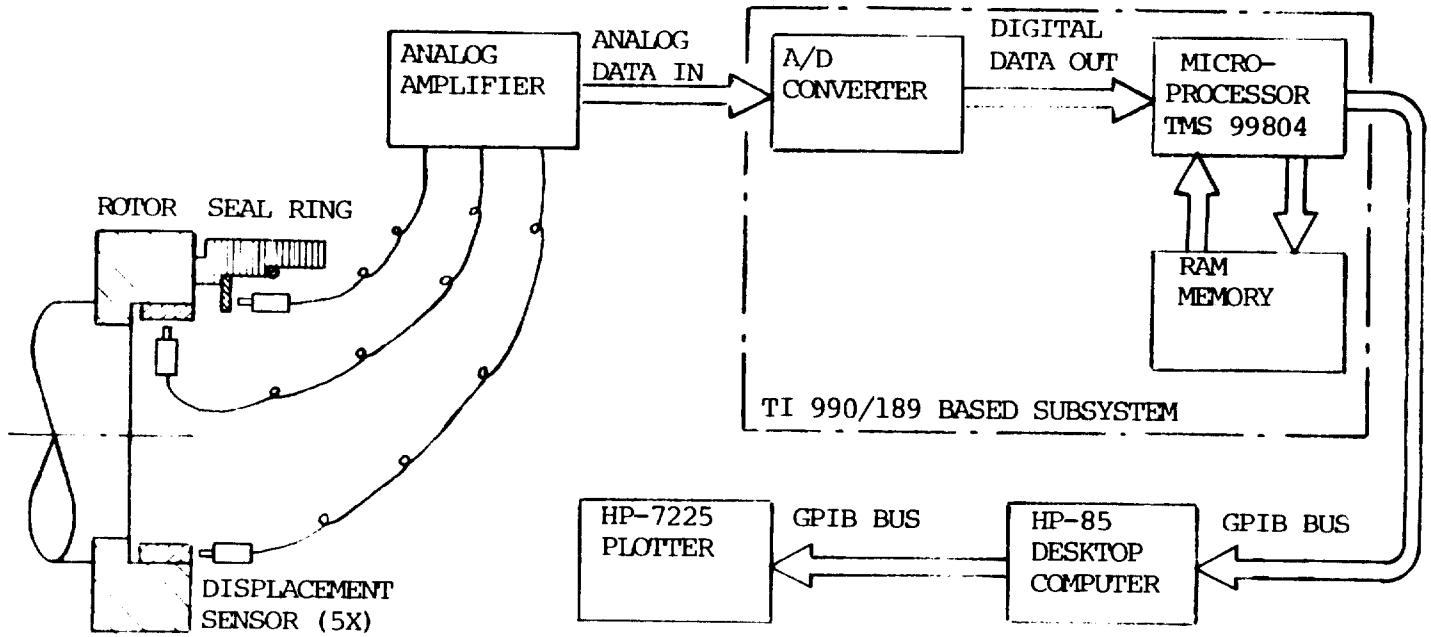

FIGURE 16 - DATA ACQUISITION SYSTEM SCHEMATIC.

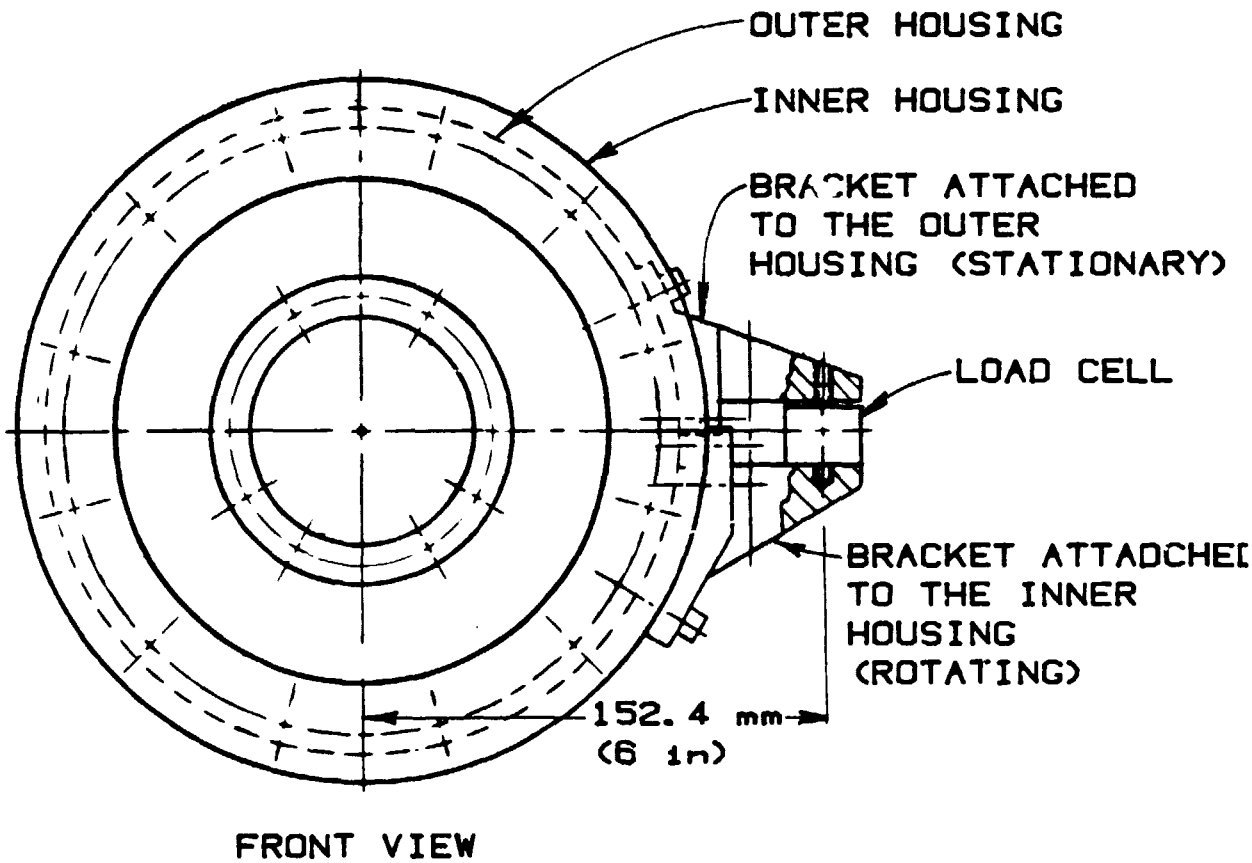

FIGURE 17- DETAIL OF THE TORQUE SENSING ARRANGEMENT.

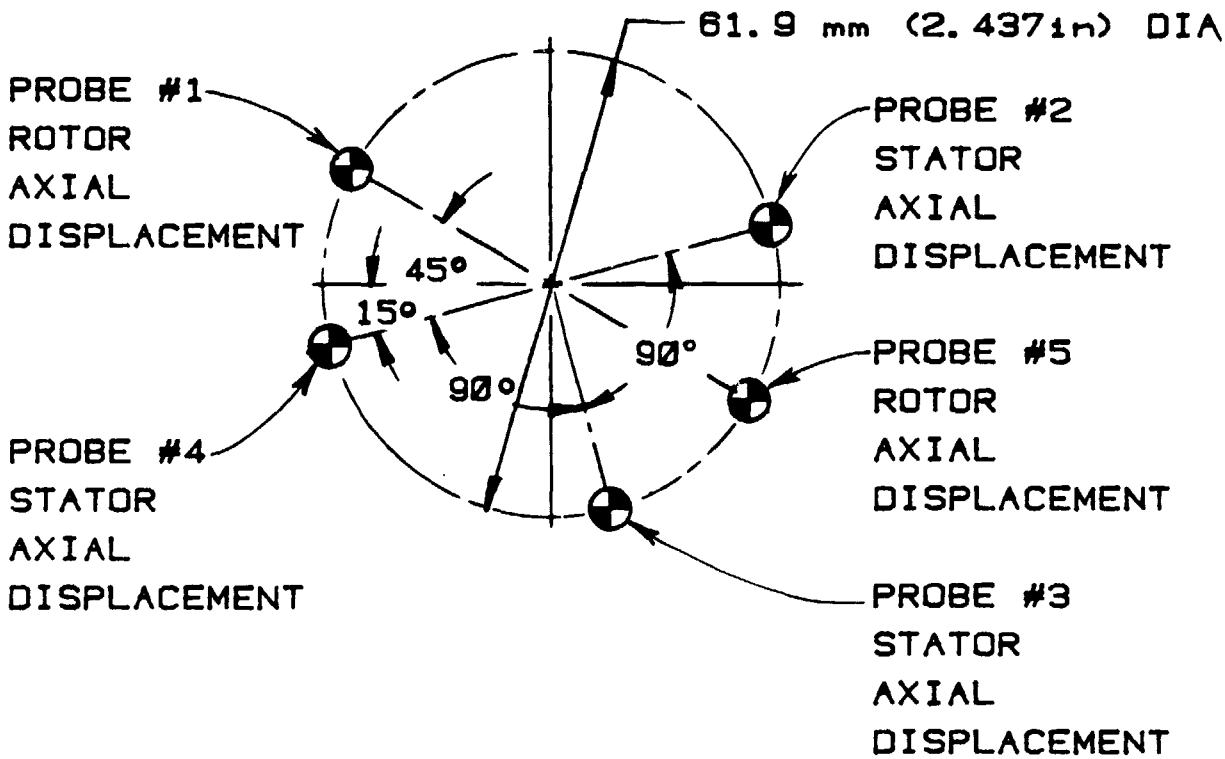

FIGURE 18 - POSITIONING OF THE DISPLACEMENT PROBES.

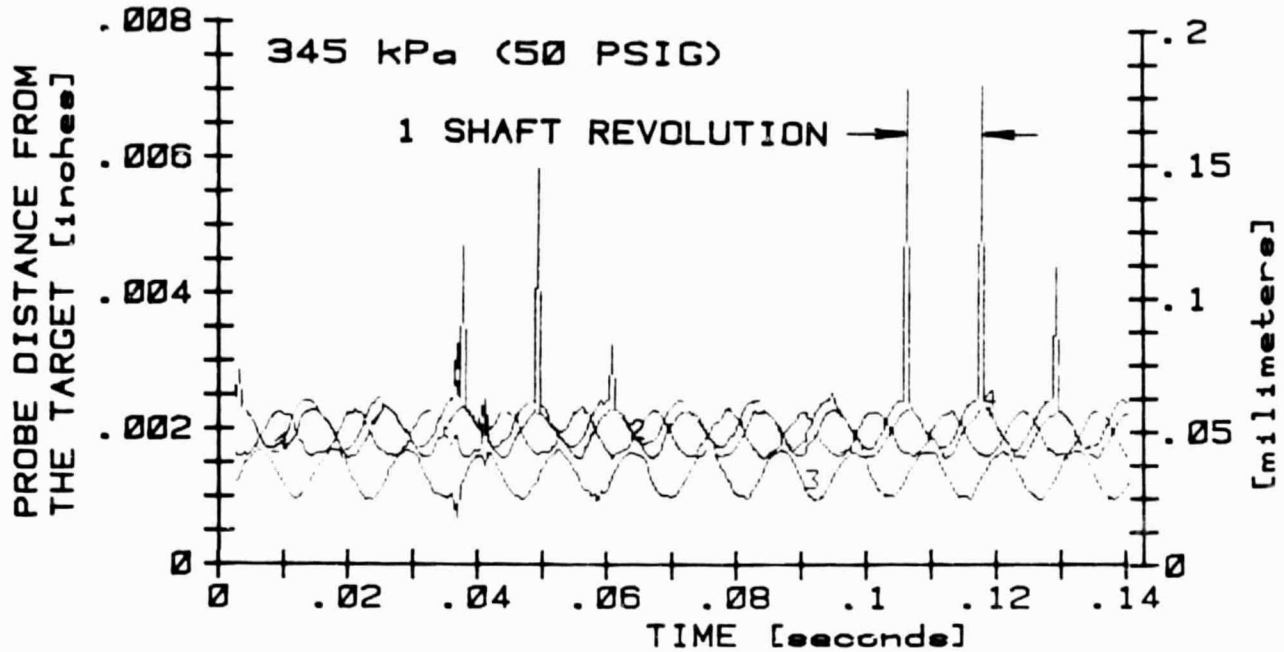

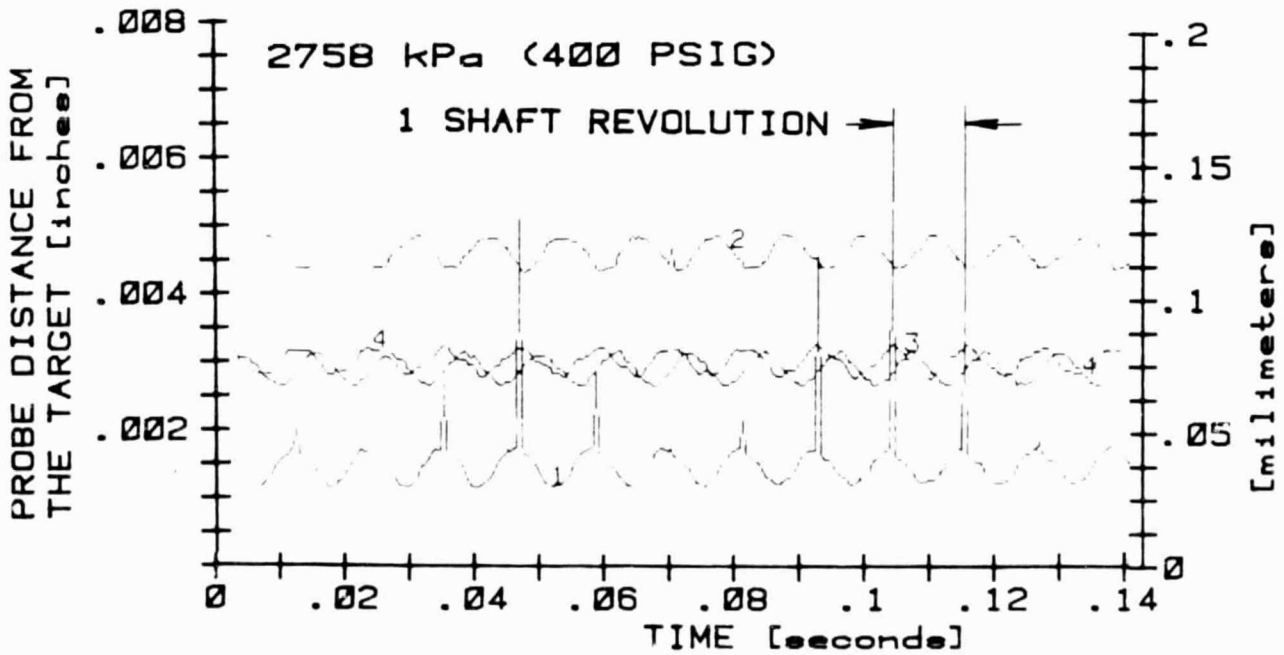

FIGURE 19 - TYPICAL DISPLACEMENT TRACES ON THE PRINTOUT FROM THE DESKTOP COMPUTER HP-85. THE TRACES REPRESENT INSTANTANEOUS DISTANCES BETWEEN THE PROBES AND THEIR TARGETS MOUNTED ON THE STATIONARY PRIMARY RING (#2, 3, 4) AND ON THE ROTATING MATING RING (#1, 5). SPIKES ON TRACES #1 and #5 WERE CAUSED BY A PURPOSELY MACHINED NOTCH IN THE ROTOR TARGET TO DETERMINE THE REVOLUTIONS OF THE SEAL SHAFT, ONE PEAK TO PEAK PULSE CORRESPONDS TO ONE REVOLUTION. SHOWN IS THE DYNAMIC AXIAL MOVEMENT OF THE FLAT FACE PUSHER TYPE SEAL BALANCED TO 76.3% at 5400 rpm.

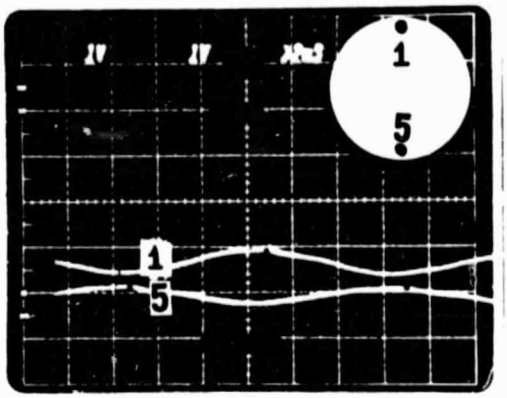

ROTOR (MATING RING), AXIAL DISPLACEMENT SENSORS #1 AND #5 ARE 180° APART

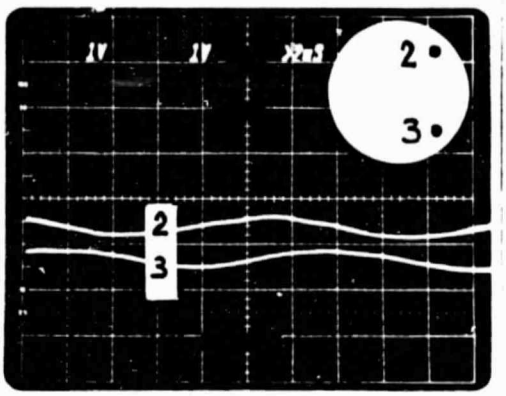

STATIONARY PRIMARY RING, DISPLACEMENT SENSORS #2 AND #3 ARE 90° APART

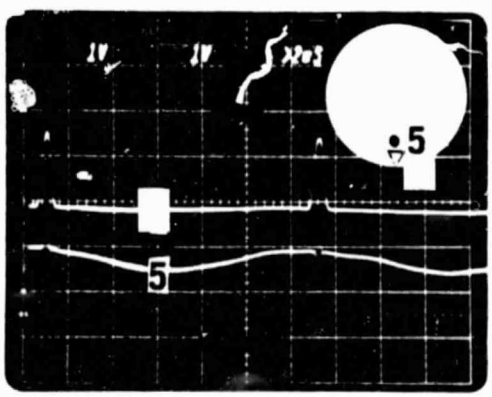

ROTOR, AXIAL DISPLACEMENT (#5 SENSOR) AND ROTOR RADIAL RUNOUT WITH THE TIMING SPIKES INDICATING 1 REVOLUTION OF THE SHAFT

FIGURE 20 - OSCILLOSCOPE TRACES SHOWING THE DYNAMIC AXIAL MOVEMENT OF THE FLAT FACE PUSHER TYPE SEAL AT 3600 RPM AND 1034 kPa (150 PSIG).

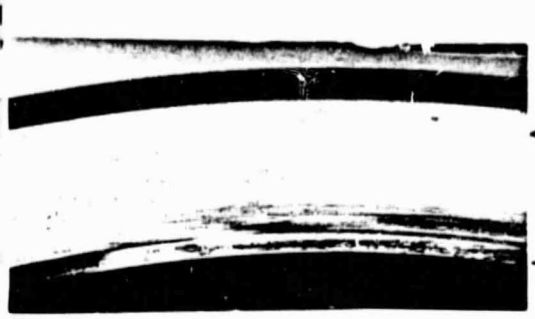

PRIMARY RING (STATOR)

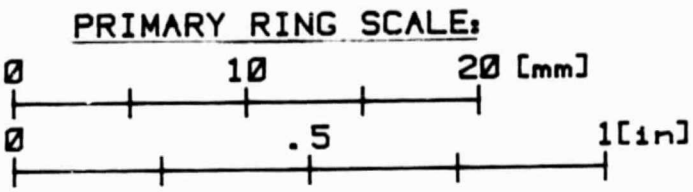

PRIMARY RING (STATOR)

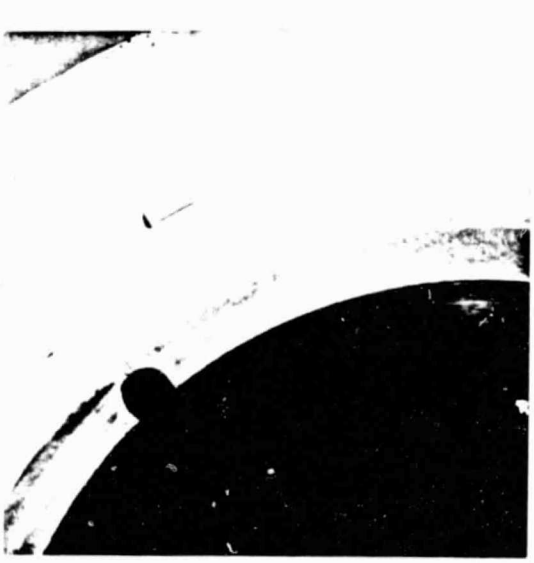

MATING RING (ROTOR) FACE SHOWING CRACK AND GALLING ⟶

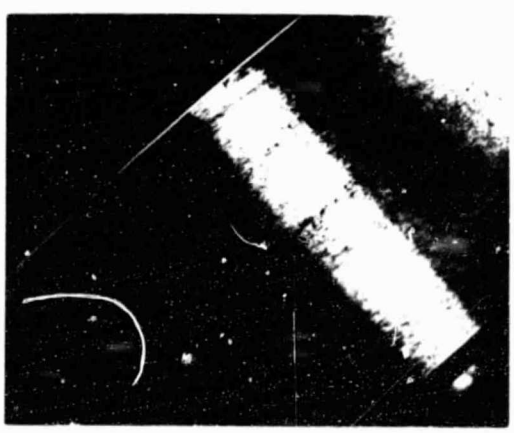

EDGE OF ROTOR SHOWING CRACK COMPLETELY THROUGH

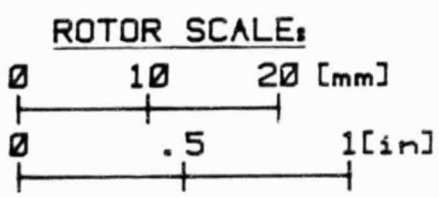

FIGURE 21 - PHOTOGRAPHS OF POST TEST FACE SURFACES OF THE CONED FACE PUSHER TYPE SEAL BALANCED TO 76.3%. ROTOR CRACKED AT THE END OF THE TEST AT 5400 RPM AND 0 kPa SYSTEM PRESSURE.

REAR SEAL

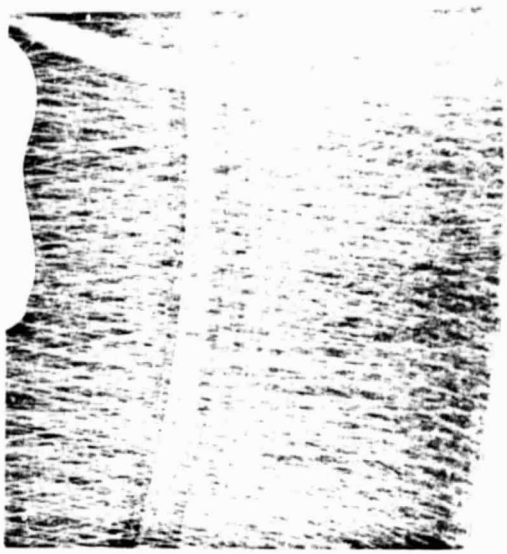

MATING RING (ROTOR)

PRIMARY RING SCALE:

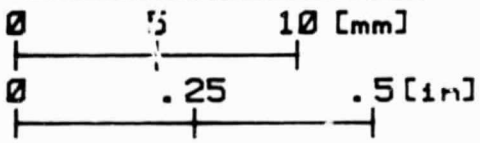

ROTOR SCALE:

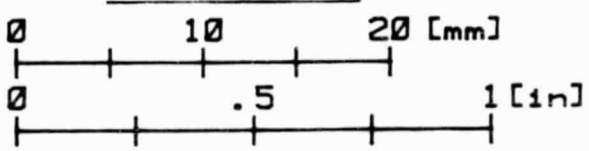

FRONT SEAL

PRIMARY RING (INSERT)

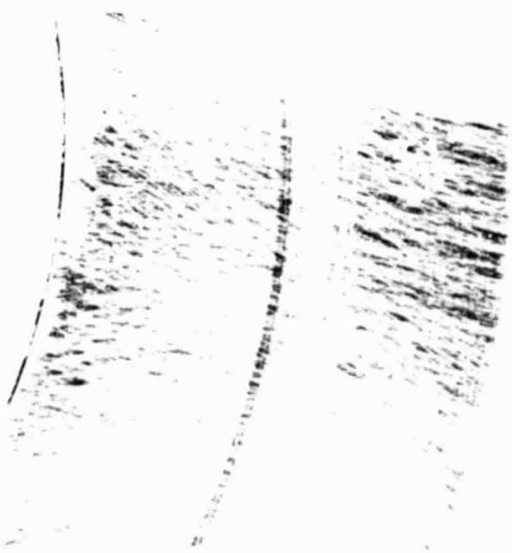

MATING RING (ROTOR)

FIGURE 22 - PHOTOGRAPHS OF POST TEST FACE SURFACES OF THE BELLOWS TYPE CONED FACE SEAL.

ORIGINAL PAGE IS
OF POOR QUALITY

PRIMARY RINGS
(STATOR)
FACE OD FACE ID

MATING RINGS
(ROTOR)

FRONT SEAL WITH
NON-CONTACTING
TUNGSTEN CARBIDE
FACES.

PRIMARY RING SCALE:

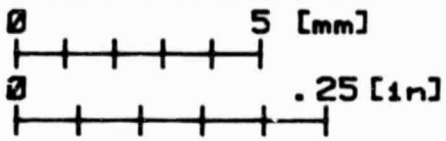

REAR SEAL WITH
CONTACTING CARBON
PRIMARY RING
(56.5% BALANCE)

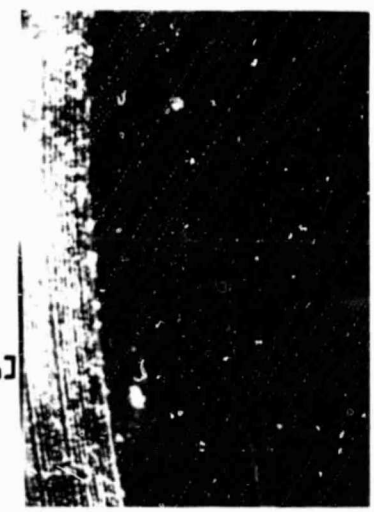

ROTOR SCALE:

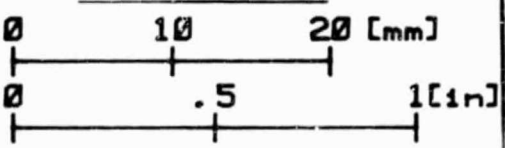

REAR SEAL WITH
NON-CONTACTING
TUNGSTEN CARBIDE
PRIMARY RING

FIGURE 23 - PHOTOGRAPHS OF POST TEST FACE SURFACES OF THE CONED FACE PUSHER TYPE SEAL BALANCED TO 51.3%. NO WEAR MARKS CAN BE OBSERVED ON THE NON-CONTACTING TUNGSTEN CARBIDE FACES.

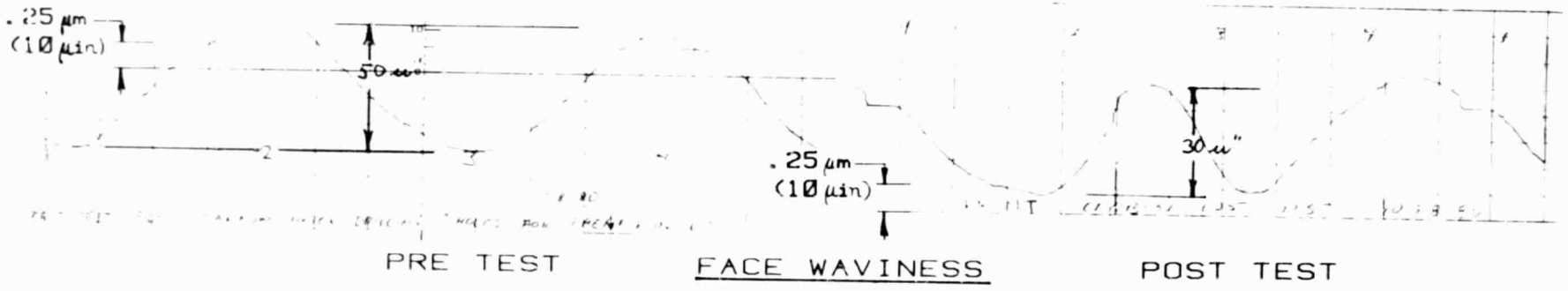

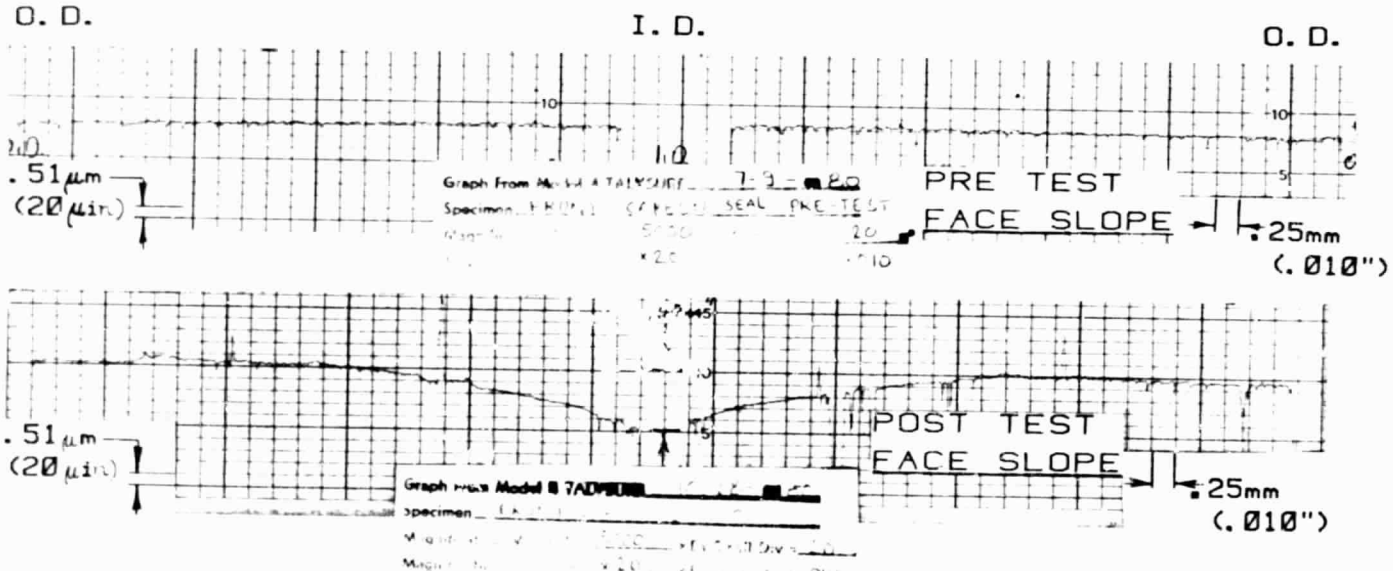

FIGURE 24. PROFILE TRACES OF THE PRIMARY RING USED IN THE TEST WITH THE STANDARD FLAT FACE PUSHER TYPE 8B SEAL BALANCED TO 76.3%

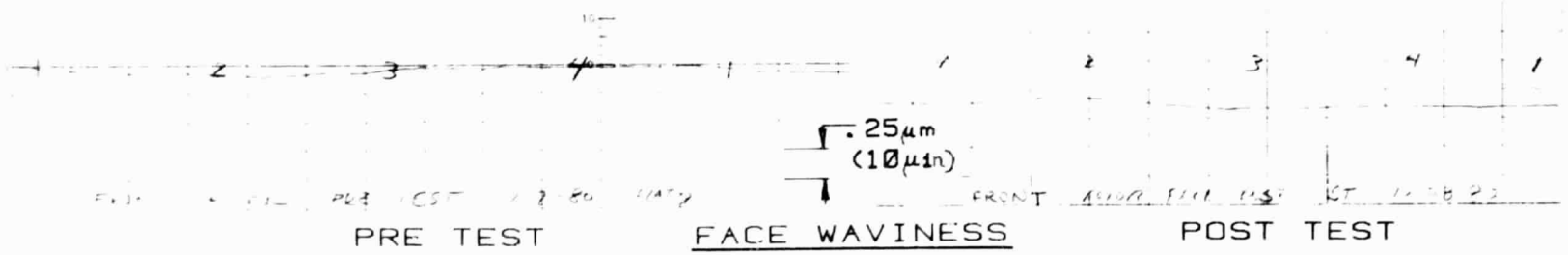

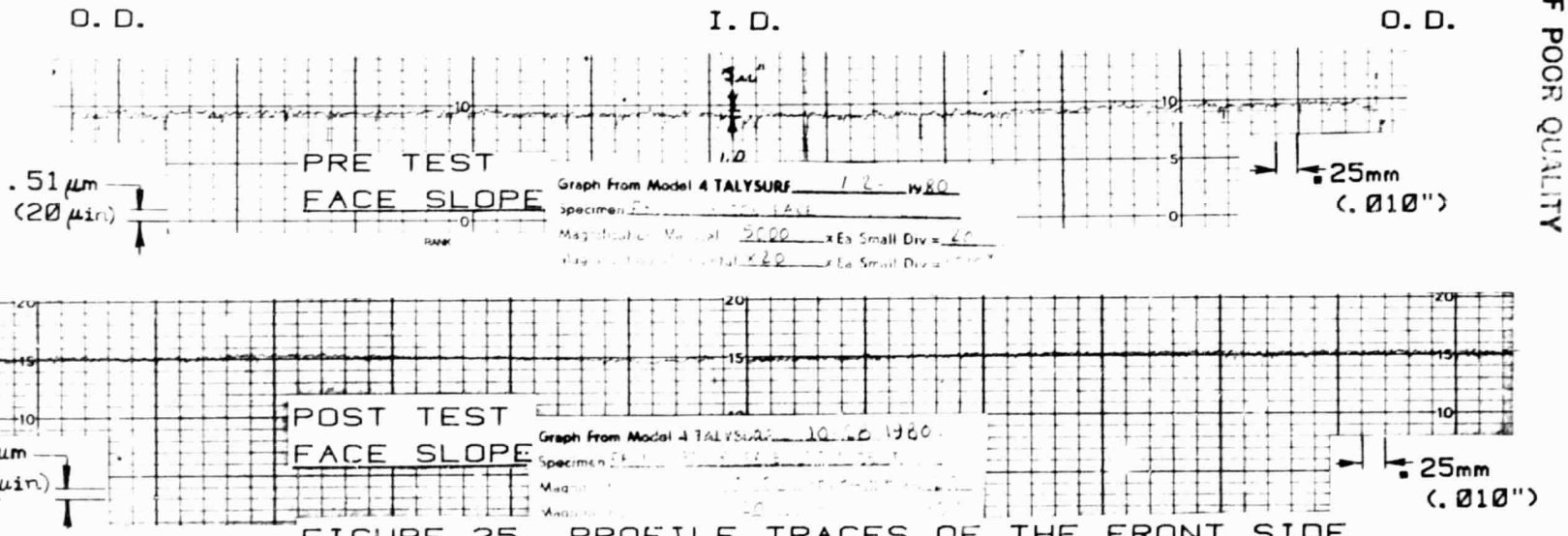

FIGURE 25. PROFILE TRACES OF THE FRONT SIDE OF THE ROTOR USED AS A MATING FACE IN THE TEST WITH THE STANDARD FLAT FACE PUSHER TYPE 8B SEAL BALANCED TO 76.3%

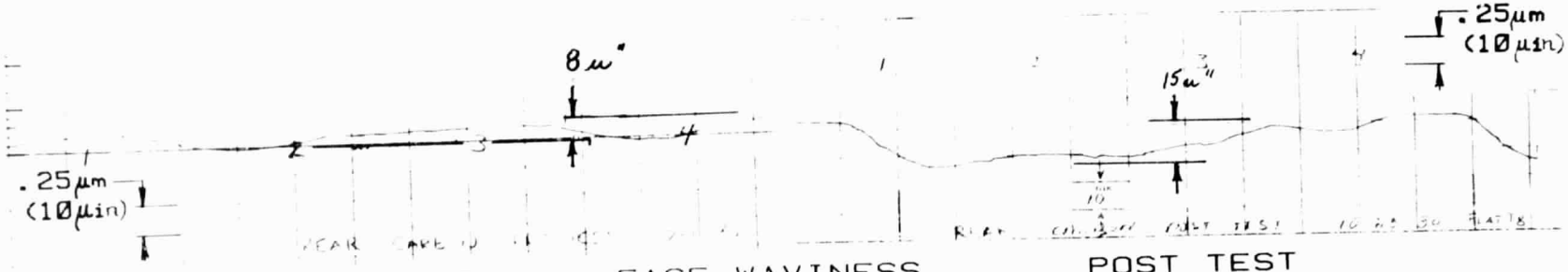

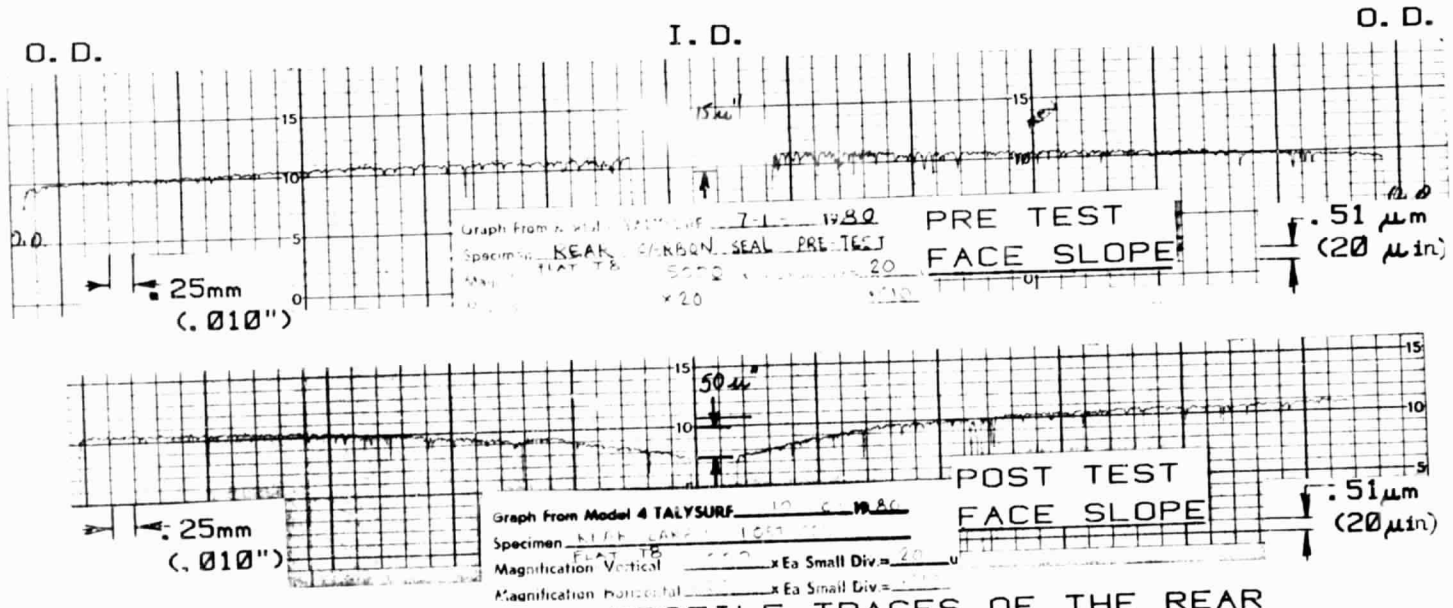

FIGURE 26. PROFILE TRACES OF THE REAR PRIMARY RING USED IN THE TEST WITH THE STANDARD FLAT FACE PUSHER TYPE 8B SEAL BALANCED TO 76.3%

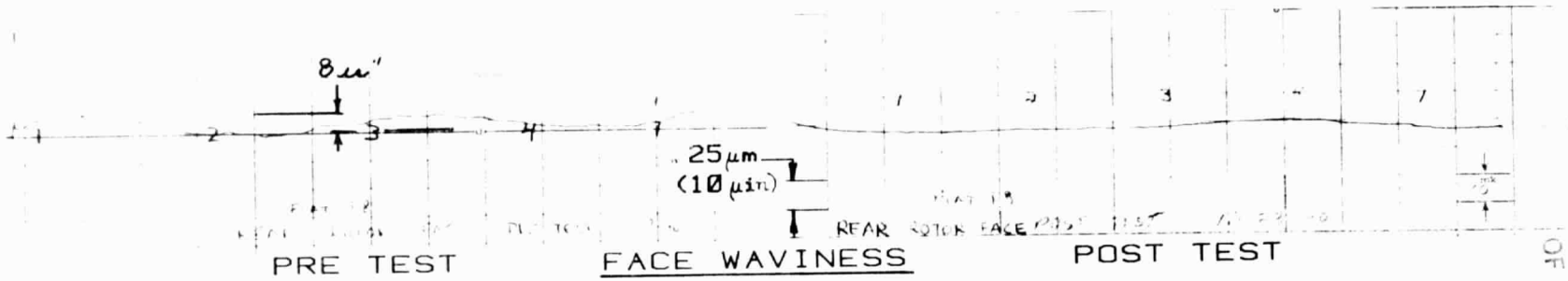

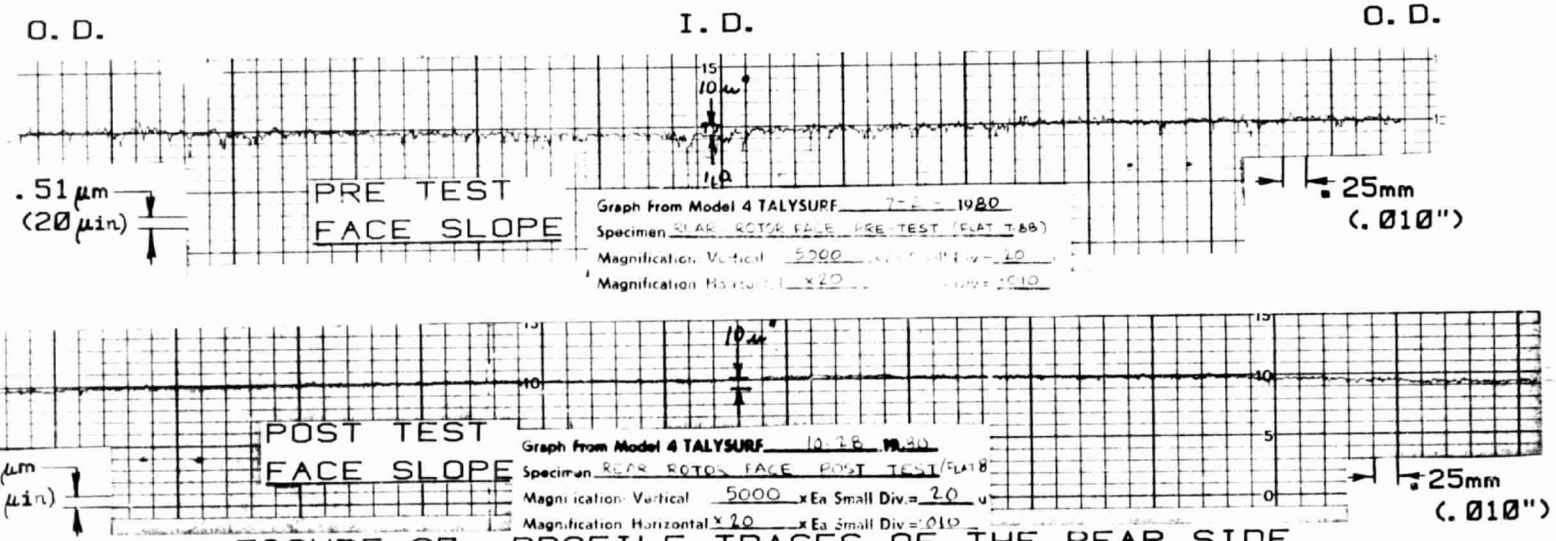

FIGURE 27. PROFILE TRACES OF THE REAR SIDE OF THE ROTOR USED AS A MATING FACE IN IN THE TEST WITH THE STANDARD FLAT FACE PUSHER TYPE 8B SEAL BALANCED TO 76.3%

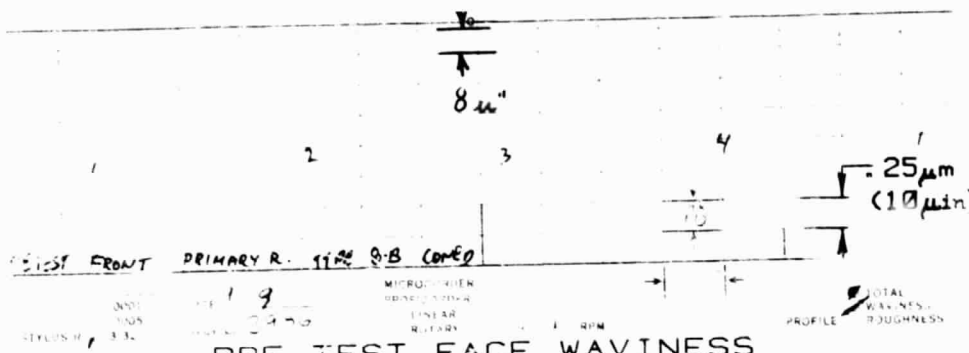

PRE TEST FACE WAVINESS

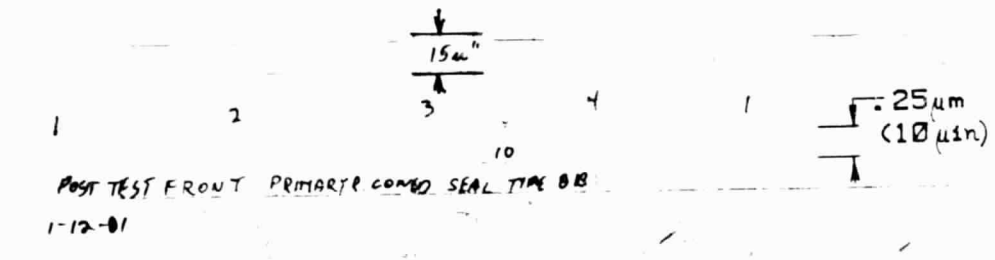

POST TEST FACE WAVINESS

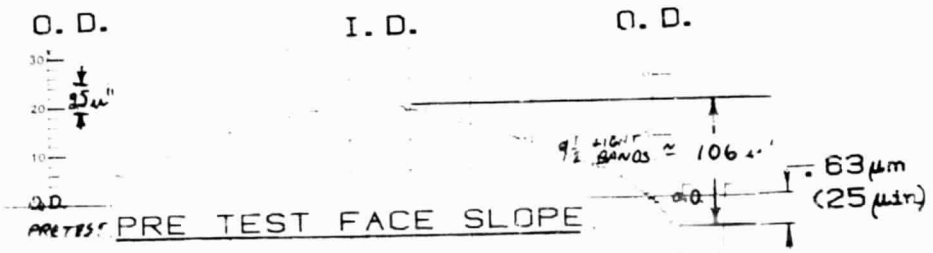

PRE TEST FACE SLOPE

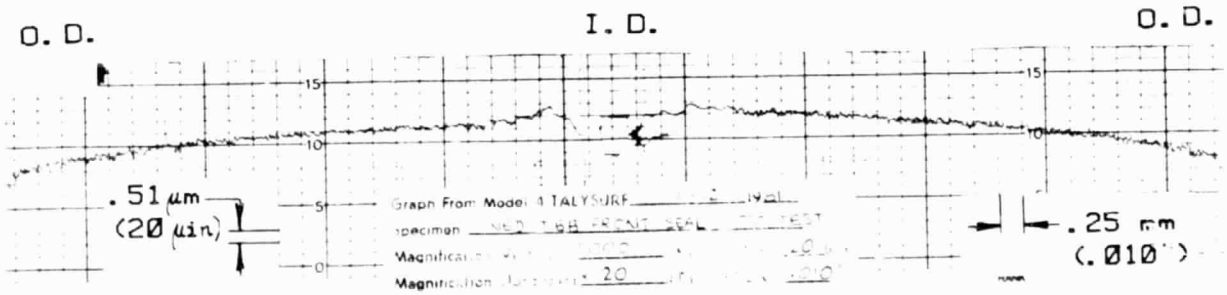

POST TEST FACE SLOPE

FIGURE 28. PROFILE TRACES OF THE FRONT PRIMARY RING USED IN THE TEST WITH THE CONE FACE PUSHER TYPE 8B SEAL BALANCED TO 70 3%

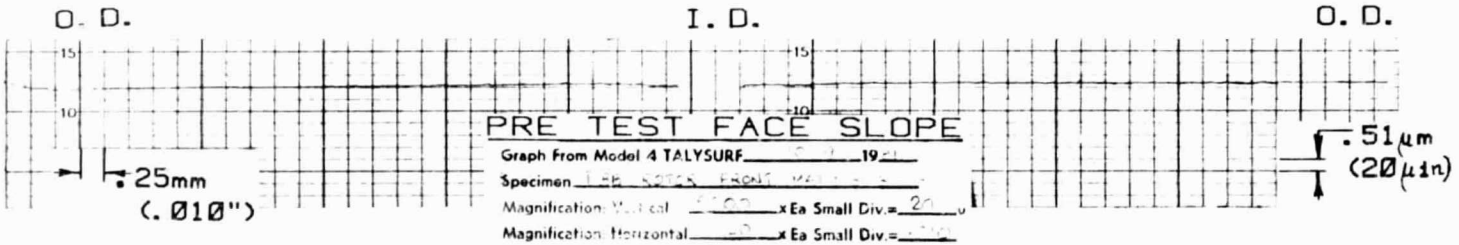

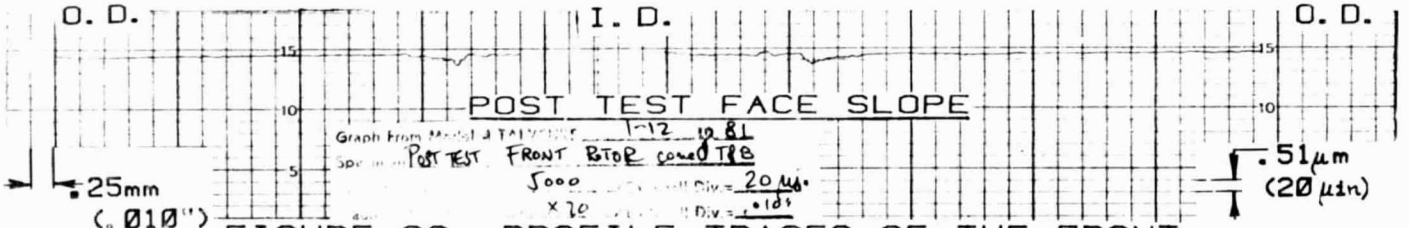

FIGURE 29. PROFILE TRACES OF THE FRONT SIDE OF THE ROTOR USED AS A MATING FACE IN THE TEST WITH THE CONE FACE PUSHER TYPE 8B SEAL BALANCED TO 76.3%. THE ROTOR CRACKED DUE TO THE THERMAL EXPANSION.

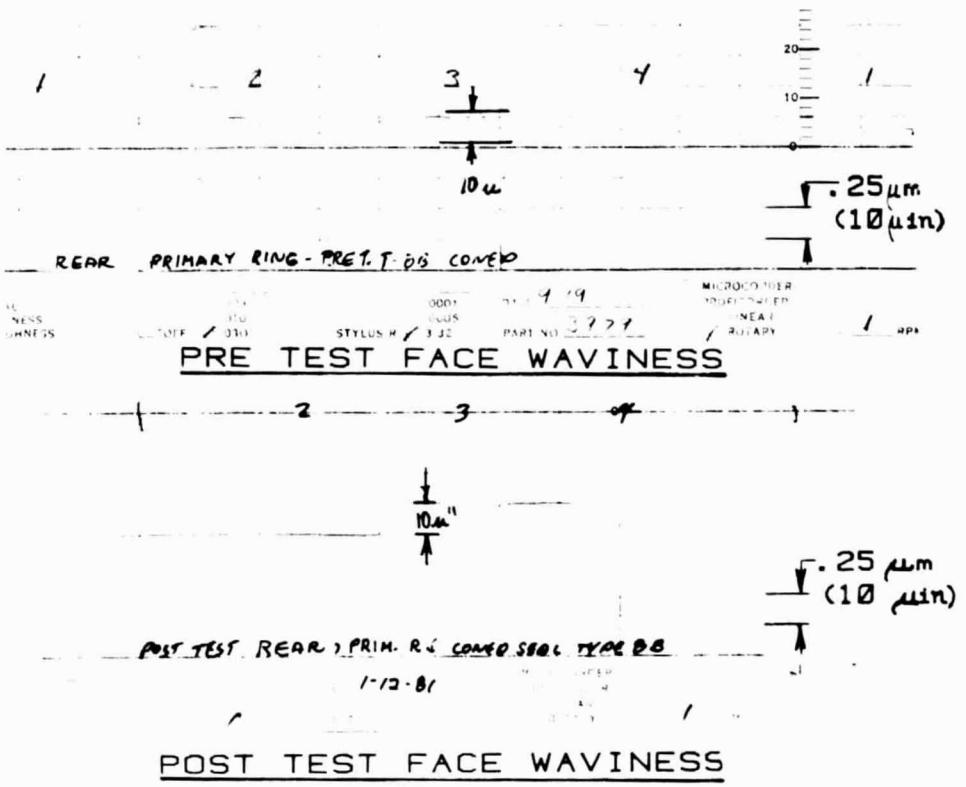

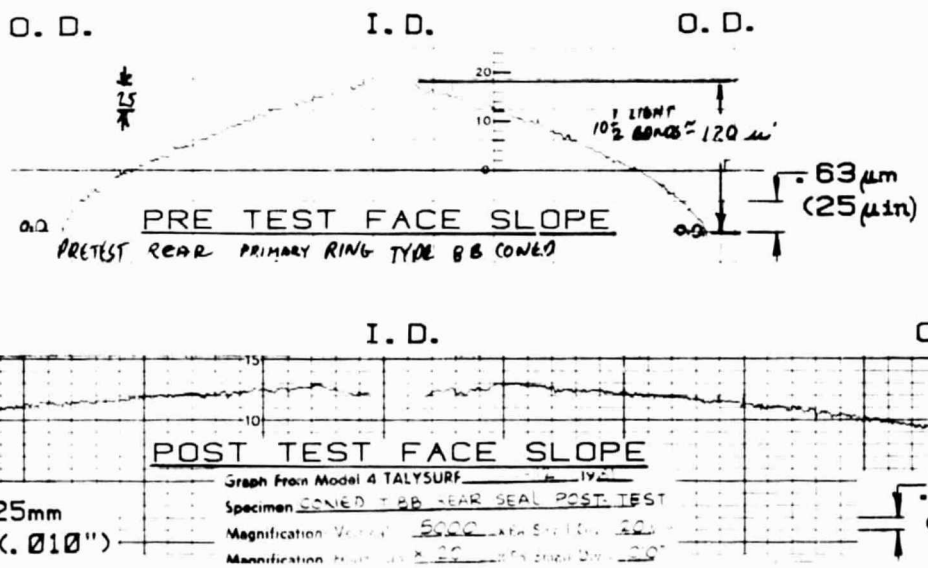

FIGURE 30. PROFILE TRACES OF THE REAR PRIMARY RING USED IN THE TEST WITH THE CONE FACE PUSHER TYPE 8B SEAL BALANCED TO 76.3%

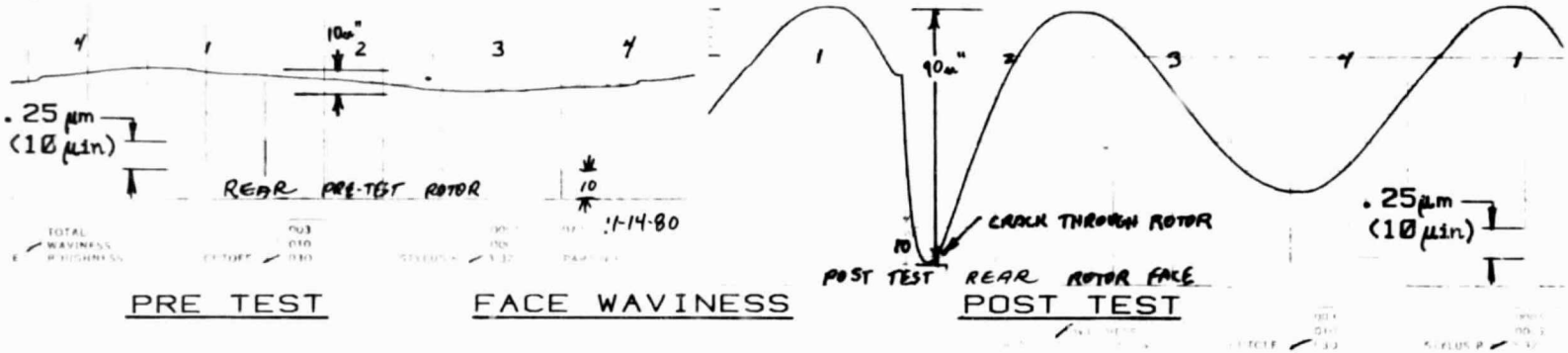

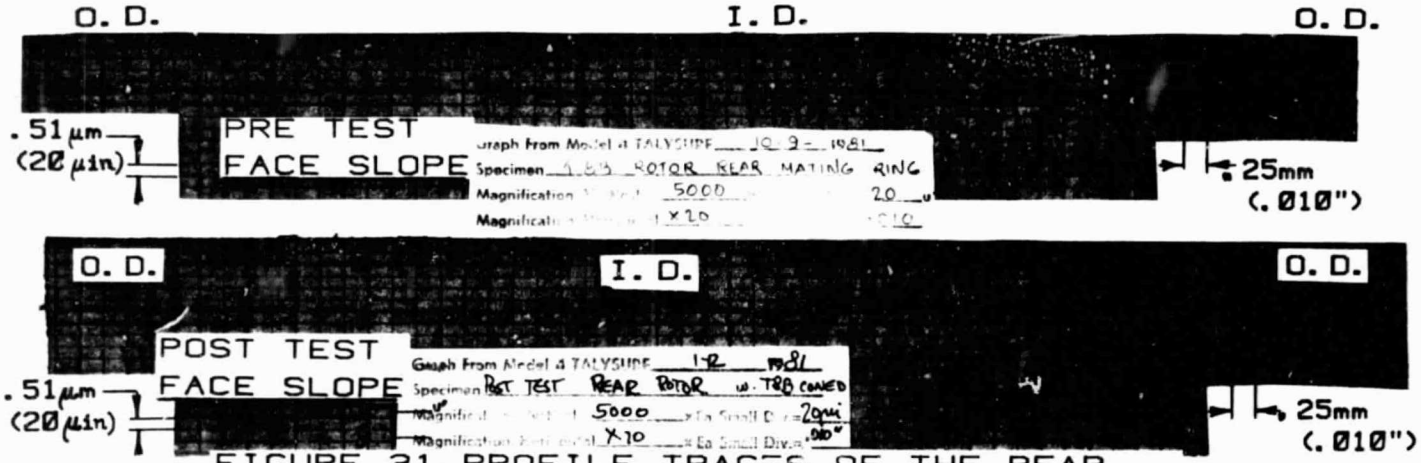

FIGURE 31. PROFILE TRACES OF THE REAR SIDE OF THE ROTOR USED AS A MATING FACE IN THE TEST WITH THE CONE FACE PUSHER TYPE 8B SEAL BALANCED TO 76.3%

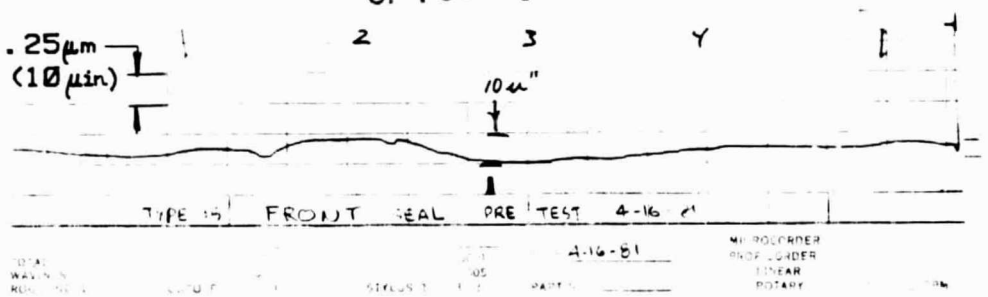

PRE TEST FACE WAVINESS

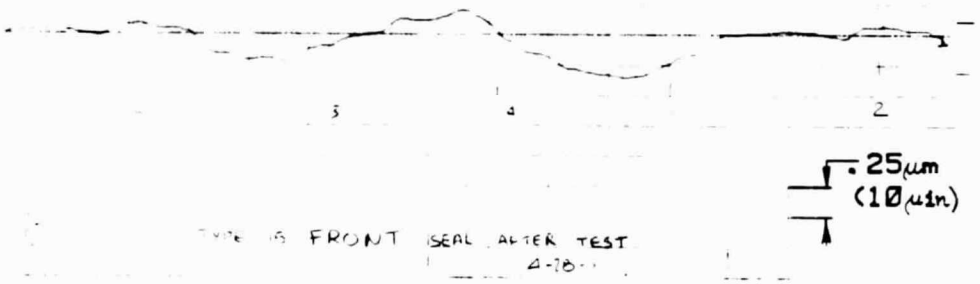

POST TEST FACE WAVINESS

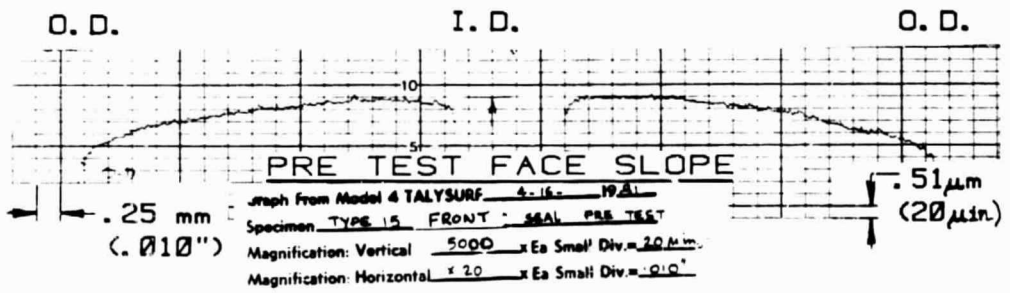

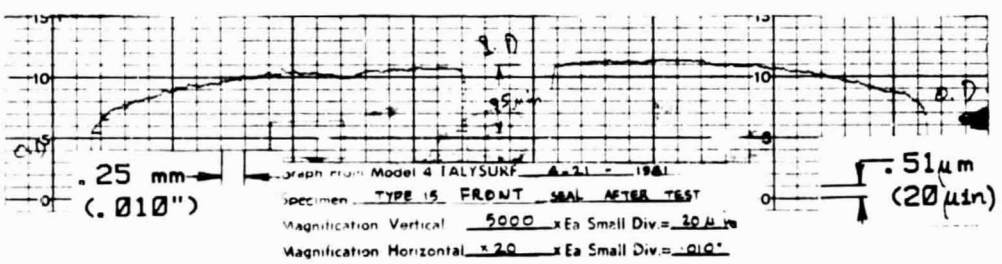

POST TEST FACE SLOPE

FIGURE 32. PROFILE TRACES OF THE FRONT PRIMARY RING (INSERT) USED IN THE TEST WITH THE CONE BELLOWS TYPE 15 SEAL. WEAR OCCURED ON THE I. D. OF THE SEAL FACES.

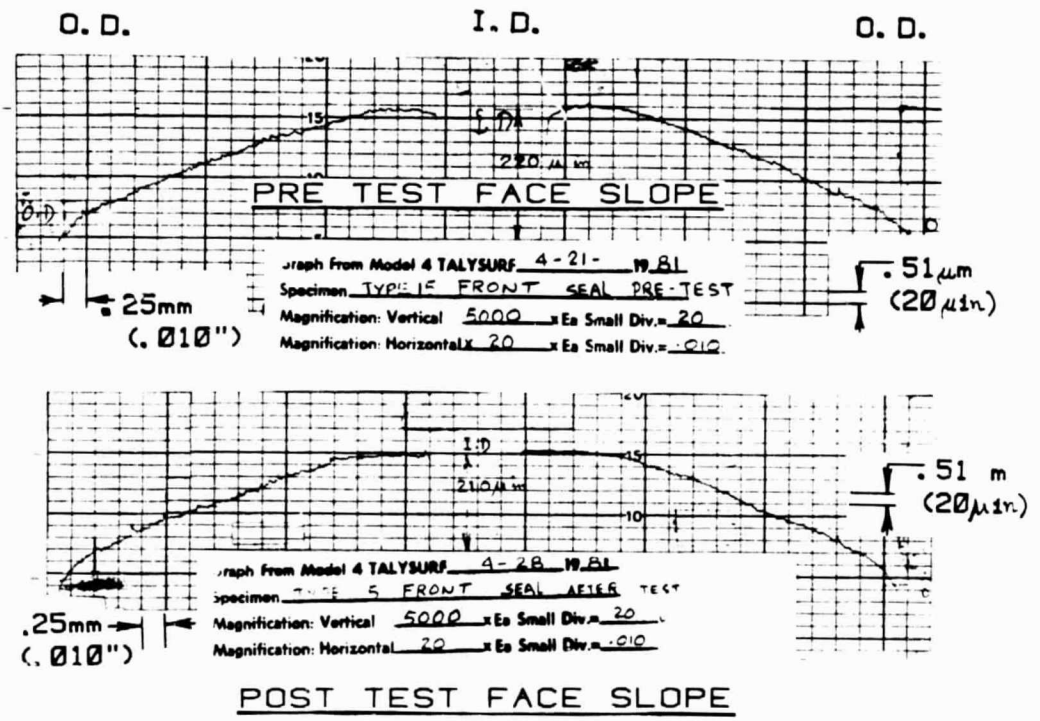

FIGURE 33. PROFILE TRACES OF THE FRONT PRIMARY RING (INSERT) USED IN THE TEST WITH THE CONE BELLOWS TYPE 15 SEAL. NO WEAR OCCURED ON THE SEAL FACES.

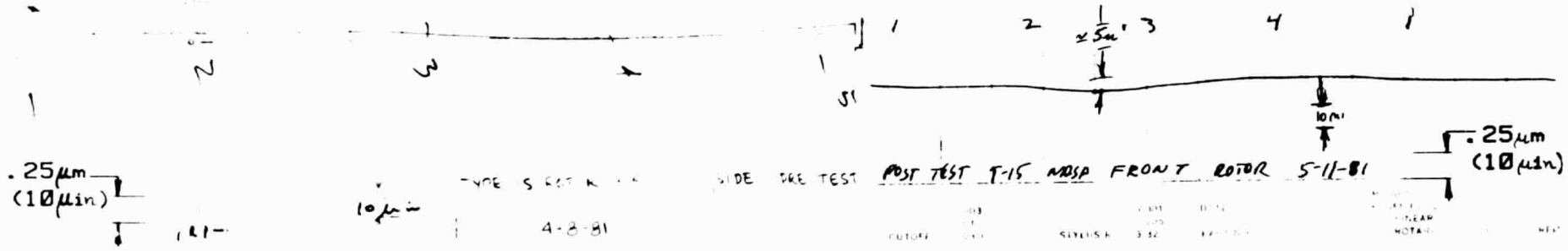

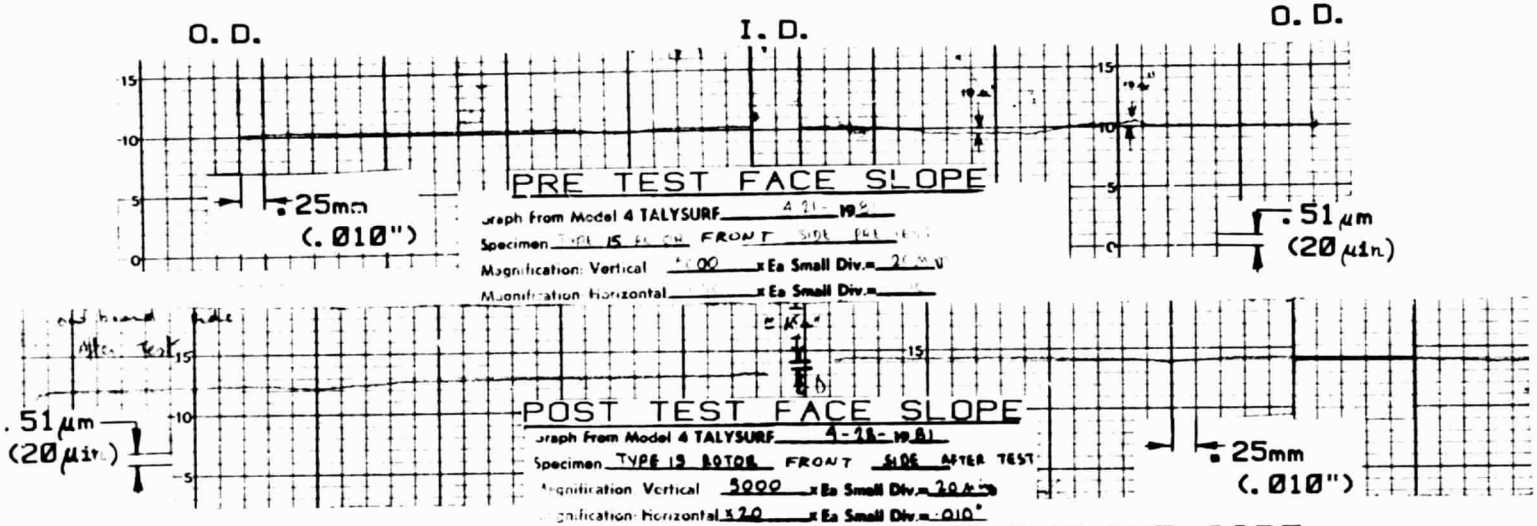

FIGURE 34. PROFILE TRACES OF THE FRONT SIDE OF THE ROTOR USED AS A MATING SURFACE DURING THE TESTS WITH THE CONED FACE BELLOWS TYPE SEAL.

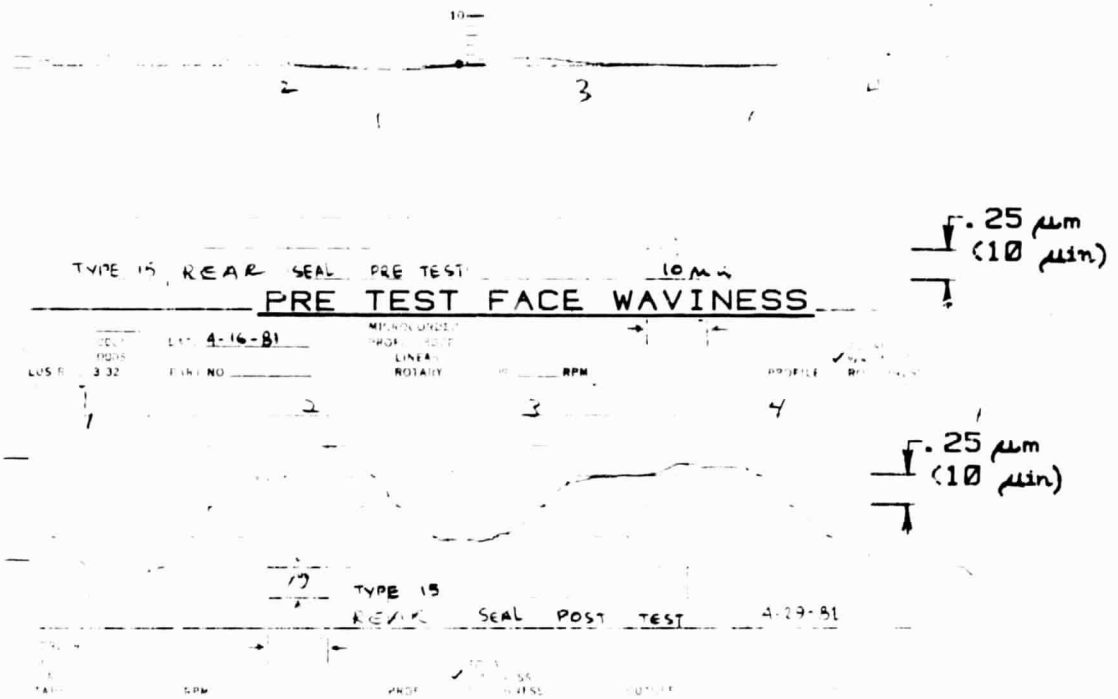

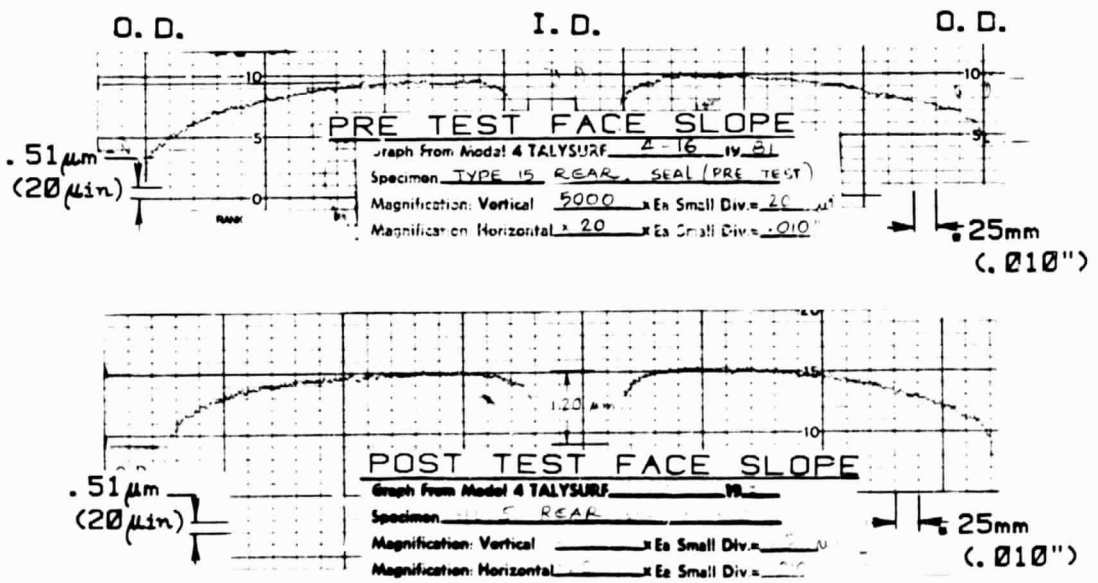

FIGURE 35. PROFILE TRACES OF THE REAR PRIMARY RING (INSERT) USED IN THE TEST WITH THE COINED FACE BELLOWS TYPE SEAL.

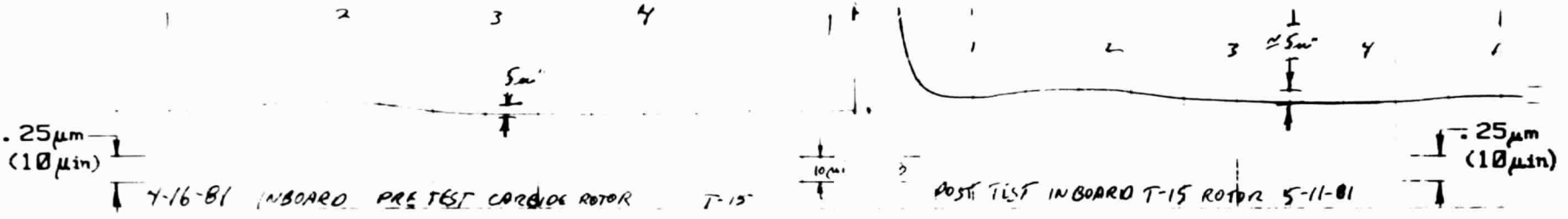

PRE TEST FACE WAVINESS POST TEST

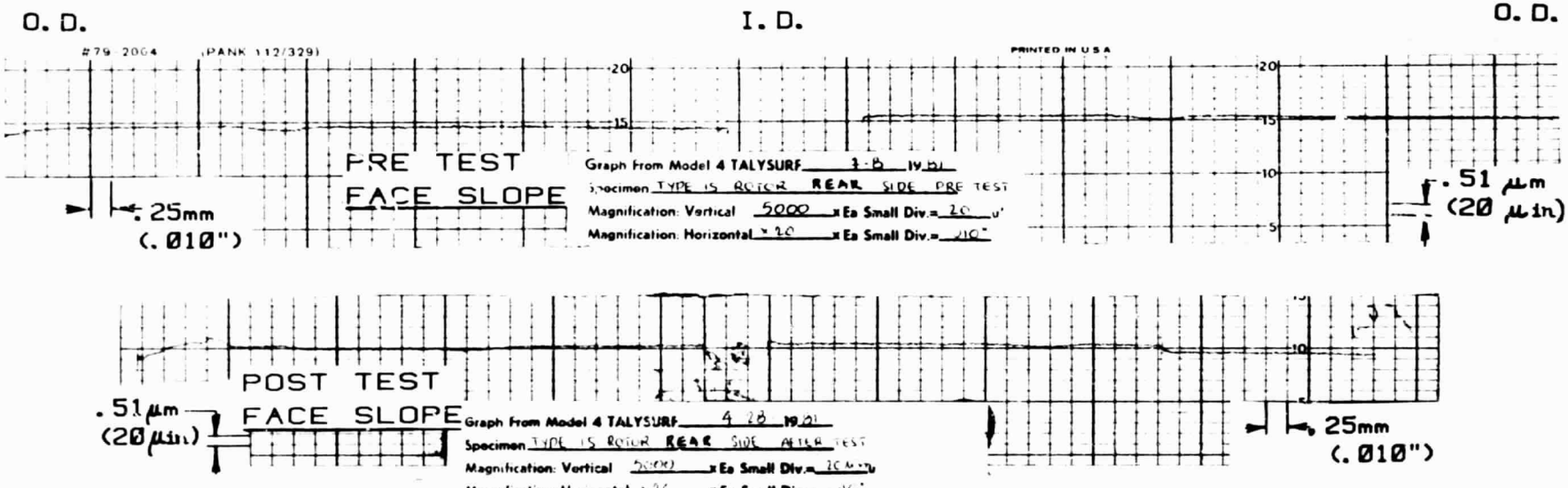

FIGURE 36. PROFILE TRACES OF THE REAR SIDE OF THE ROTOR USED AS A MATING SURFACE DURING THE TEST WITH THE CONED FACE BELLOWS TYPE SEAL

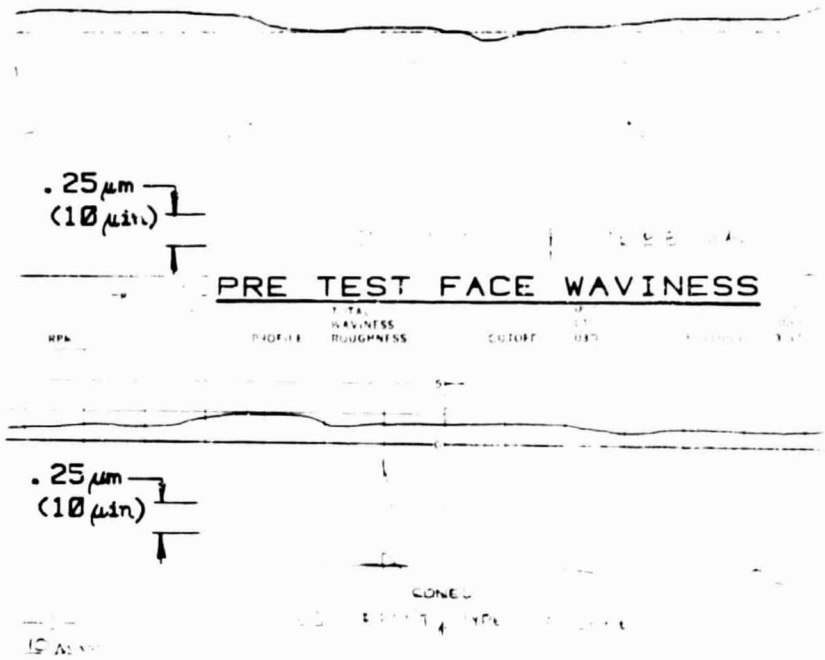

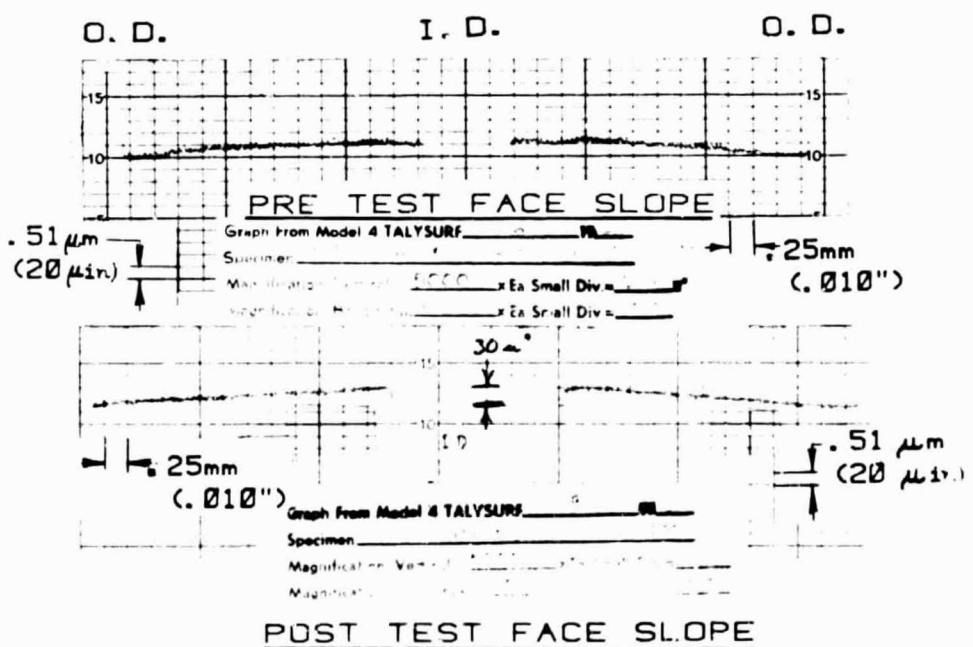

FIGURE 37. PROFILE TRACES OF THE FRONT PRIMARY RING USED IN THE TEST WITH THE CONED FACE PUSHER TYPE SEAL BALANCED TO 51.3%.

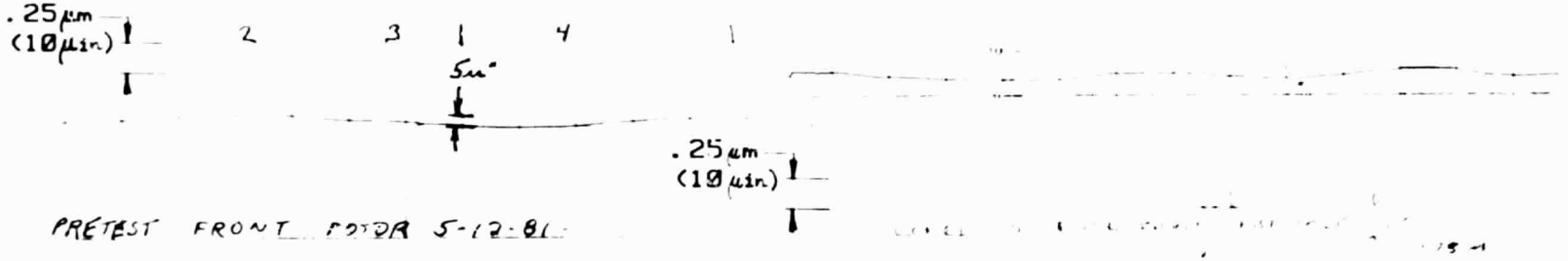

PRE TEST FACE WAVINESS POST TEST

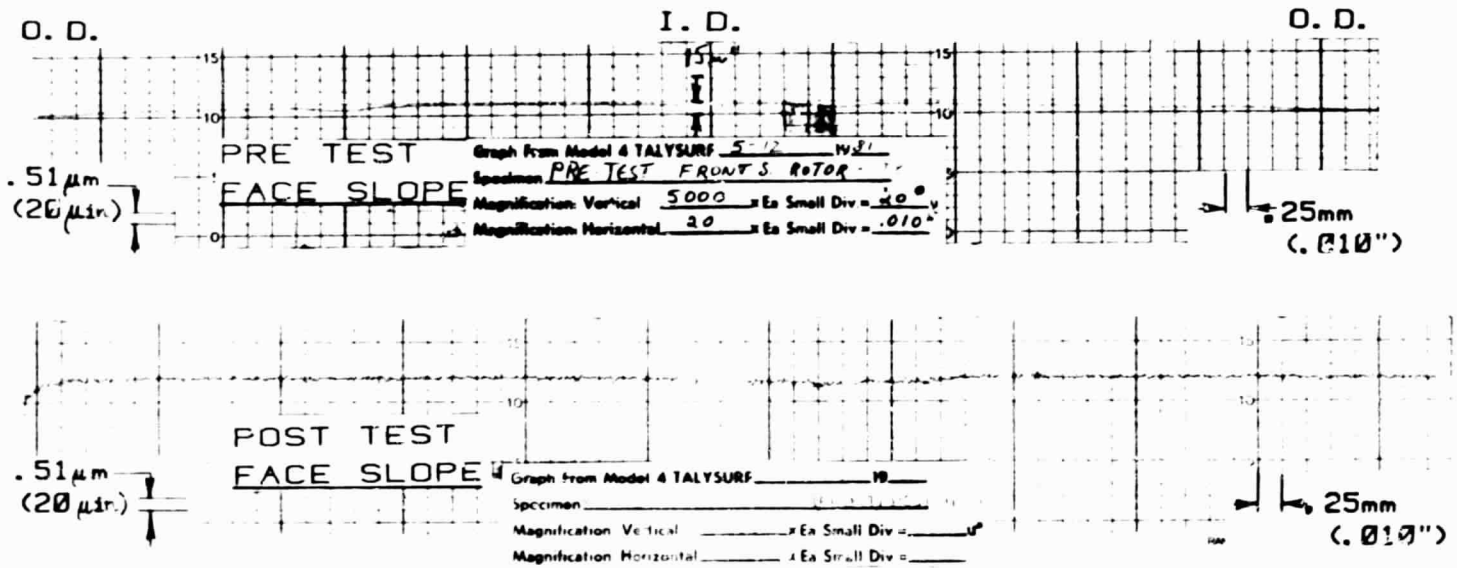

FIGURE 38. PROFILE TRACES OF THE FRONT SIDE OF THE ROTOR USED AS A MATING FACE IN THE TEST WITH THE CONED FACE PUSHER TYPE SEAL BALANCED TO 51.3%

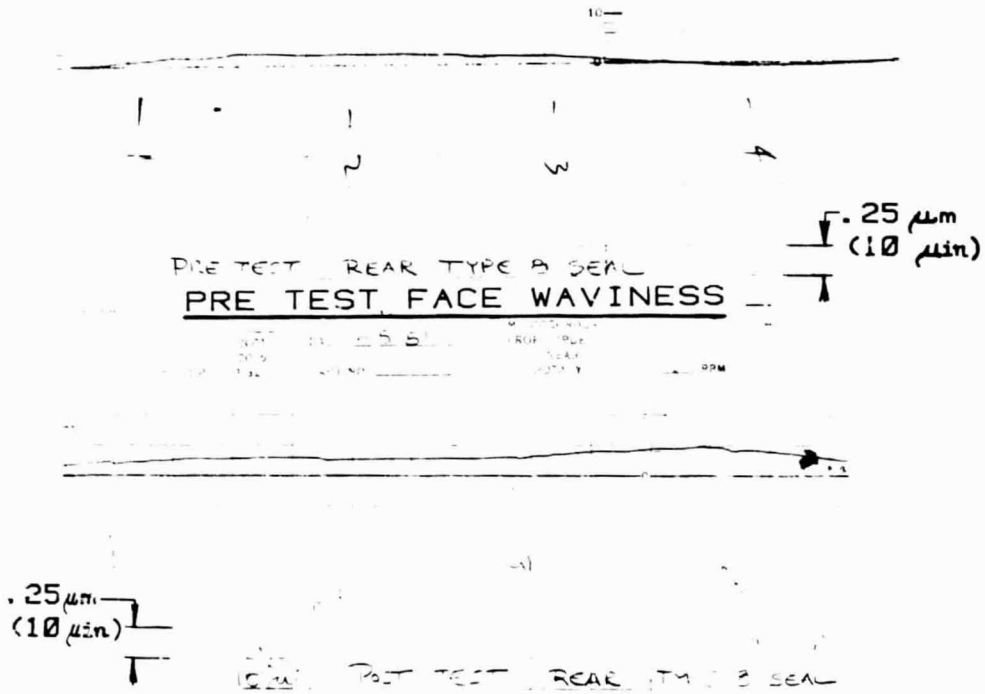

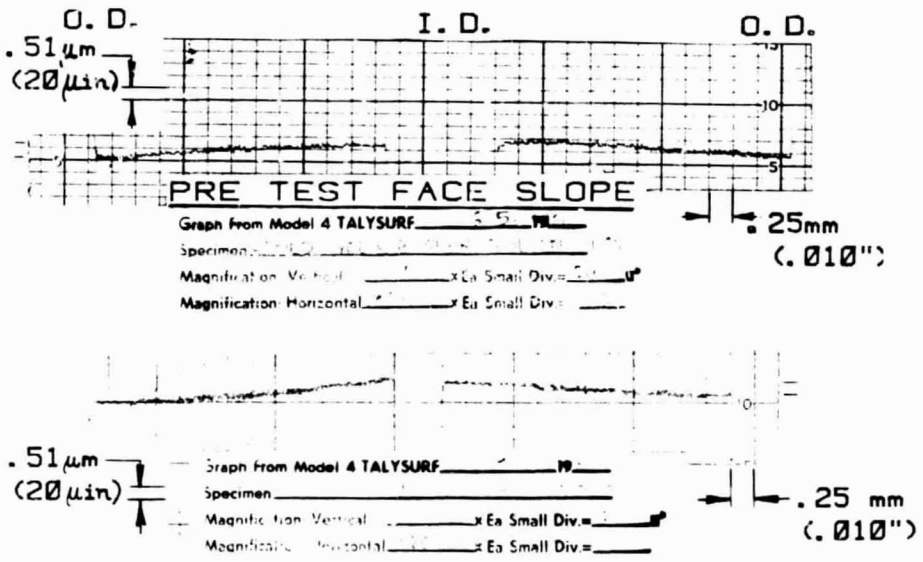

FIGURE 39. PROFILE TRACES OF THE REAR PRIMARY RING USED IN THE TEST WITH THE CONED FACE PUSHER TYPE SEAL BALANCED TO 51.3%.

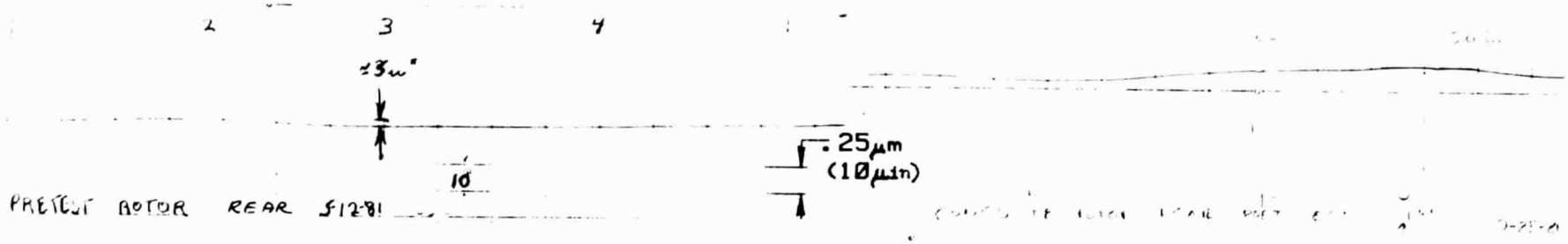

PRE TEST FACE WAVINESS POST TEST

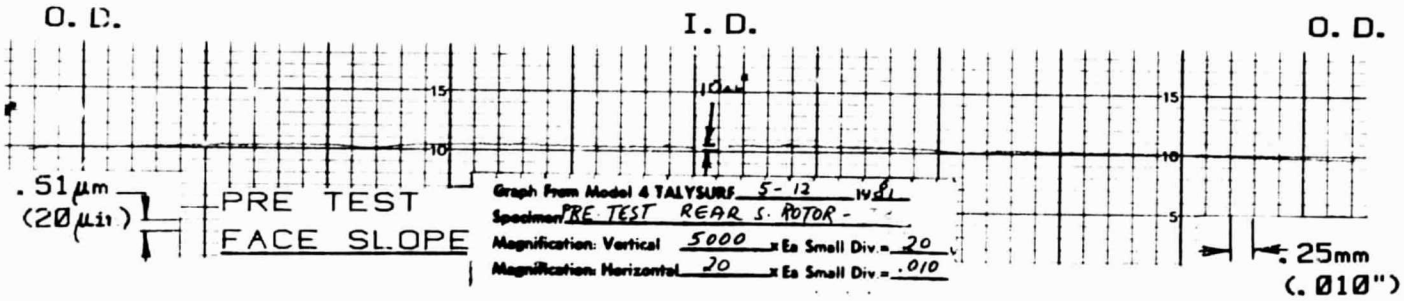

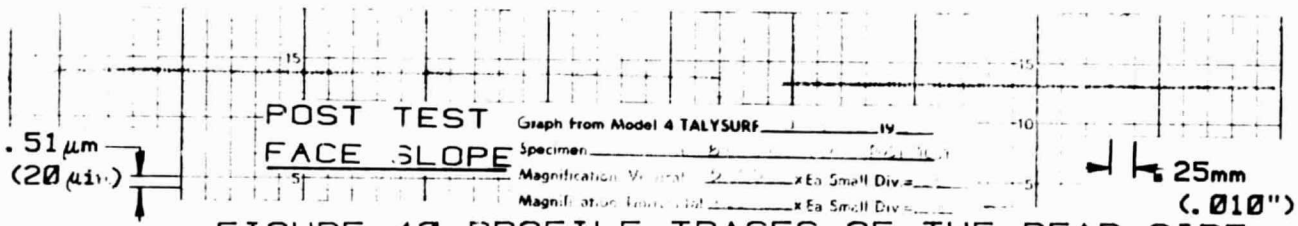

FIGURE 40. PROFILE TRACES OF THE REAR SIDE OF THE ROTOR USED IN THE TEST WITH THE CONED FACE PUSHER TYPE SEAL BALANCED TO 51.3%

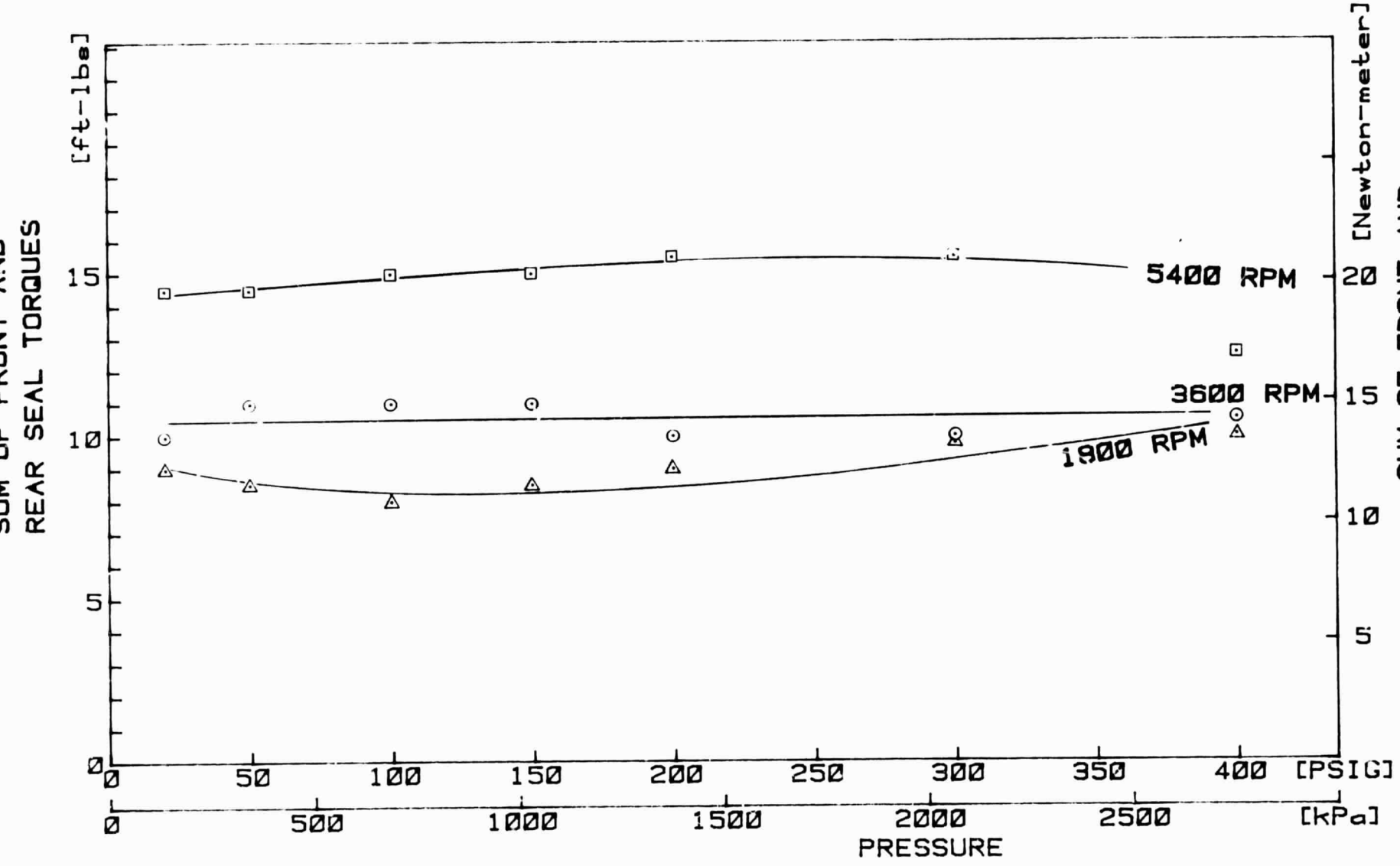

FIGURE 41 -- TYPICAL PEAK TORQUE AT VARIOUS PRESSURES AND SPEEDS OF THE FLAT FACE PUSHER TYPE FRONT AND REAR SEALS AS RECORDED DURING A 3 MINUTE INTERVAL UNDER THE STABILIZED SEAL FACE TEMPERATURE.

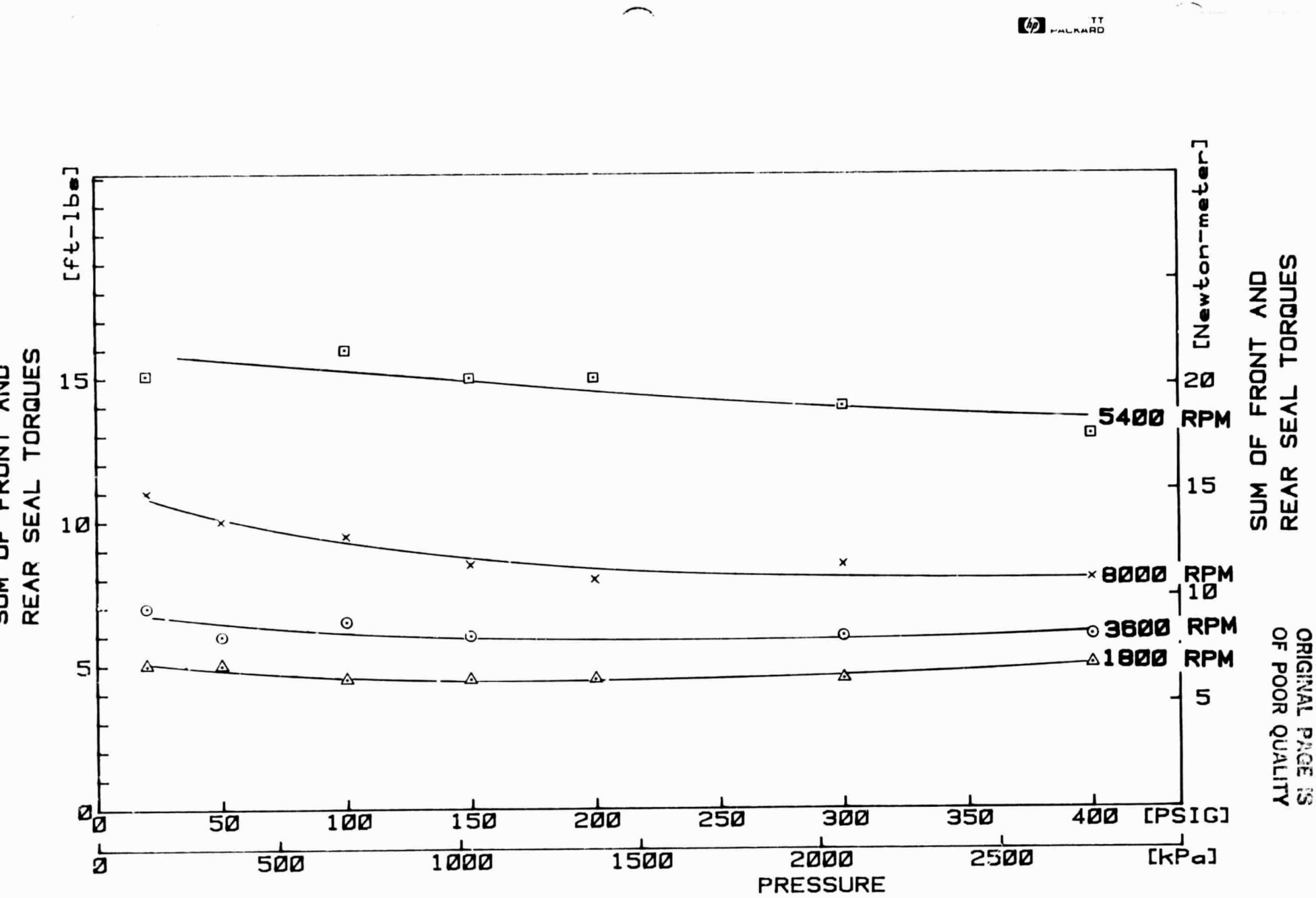

FIGURE 42 - TYPICAL PEAK TORQUE AT VARIOUS PRESSURES AND SPEEDS OF THE CONED FACE PUSHER TYPE FRONT AND REAR SEALS RECORDED DURING A 3 MINUTE INTERVAL UNDER THE STABILIZED SEAL FACE TEMPERATURE.

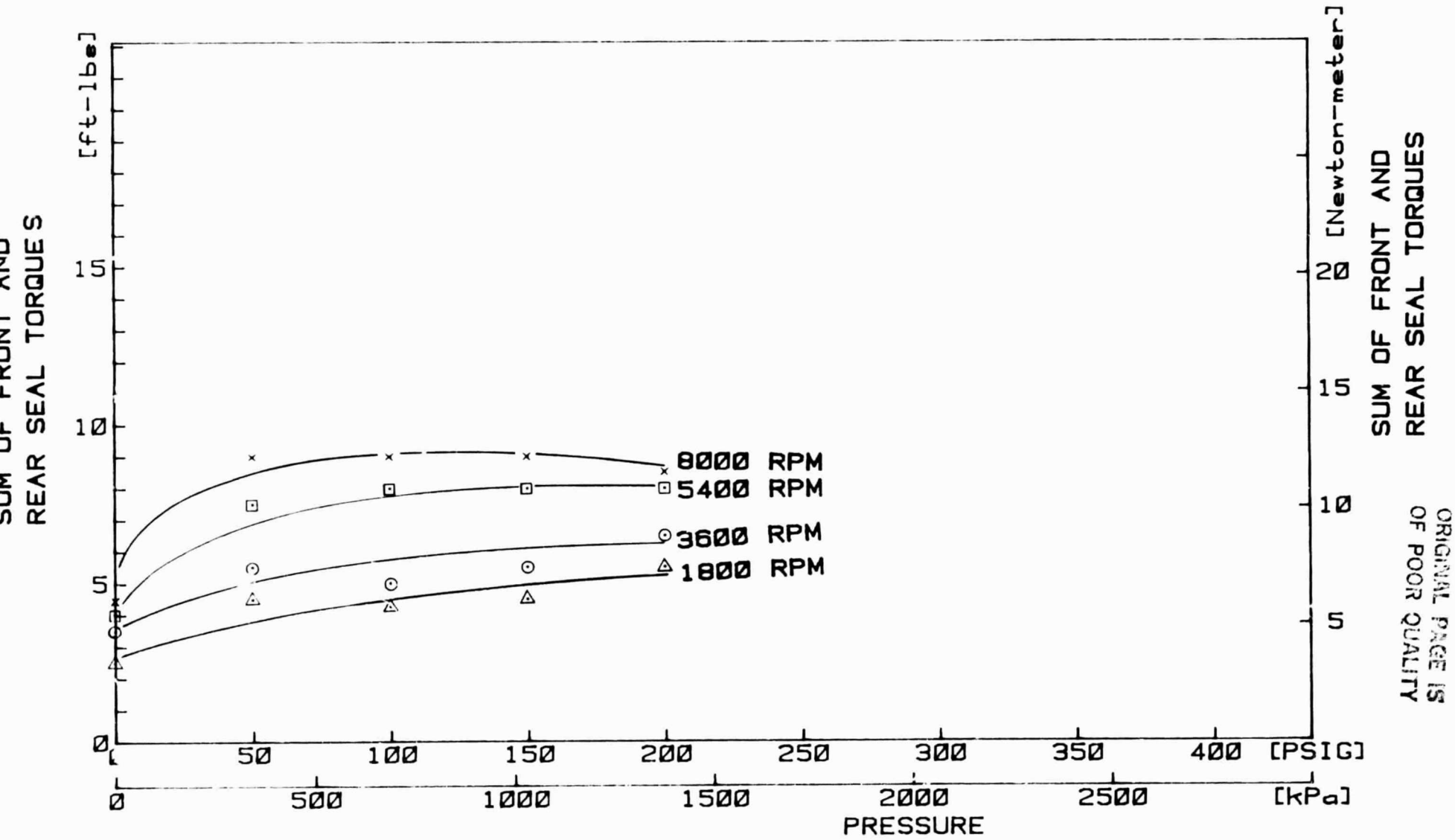

FIGURE 43 - TYPICAL PEAK TORQUE AT VARIOUS PRESSURES AND SPEEDS OF THE CONED FACE BELLOWS TYPE FRONT AND REAR SEALS RECORDED DURING A 3 MINUTE INTERVAL UNDER THE STABILIZED SEAL FACE TEMPERATURE.

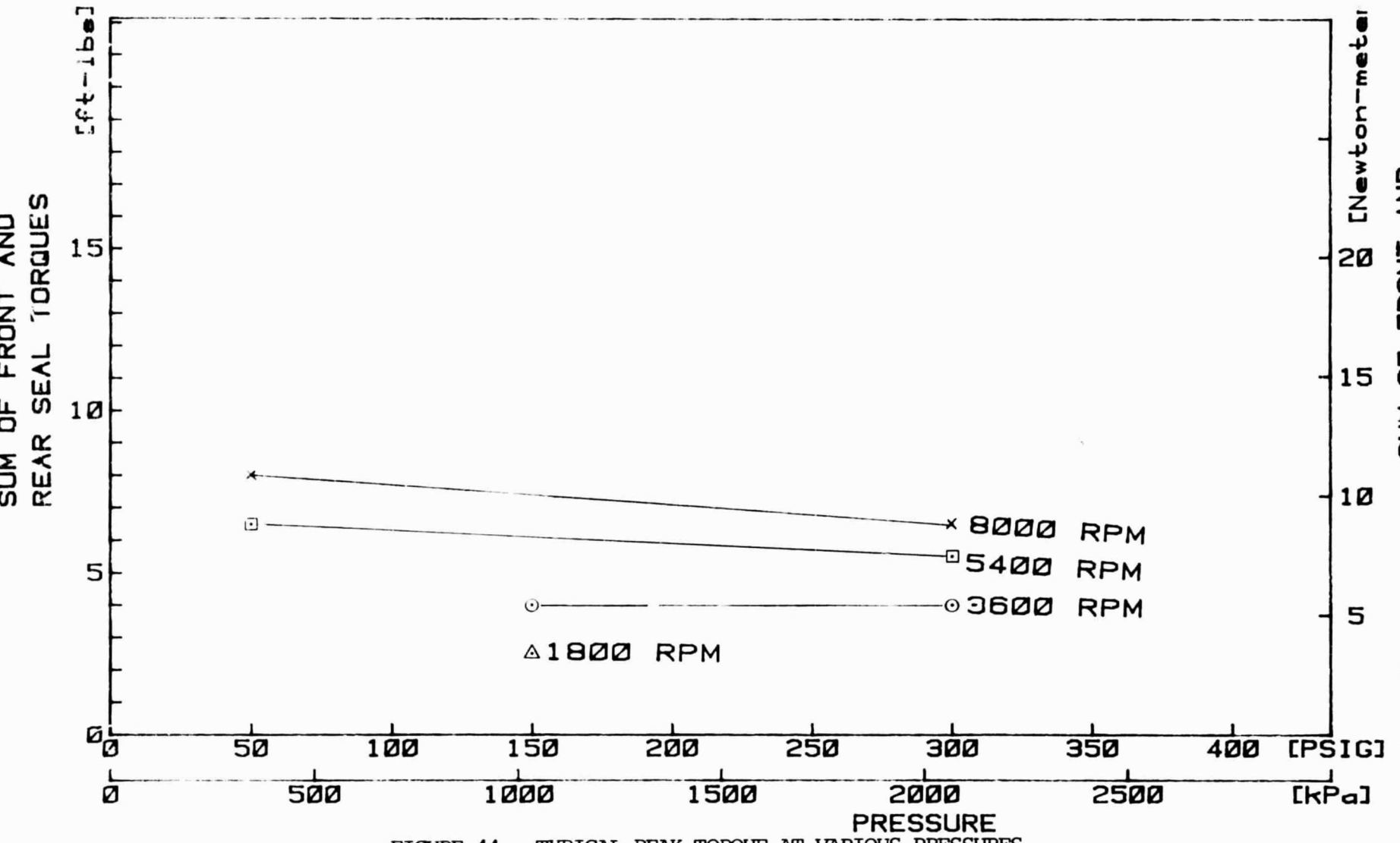

FIGURE 44 - TYPICAL PEAK TORQUE AT VARIOUS PRESSURES AND SPEEDS OF THE CONED FACE PUSHER TYPE SEAL, BALANCED TO 51.3%. THE CURVES REPRESENT CHARACTERISTIC MAXIMUM TORQUE AS RECORDED DURING A 3 MINUTE INTERVAL UNDER THE STABILIZED SEAL FACE TEMPERATURE.

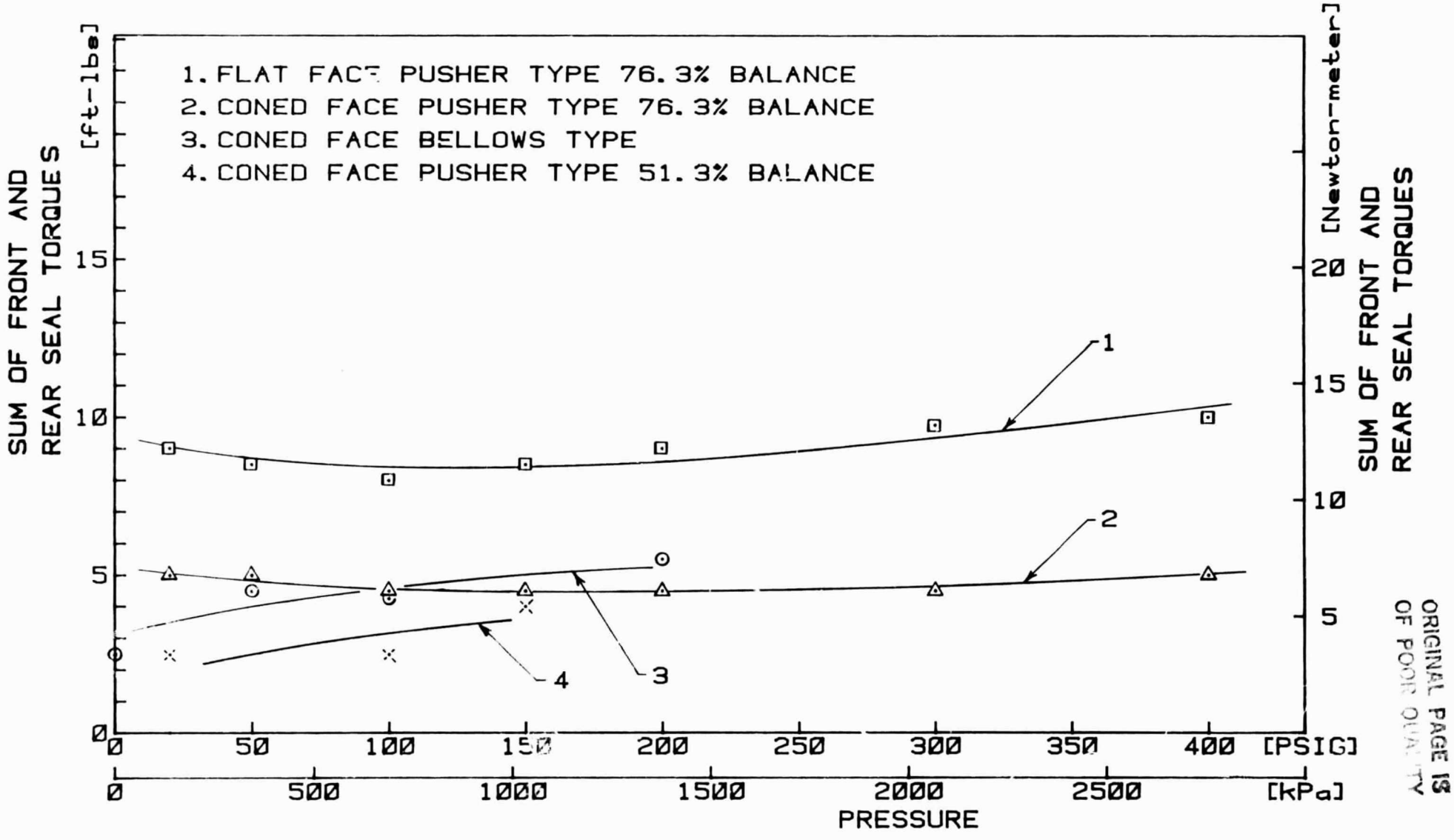

FIGURE 45 - COMPARISON OF THE TYPICAL PEAK TORQUE VALUES OF THE TESTED SEALS AT 1800 RPM AND VARIOUS PRESSURES.

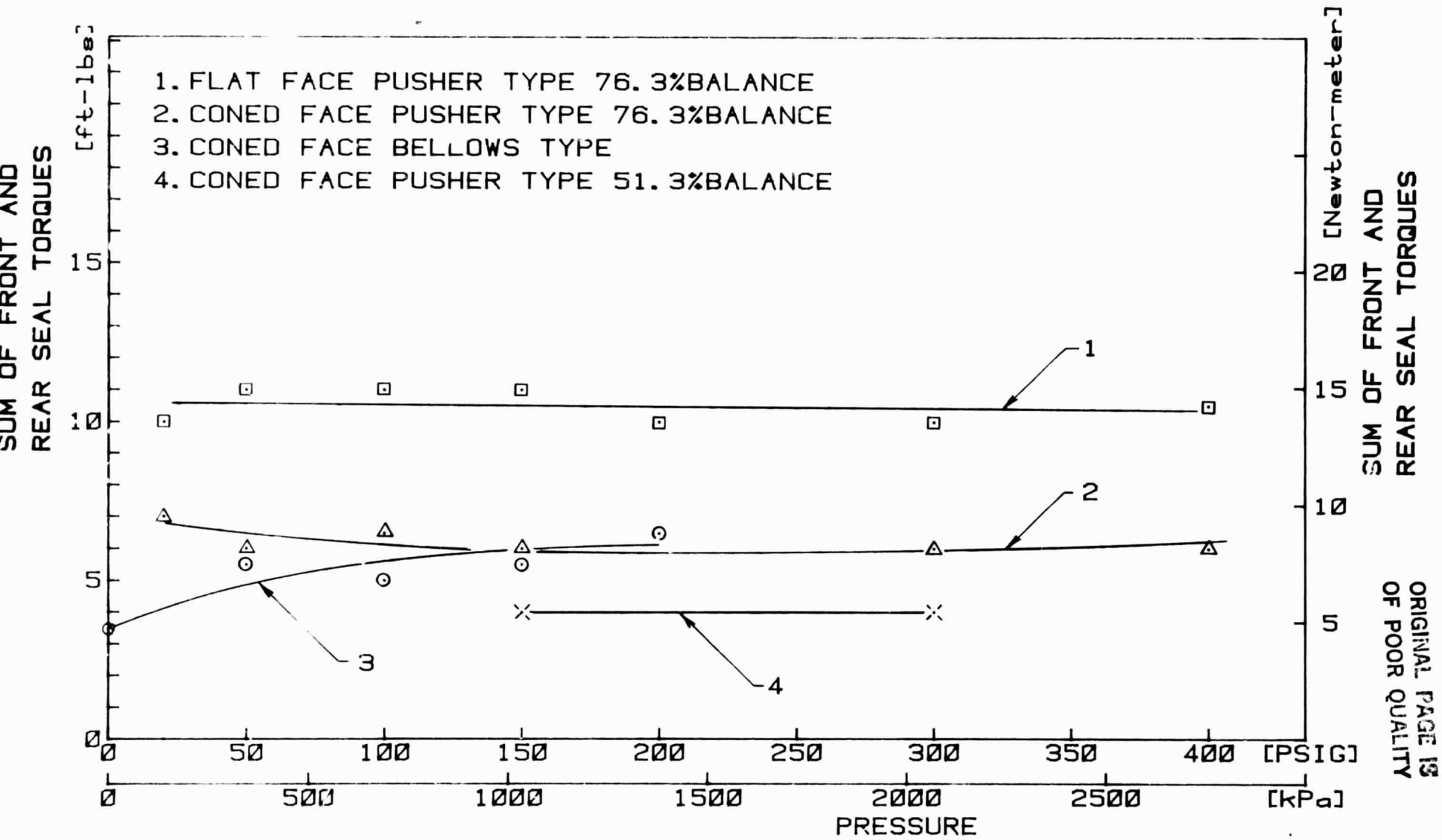

FIGURE 46 - COMPARISON OF THE TYPICAL PEAK TORQUE VALUES OF THE TESTED SEALS AT 3600 RPM AND VARIOUS PRESSURES.

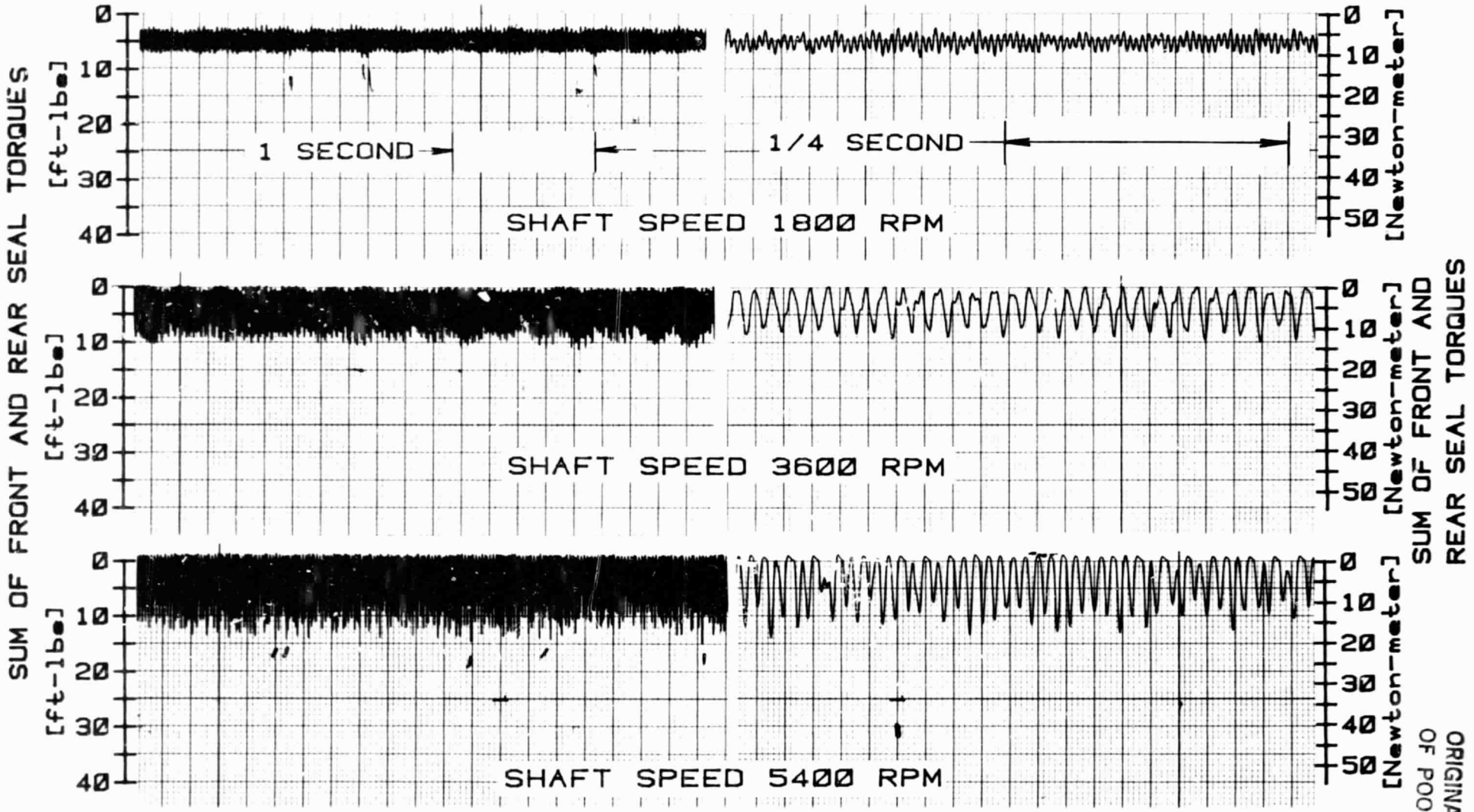

FIGURE 47 - TYPICAL TORQUE RECORDING OF THE FLAT FACE FRONT AND REAR PUSHER TYPE SEAL, BALANCED TO 76.3% AT 1034 kPa (150 PSIG) AT TWO DIFFERENT CHART SPEEDS.

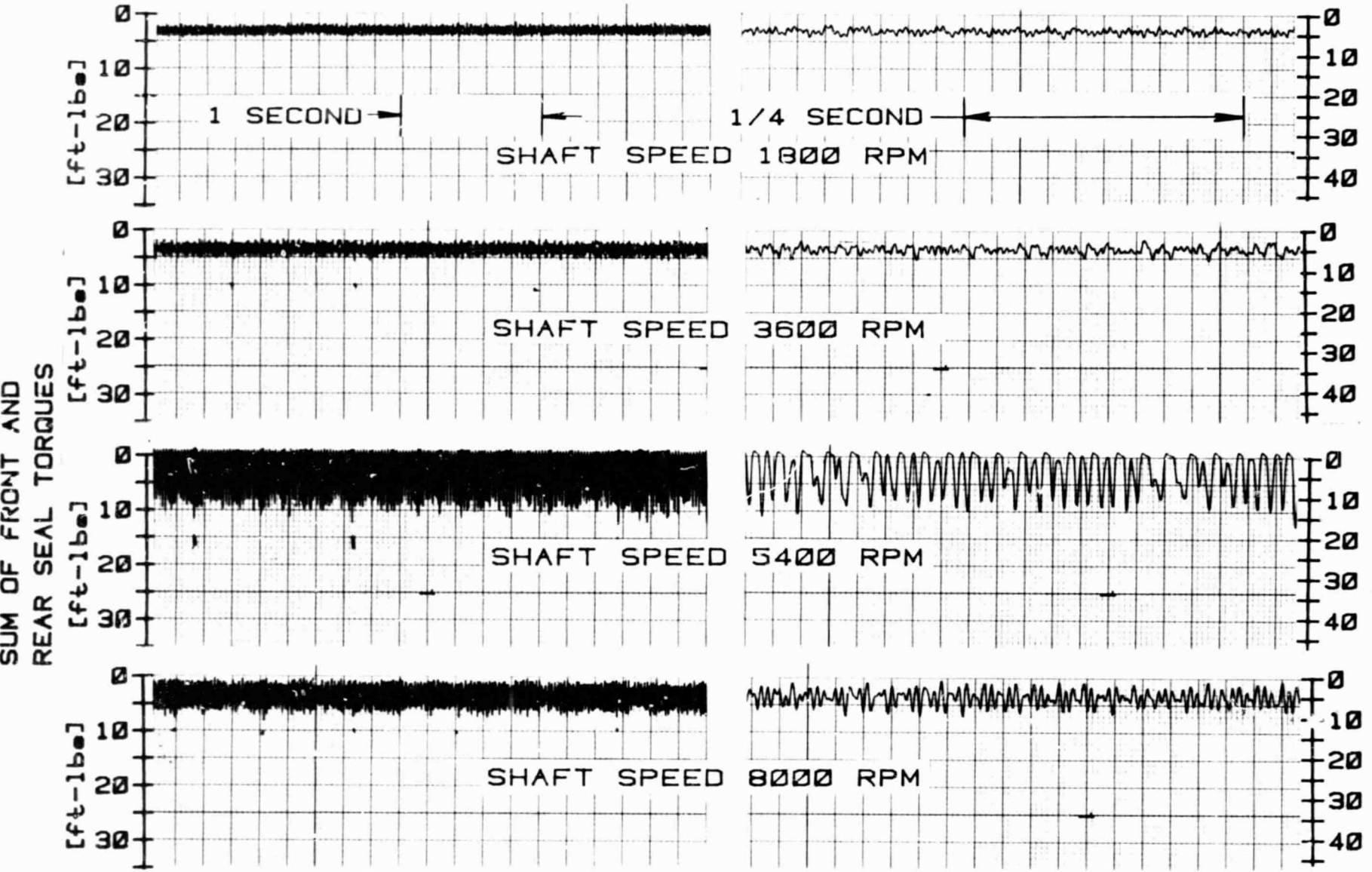

FIGURE 48 - TYPICAL TORQUE RECORDING OF THE CONED FACE FRONT AND REAR PUSHER TYPE SEALS AT 1034 kPa (150 PSIG).

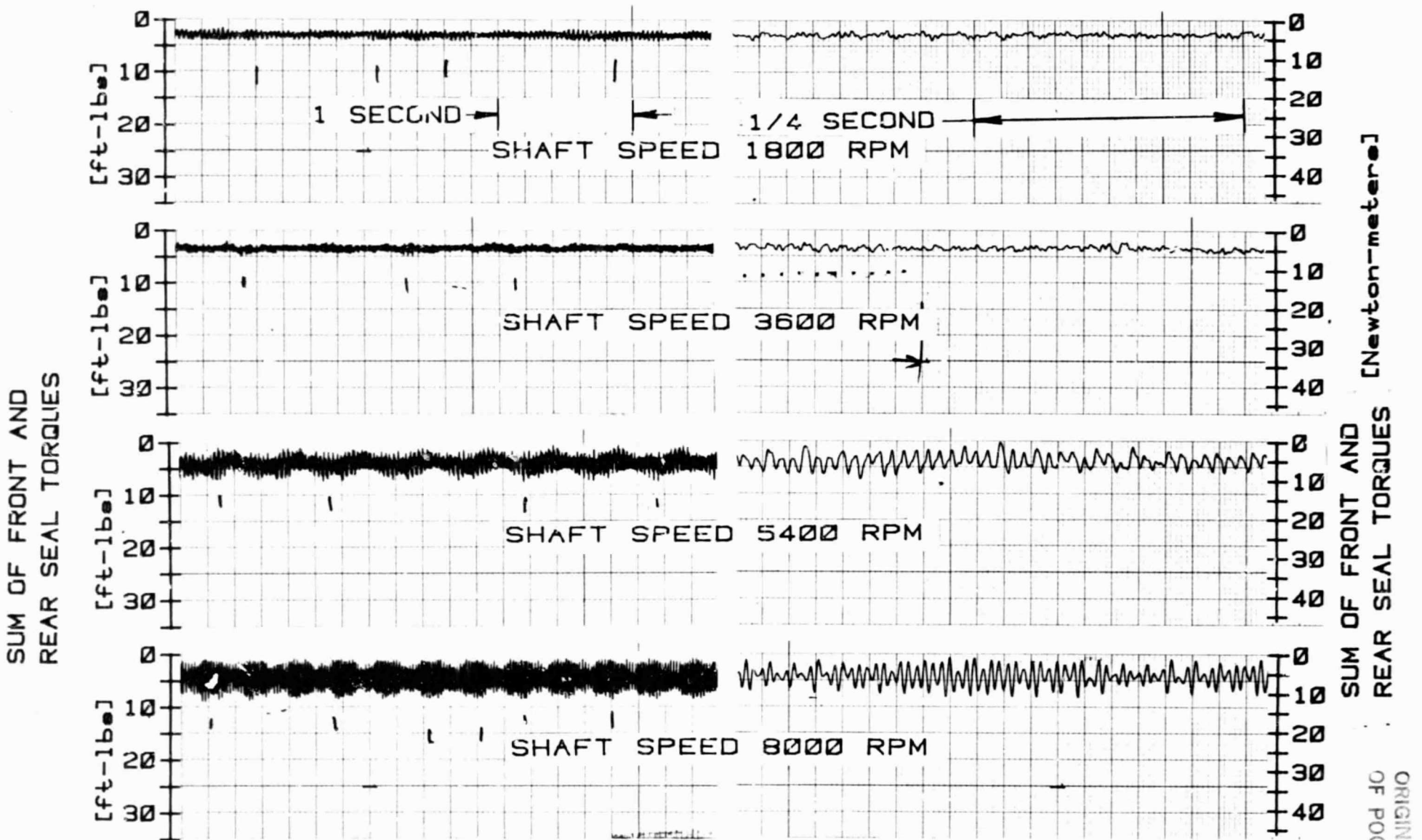

FIGURE 49 - TYPICAL TORQUE RECORDING OF THE CONED FACE FRONT AND REAR BELLOWS TYPE SEALS AT 1034 kPa (150 PSIG).

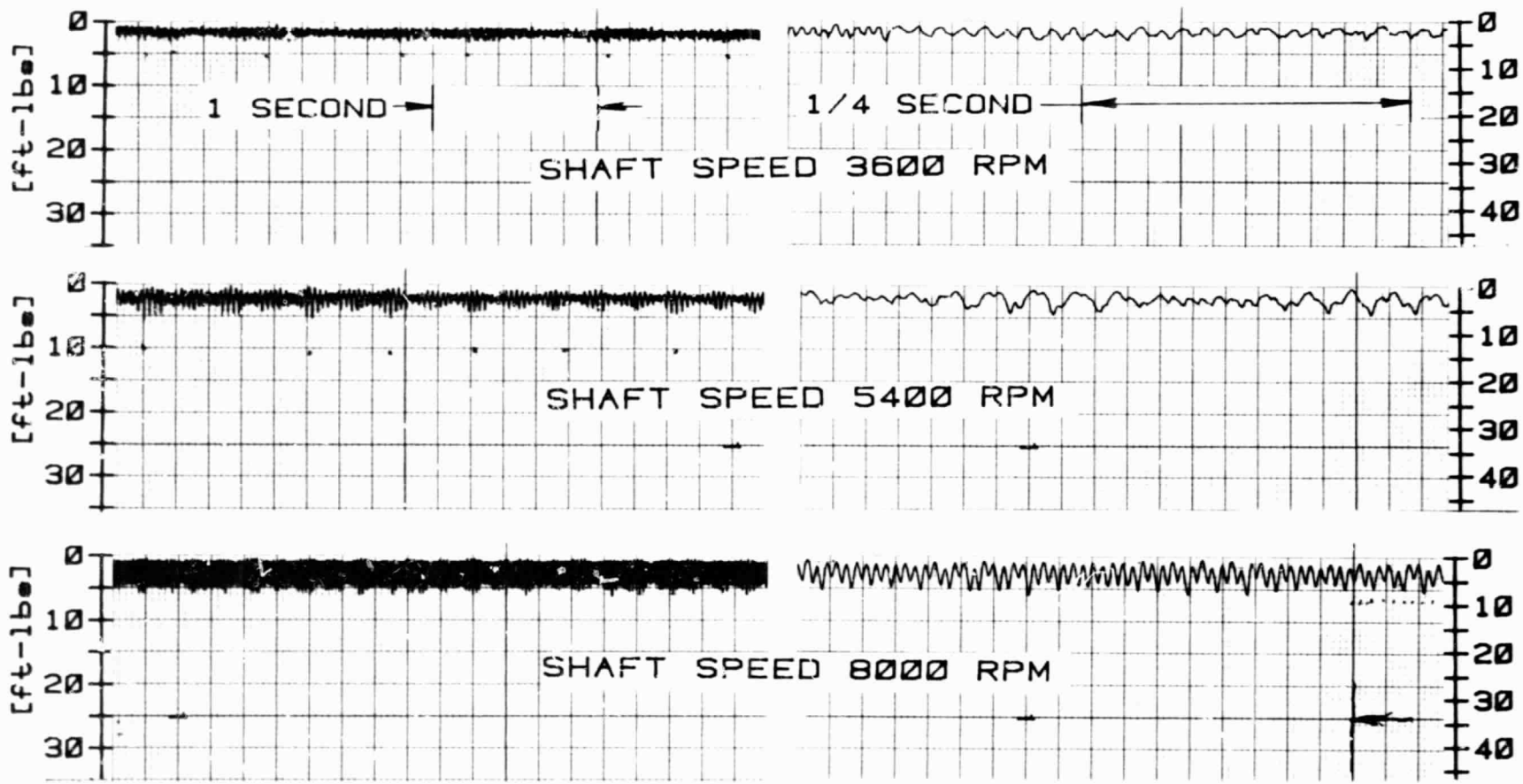

FIGURE 50 - TYPICAL TORQUE RECORDING OF THE CONED FACE FRONT AND REAR PUSHER TYPE SEALS, BALANCED TO 51.3% AT 1034 kPa (150 PSIG).

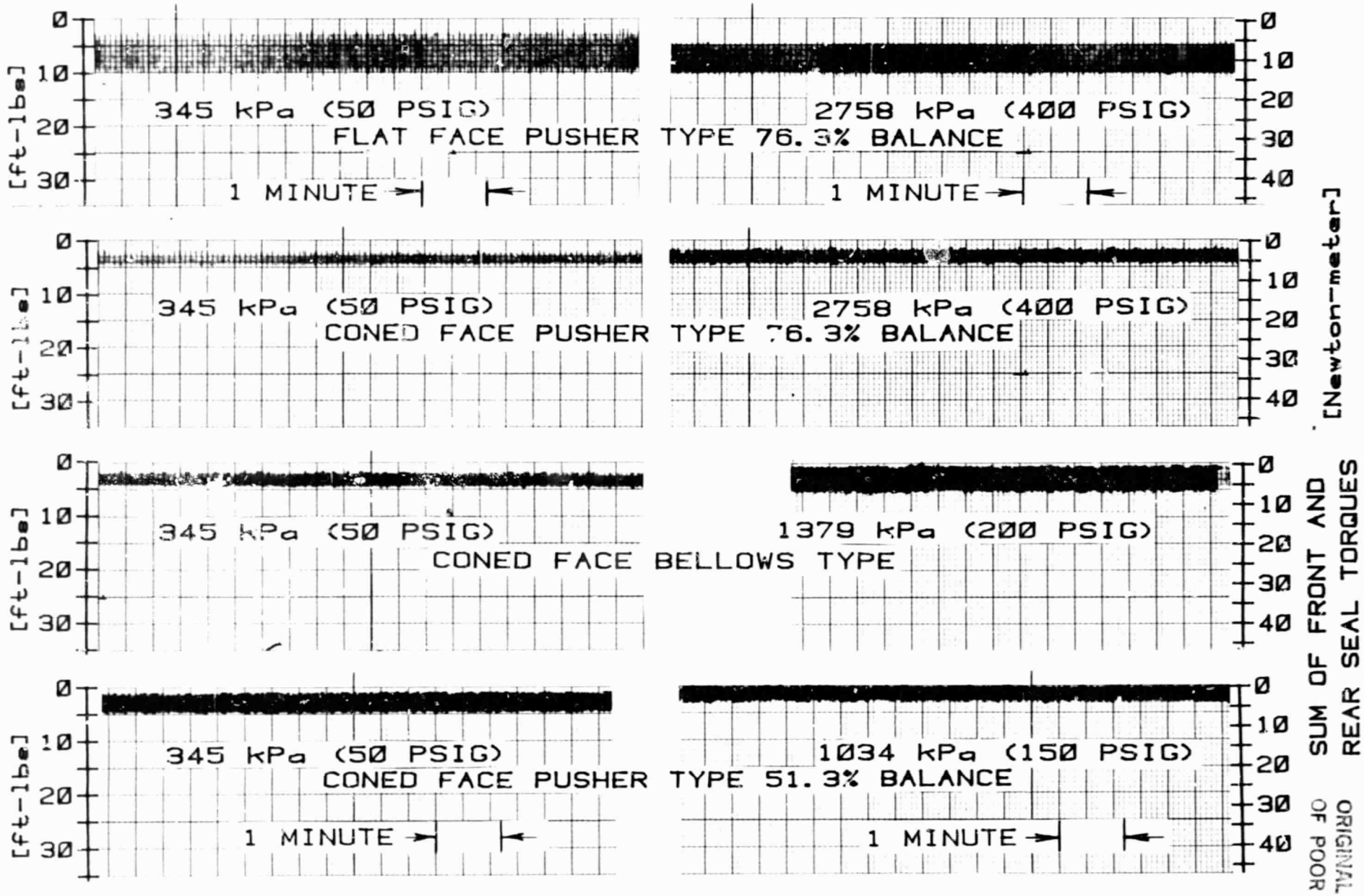

FIGURE 51 - TORQUE COMPARISON OF THE TESTED SEALS AT 1800 RPM AND VARIOUS PRESSURES.

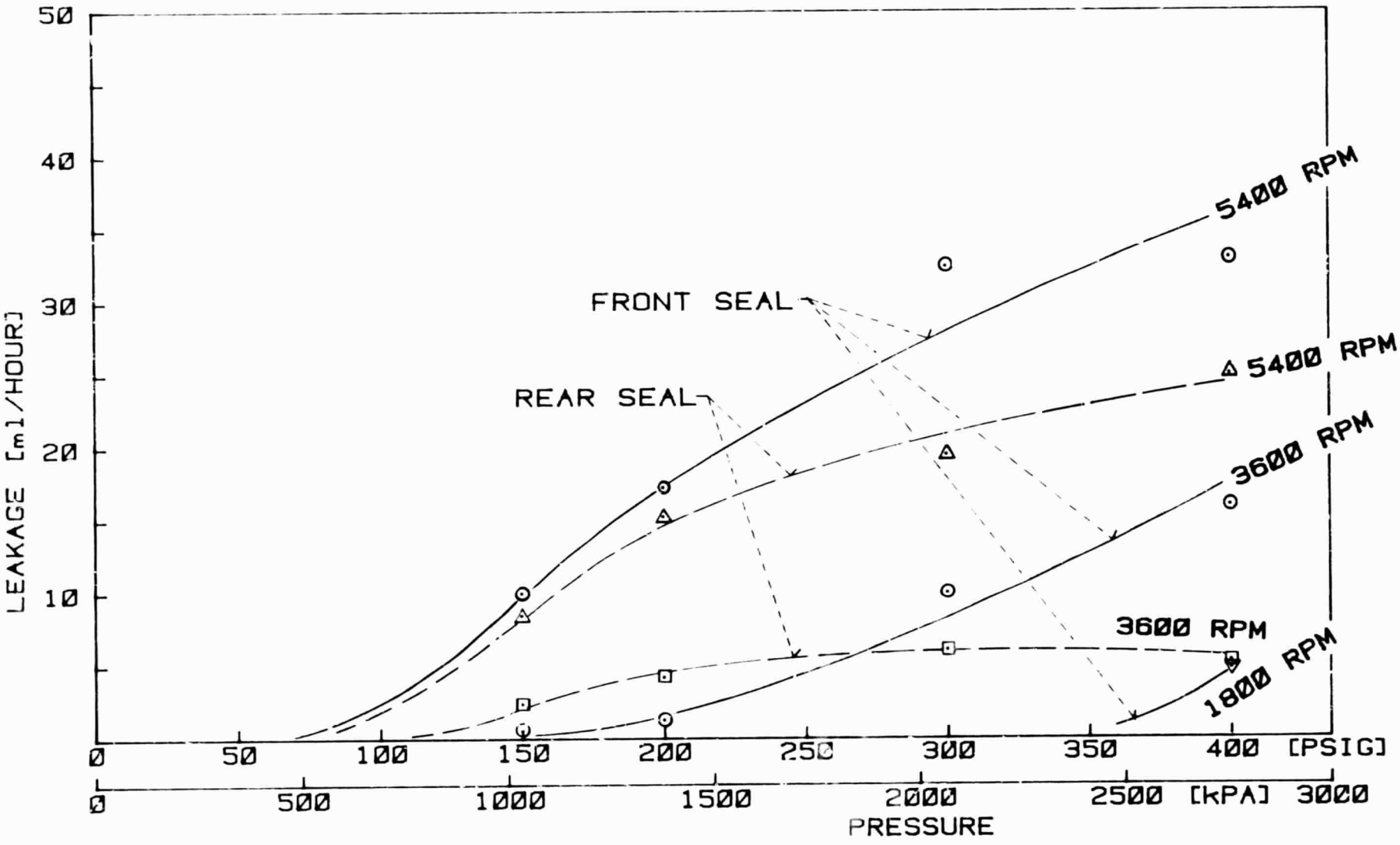

FIGURE 52 - LEAKAGE OF THE FLAT FACE PUSHER TYPE SEAL AT DIFFERENT PRESSURES AND SPEEDS.

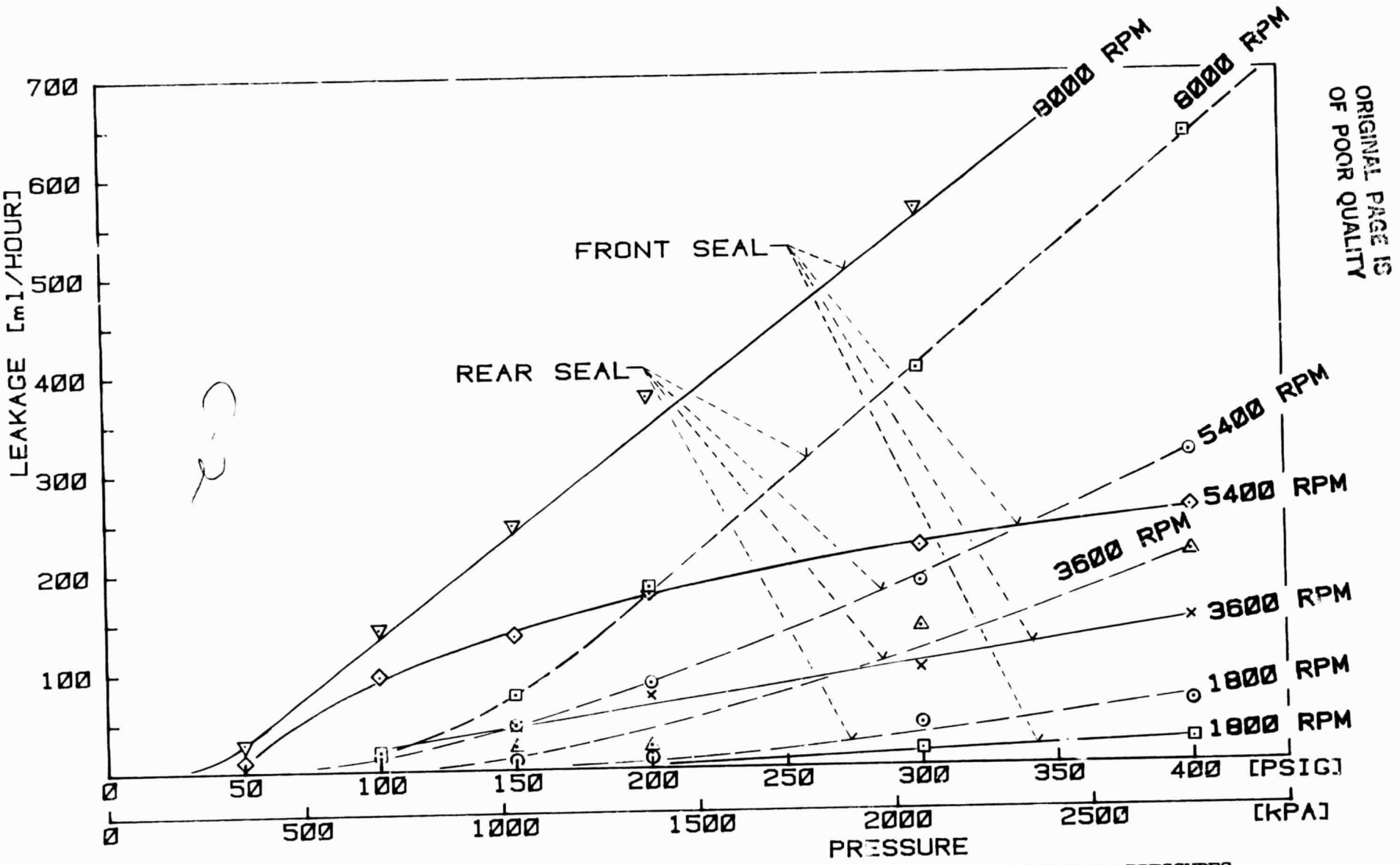

FIGURE 53 - LEAKAGE OF THE CONED FACE PUSHER TYPE SEAL BALANCED TO 76.3% AT DIFFERENT PRESSURES AND SPEEDS.

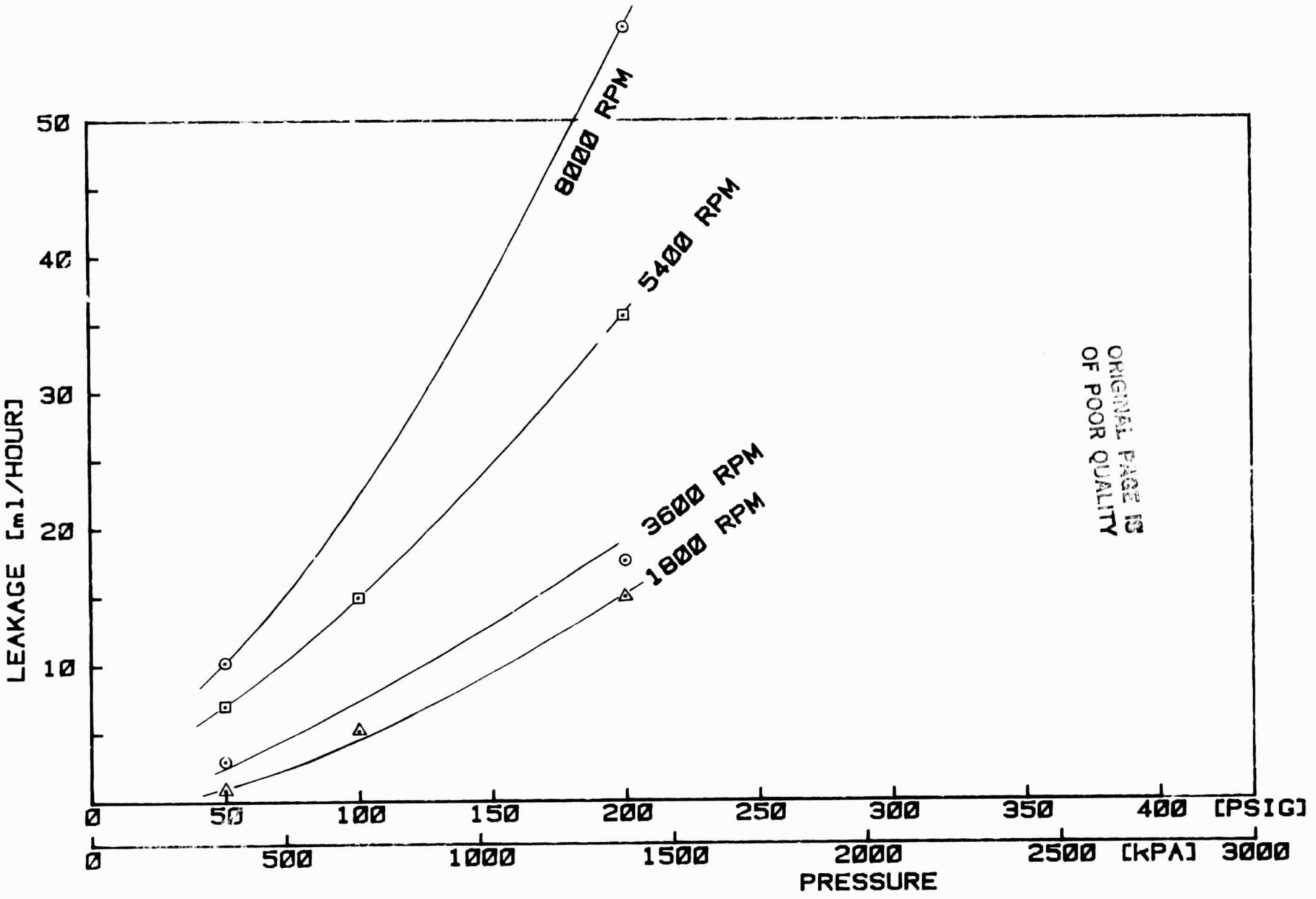

FIGURE 54 - LEAKAGE AT VARIOUS PRESSURES AND SPEEDS OF THE FRONT BELLOWS TYPE SEAL WITH THE CONED FACE PRIMARY RING.

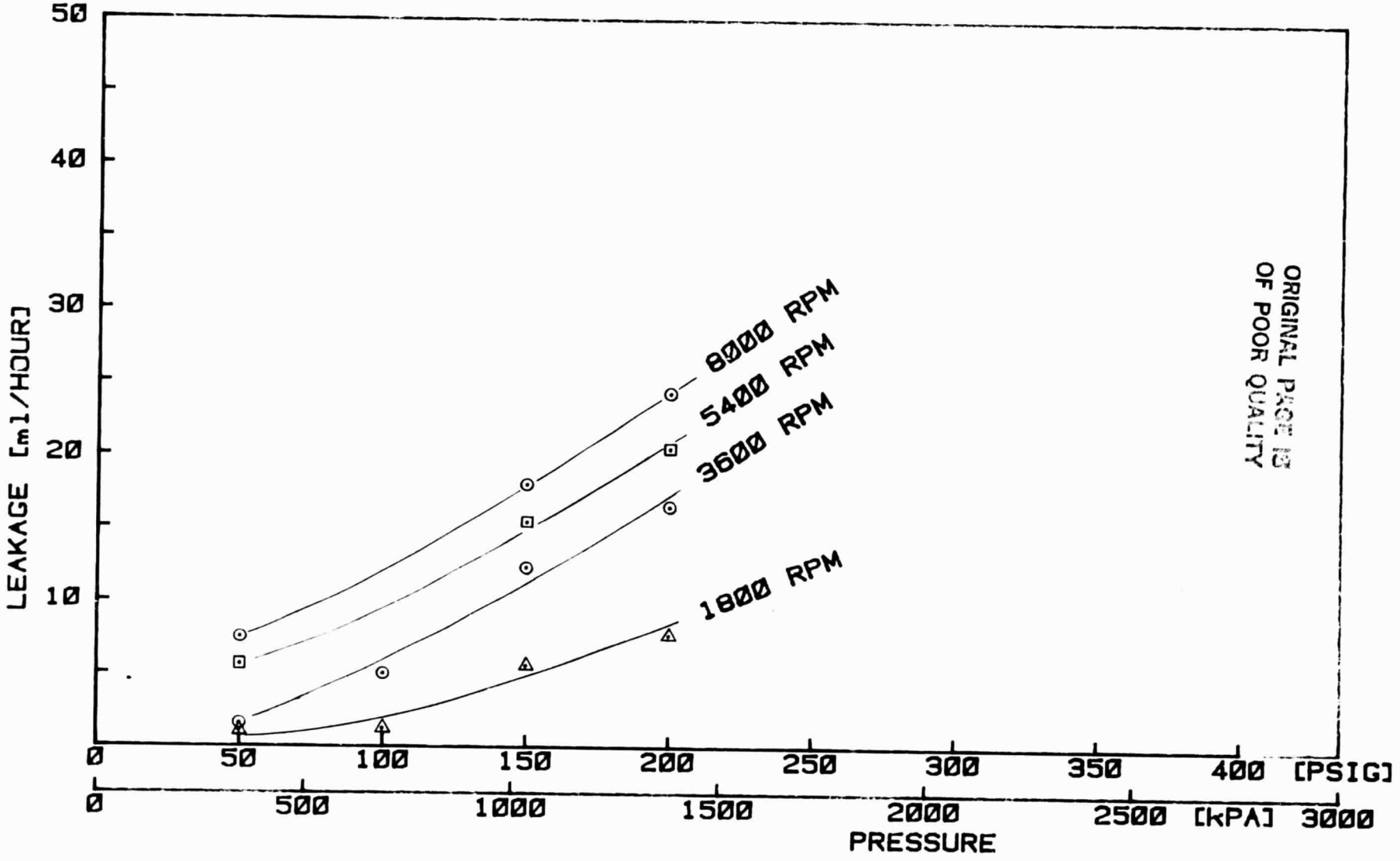

FIGURE 55 - LEAKAGE AT VARIOUS PRESSURES AND SPEEDS OF THE REAR BELLOWS TYPE SEAL WITH THE CONED FACE PRIMARY RING.

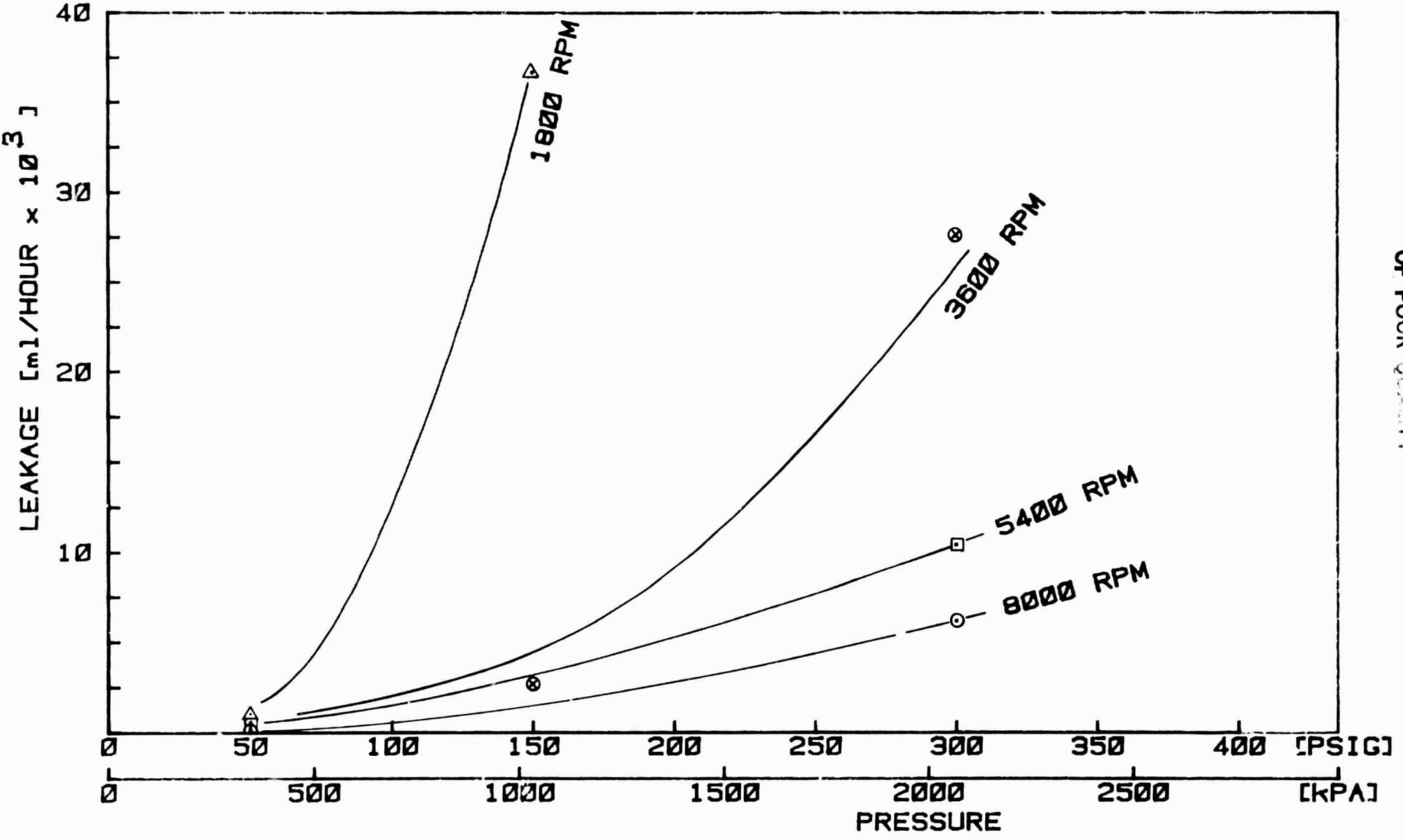

FIGURE 56 - LEAKAGE OF THE FRONT CONED FACE PUSHER TYPE SEAL BALANCED TO 51.3% AT DIFFERENT PRESSURES AND SPEEDS.

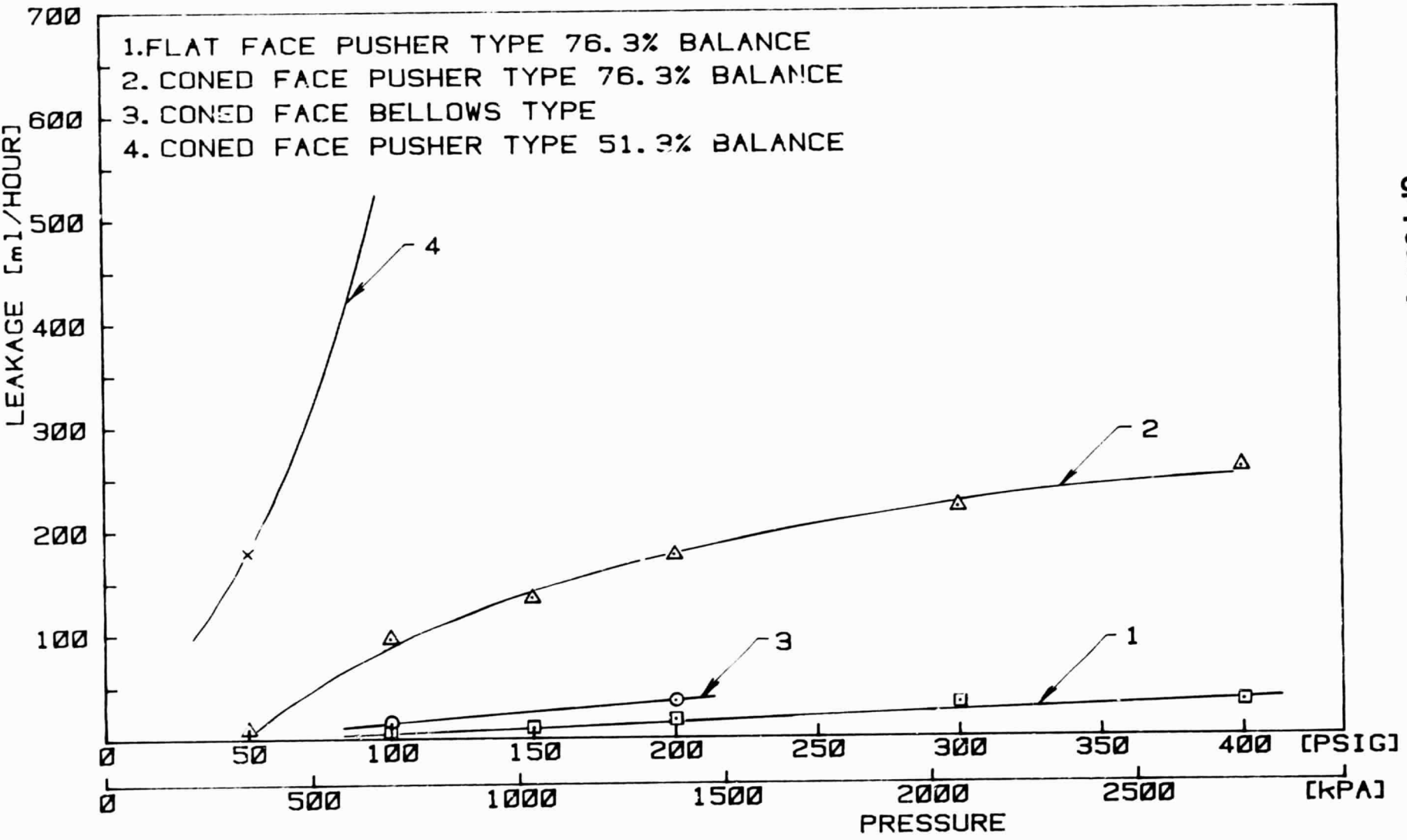

FIGURE 57 - COMPARISON OF THE TYPICAL LEAKAGE VALUES OF THE TESTED FRONT SEALS AT 5400 RPM AND VARIOUS PRESSURES.

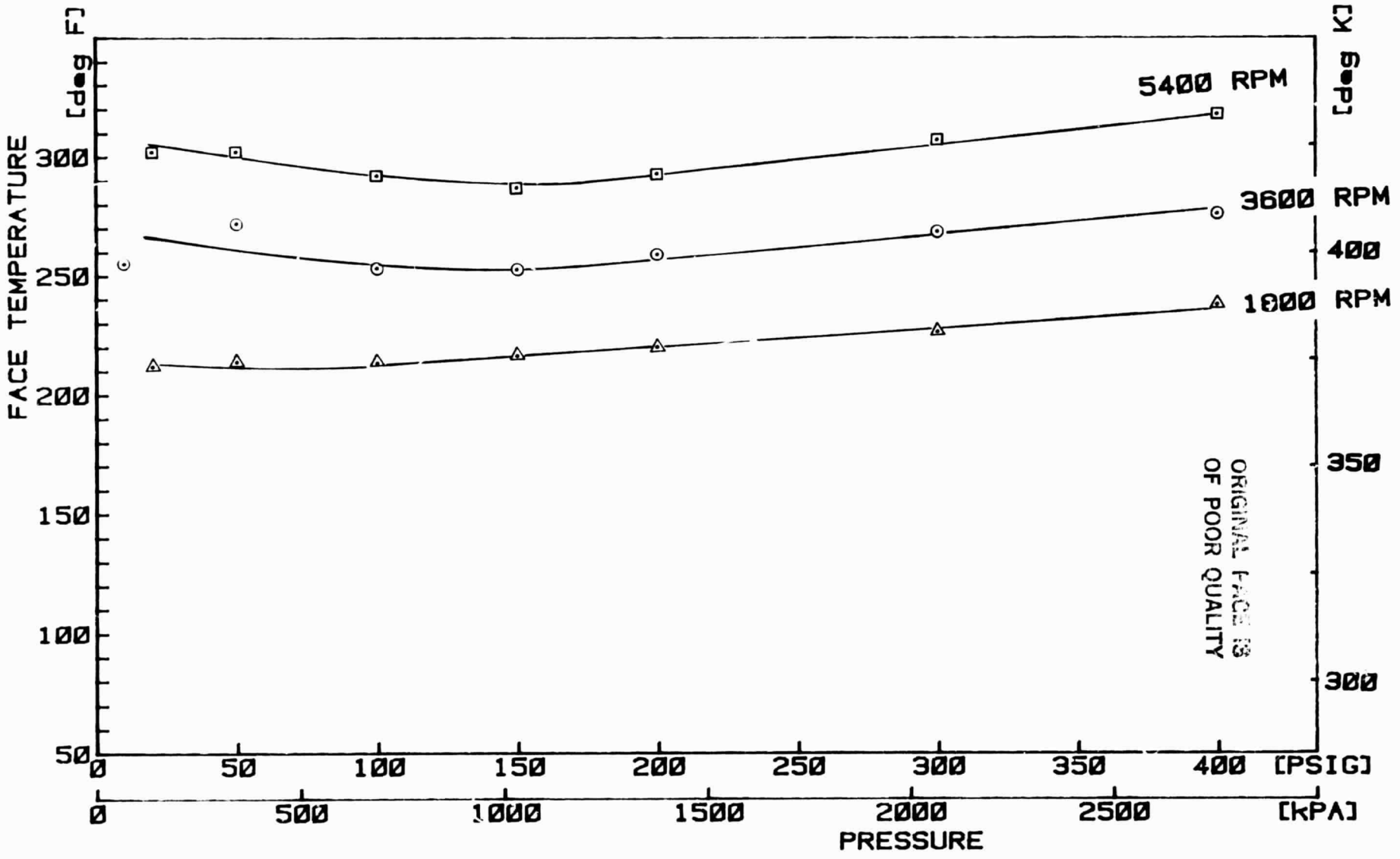

FIGURE 58 - FACE TEMPERATURE OF THE FLAT FACE PUSHER TYPE SEAL AT VARIOUS PRESSURES AND SPEEDS.

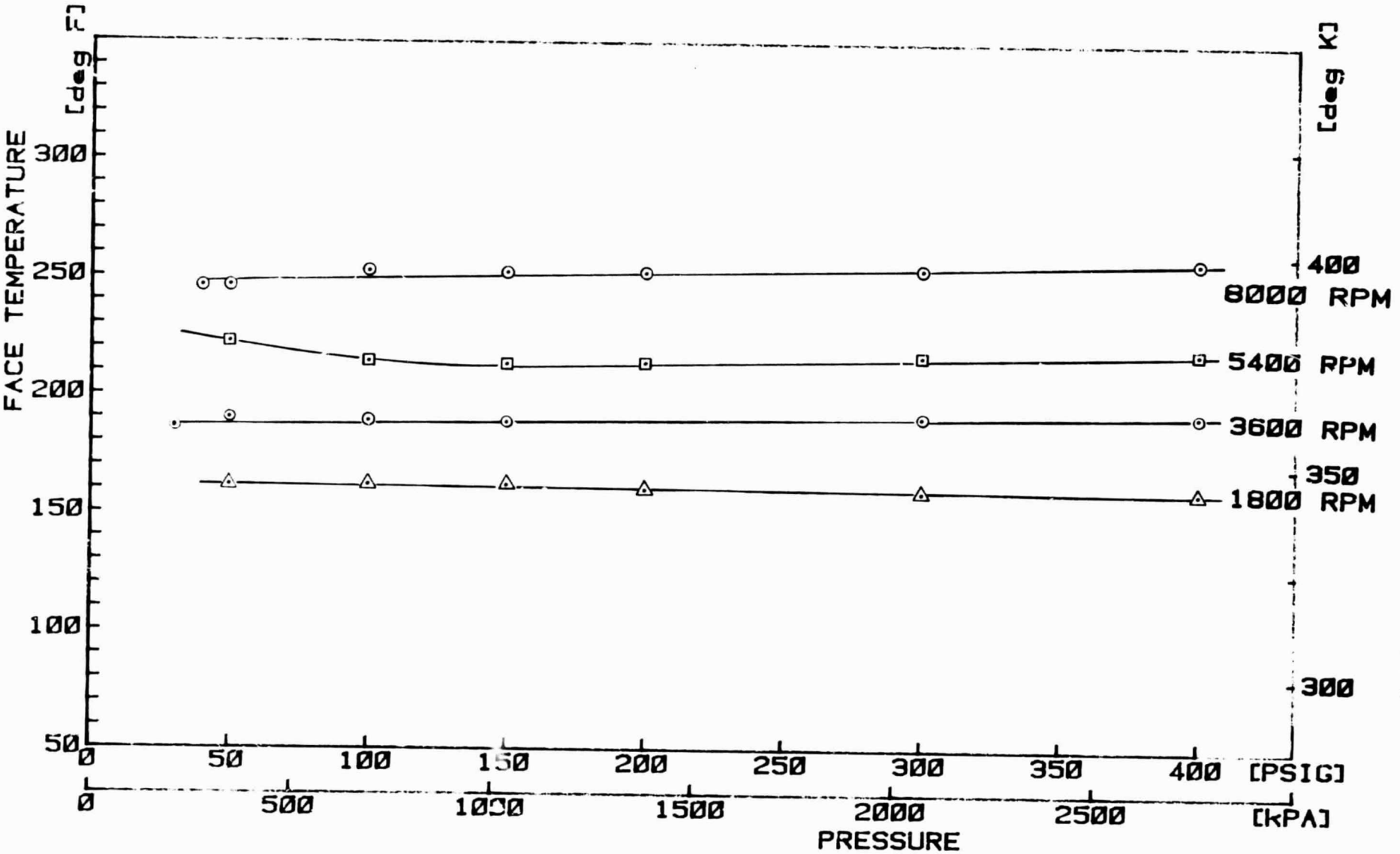

FIGURE 59 - FACE TEMPERATURE OF THE CONED FACE PUSHER TYPE SEAL BALANCED TO 76.3% AT VARIOUS PRESSURES AND SPEEDS.

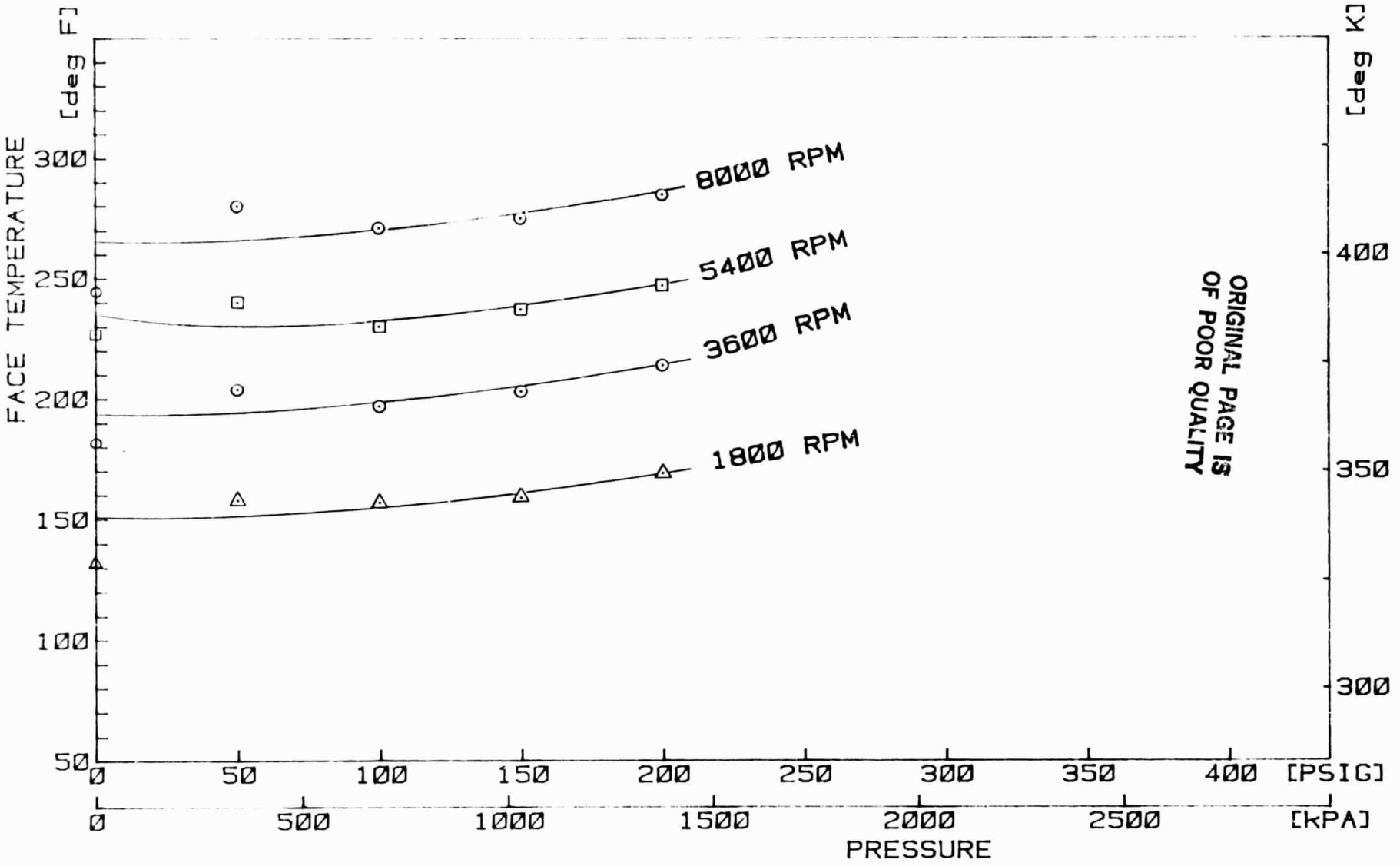

FIGURE 60 - FACE TEMPERATURE OF THE CONED FACE BELLOWS TYPE SEAL AT VARIOUS PRESSURES AND SPEEDS.

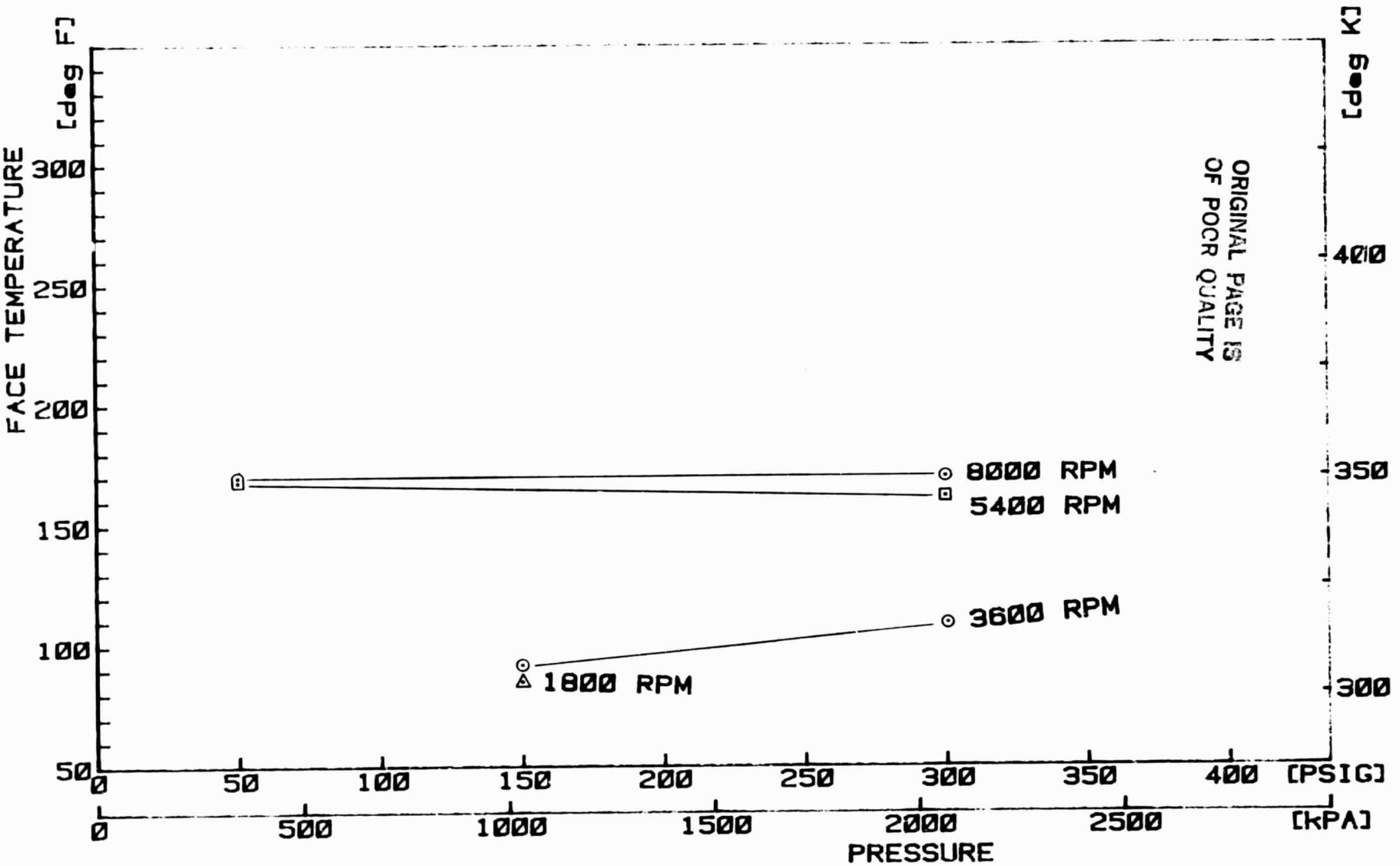

FIGURE 61 - FACE TEMPERATURE AT VARIOUS PRESSURES AND SPEEDS OF THE CONED FACE PUSHER TYPE SEAL, BALANCED TO 51.3%.

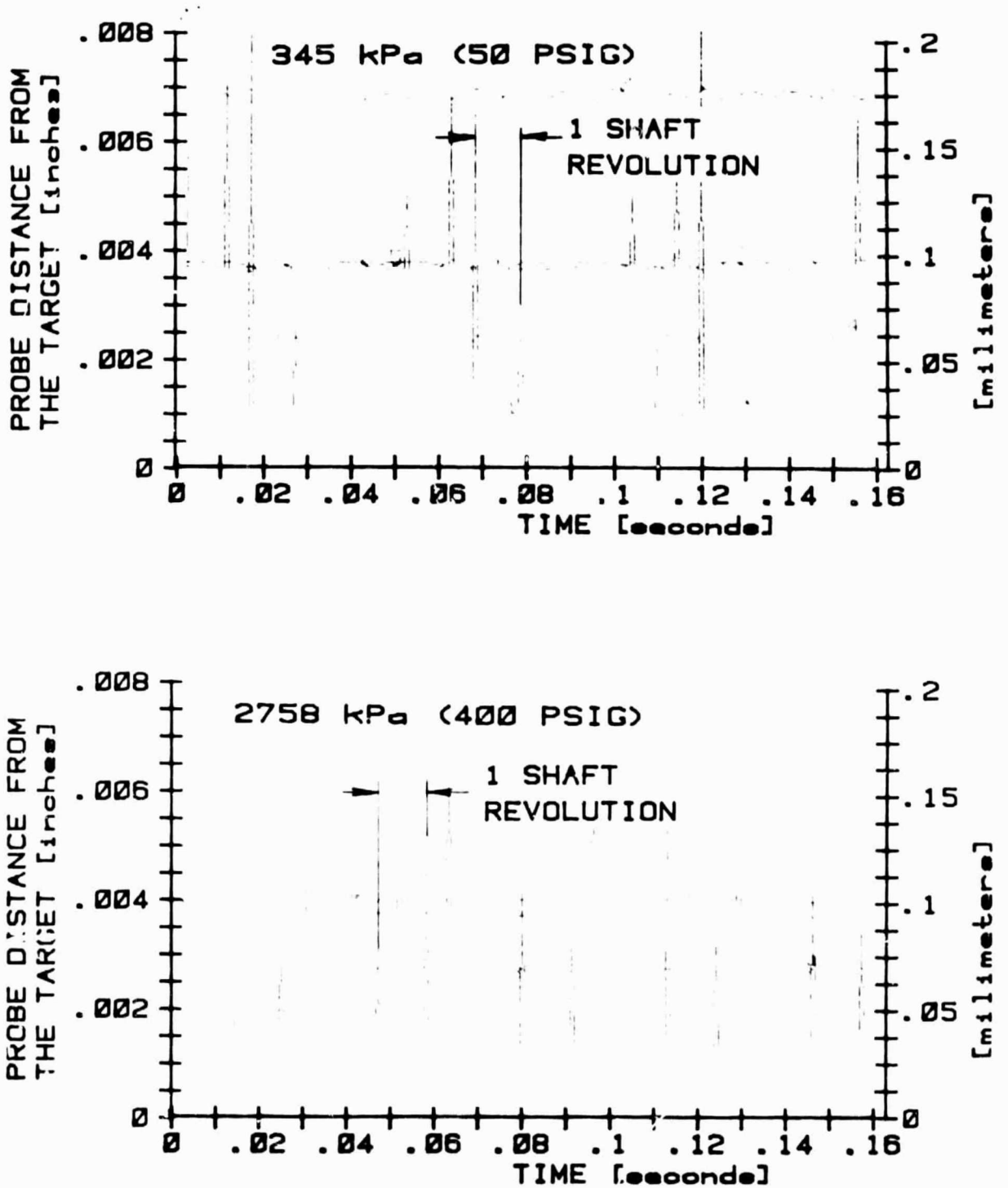

FIGURE 62 - RECORDING OF THE TYPICAL AXIAL MOVEMENT OF THE CONED FACE PUSHER TYPE SEAL (76.3% BALANCE) AT 5400 RPM ON THE PRINTOUT FROM THE DESKTOP COMPUTER HP-85. TRACES #2, 3, AND 4 ARE INSTANTANEOUS AXIAL DISTANCES BETWEEN THE PROBE TIPS AND THE TARGET ATTACHED TO A STATIONARY PRIMARY RING. TRACES #1 AND #5 ARE AXIAL DISTANCES BETWEEN THE PROBES AND THE ROTOR TARGET RING. ONE PEAK TO PEAK PULSE CORRESPONDS TO ONE REVOLUTION OF THE SEAL SHAFT.

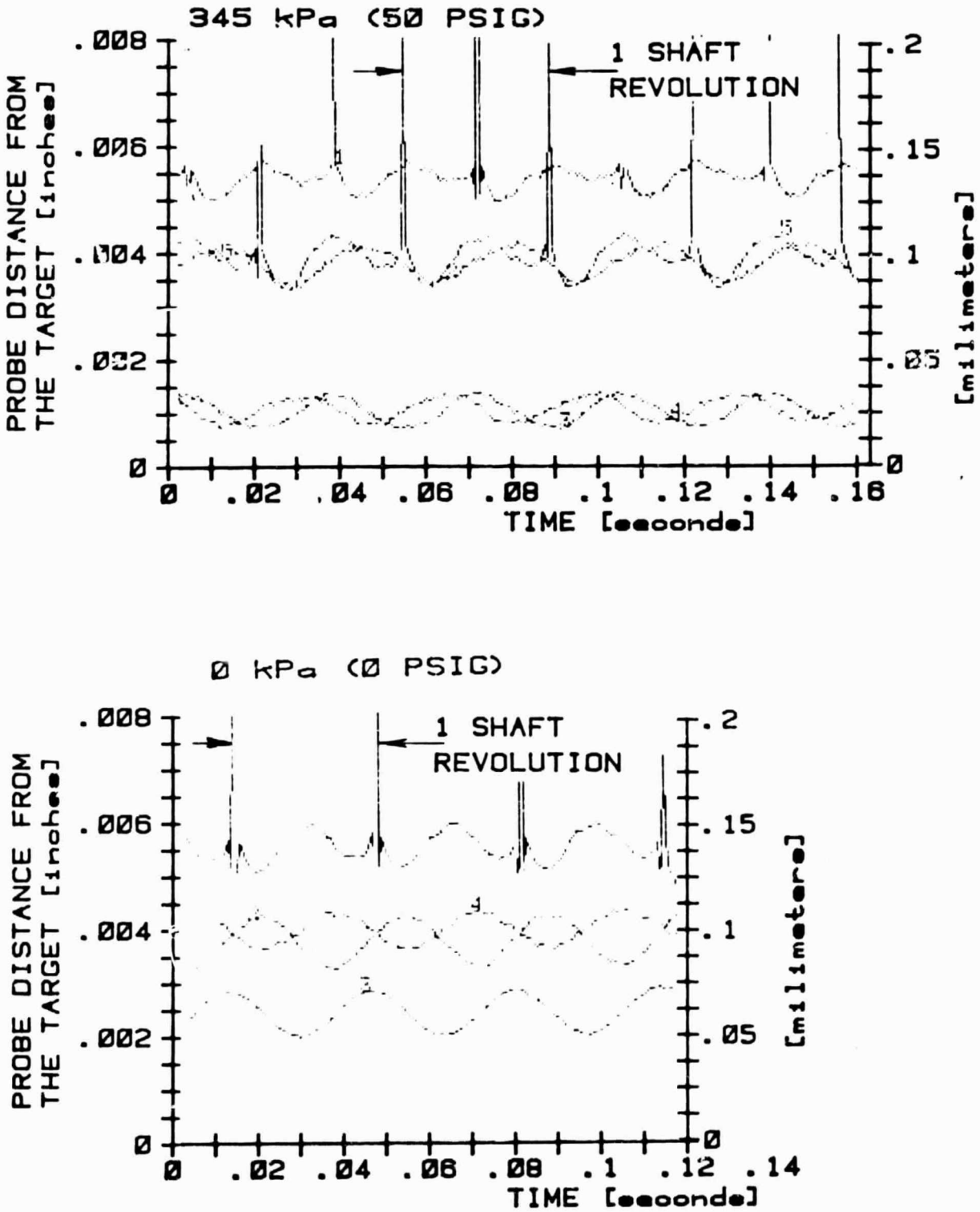

FIGURE 63 - RECORDING OF THE TYPICAL AXIAL MOVEMENT OF THE CONED FACE BELLOWS TYPE SEAL AT 1800 RPM. TRACES #2, 3, AND 4 REPRESENT INSTANTANEOUS AXIAL DISTANCES BETWEEN THE PROBE TIPS AND THE TARGET ATTACHED TO A STATIONARY PRIMARY RING. THE TRACES #1 AND #5 ARE AXIAL DISTANCES BETWEEN THE PROBES AND THE ROTOR TARGET RING. LOCATION OF EACH PROBE IS SHOWN IN FIGURE 18. ONE PEAK TO PEAK TO PEAK PULSE CORRESPONDS TO ONE REVOLUTION OF THE SEAL SHAFT.

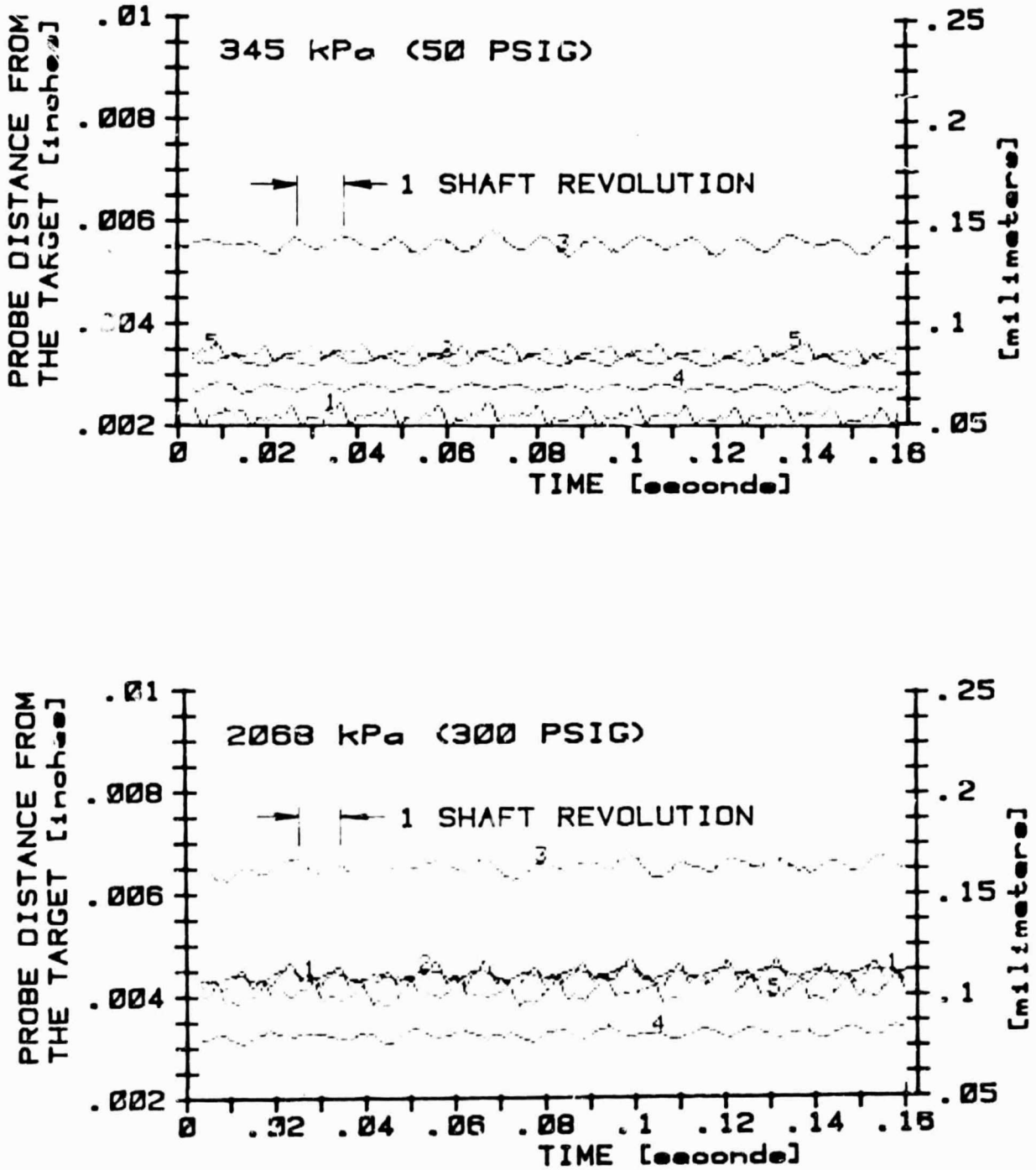

FIGURE 64 - RECORDING OF THE TYPICAL AXIAL MOVEMENT OF THE CONED FACE PUSHER TYPE SEAL (51.3% BALANCE) AT 5400 RPM. TRACES ARE INSTANTANEOUS DISTANCES BETWEEN THE PROBES AND THEIR TARGETS MOUNTED ON THE STATIONARY PRIMARY RING (#2, 3, 4) AND ON THE ROTATING MATING RING (#1, 5). RADIAL LOCATION OF THE PROBES IS SHOWN IN FIGURE 18. ONE PEAK TO PEAK PULSE CORRESPONDS TO ONE REVOLUTION OF THE SEAL SHAFT.

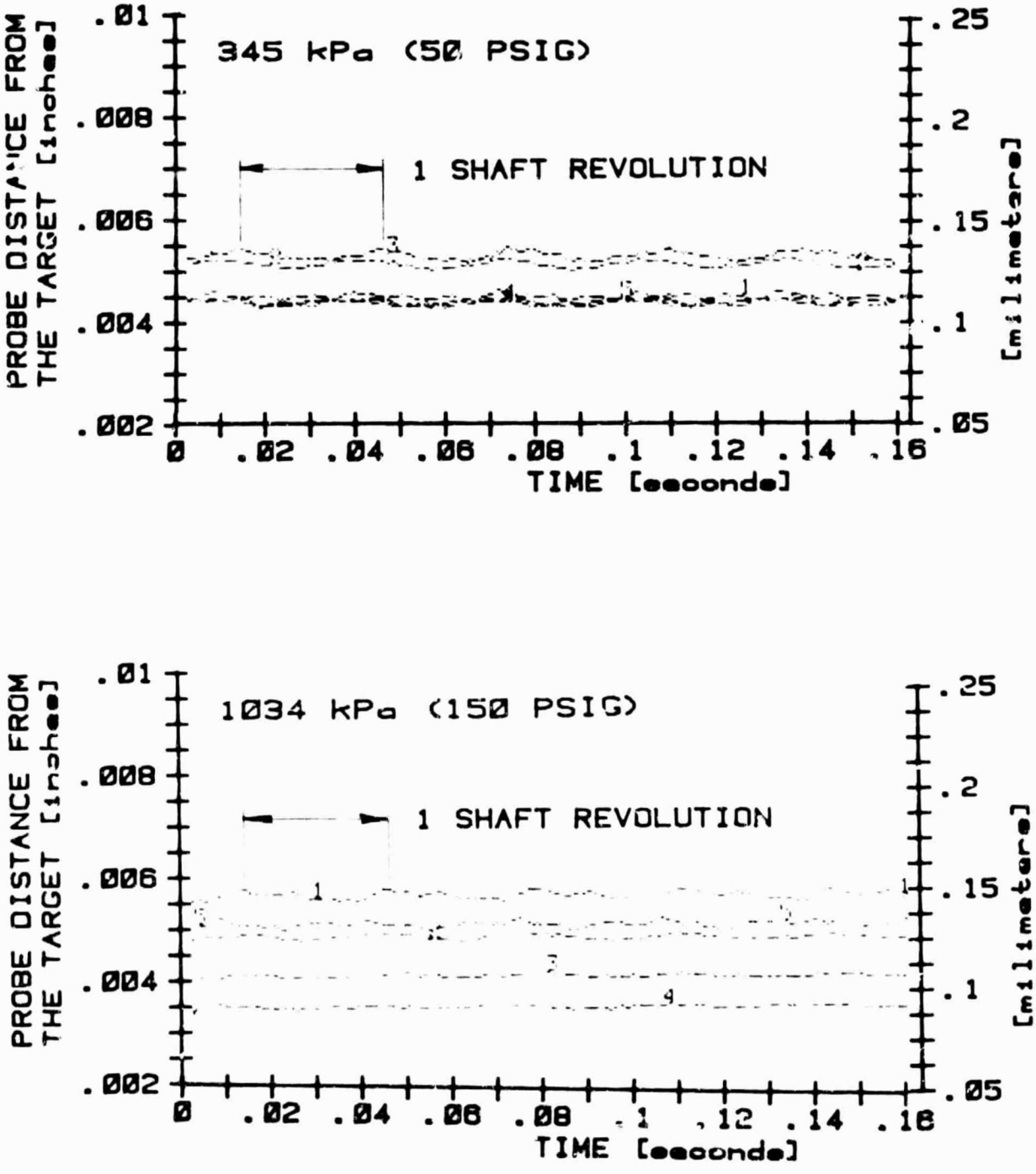

FIGURE 65 - RECORDING OF THE TYPICAL AXIAL MOVEMENT OF THE CONED FACE PUSHER TYPE SEAL (57.3% BALANCE) AT 1800 RPM. TRACES REPRESENT AXIAL DISTANCES BETWEEN THE PROBES AND THEIR RESPECTIVE TARGETS MOUNTED ON THE STATIONARY (#2, 3, 4) AND ROTATING (#1 and #5) SEAL PARTS. ONE PEAK TO PEAK PULSE CORRESPONDS TO ONE REVOLUTION OF THE SEAL SHAFT.

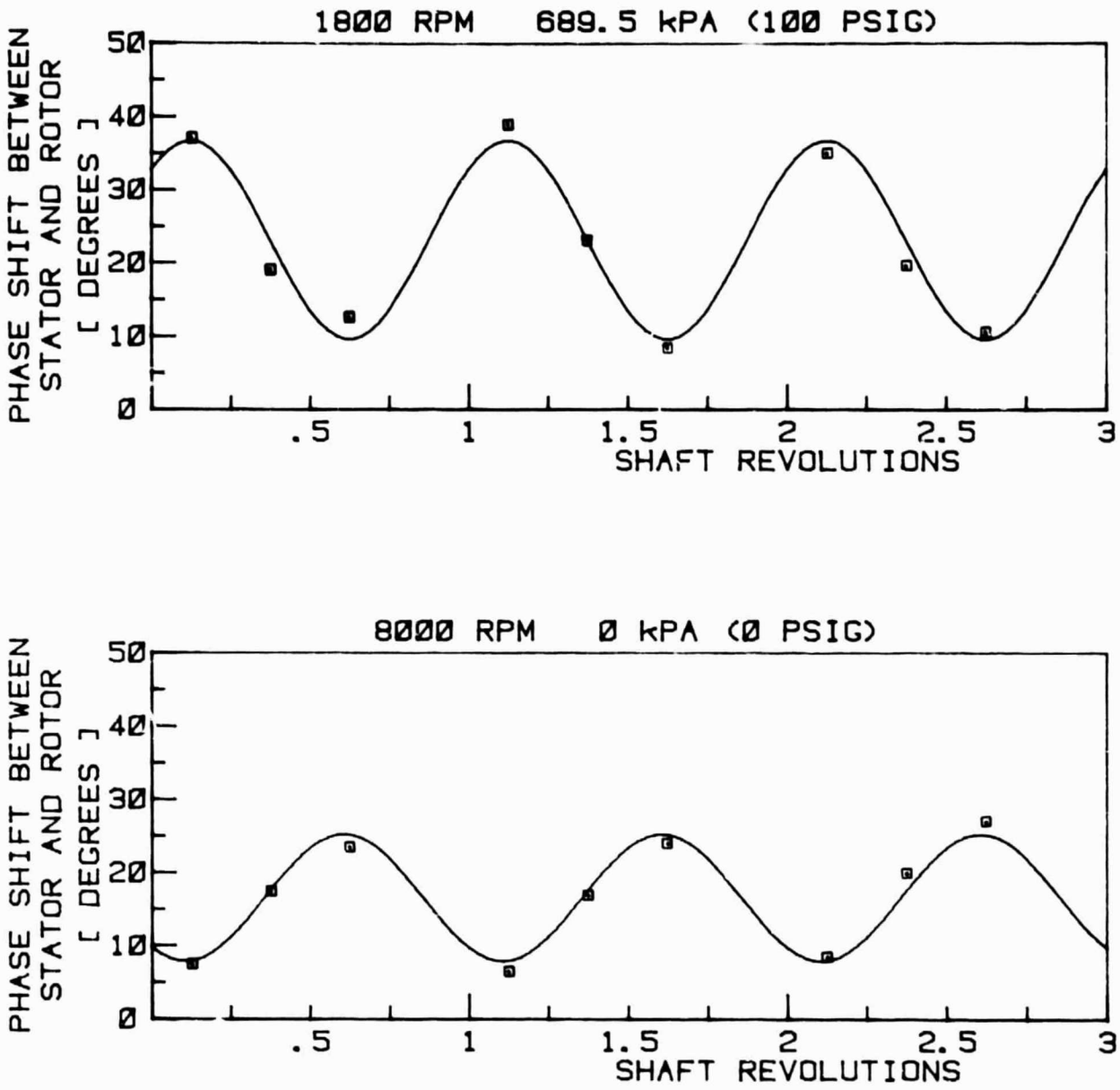

FIGURE 66 - VARIATION OF THE PHASE SHIFT BETWEEN THE ROTOR AND THE STATOR WITH TIME FOR THE CONEL FACE BELLOWS TYPE SEAL.

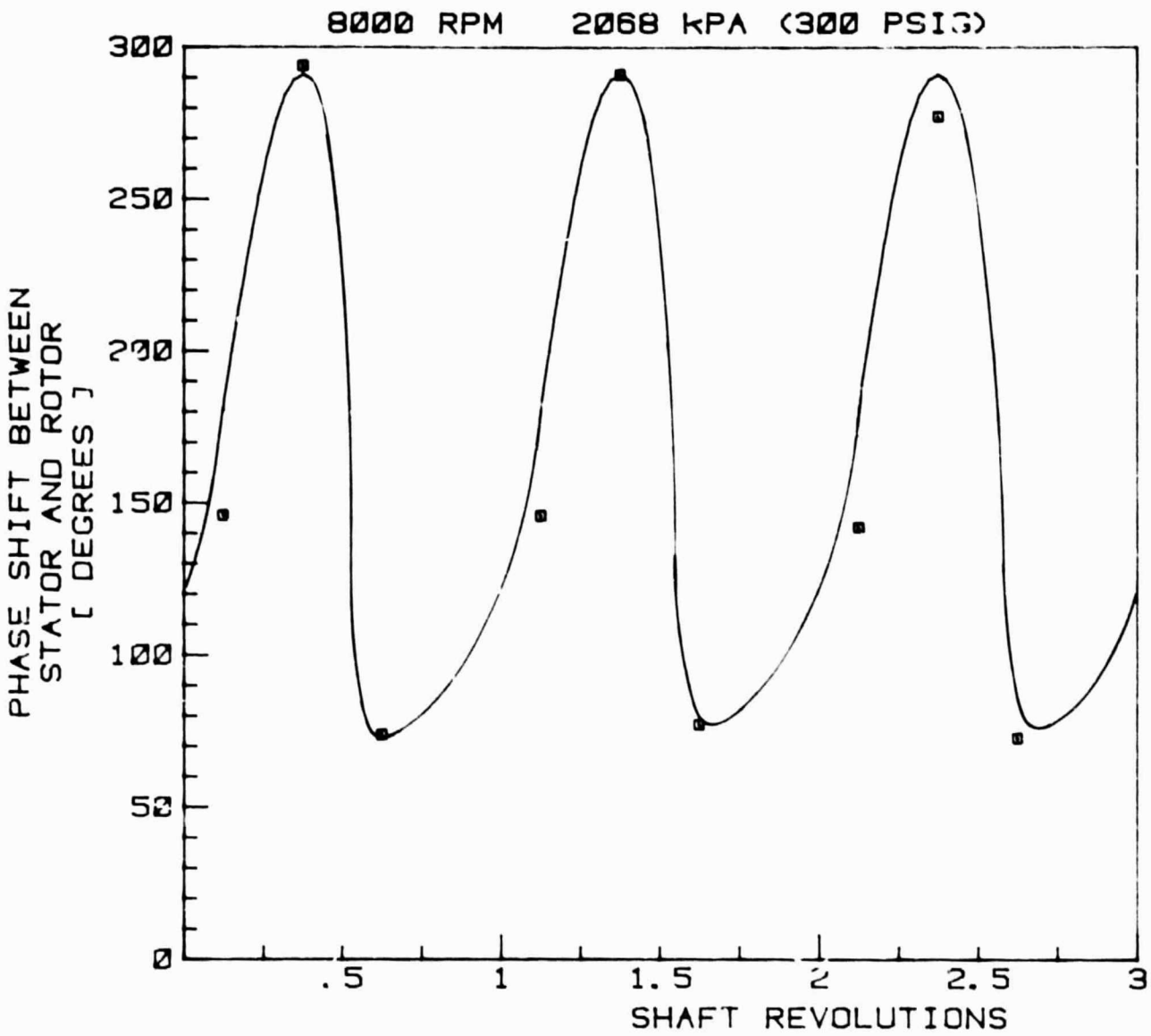

FIGURE 67 - VARIATION OF THE PHASE SHIFT BETWEEN THE ROTOR AND THE STATOR WITH TIME FOR THE CONED FACE PUSHER TYPE SEAL BALANCED TO 51.38.